

ACCEPTED MANUSCRIPT • OPEN ACCESS

## Roadmap on exsolution for energy applications

To cite this article before publication: Dragos Neagu *et al* 2023 *J. Phys. Energy* in press <https://doi.org/10.1088/2515-7655/acd146>

### Manuscript version: Accepted Manuscript

Accepted Manuscript is “the version of the article accepted for publication including all changes made as a result of the peer review process, and which may also include the addition to the article by IOP Publishing of a header, an article ID, a cover sheet and/or an ‘Accepted Manuscript’ watermark, but excluding any other editing, typesetting or other changes made by IOP Publishing and/or its licensors”

This Accepted Manuscript is © 2023 The Author(s). Published by IOP Publishing Ltd.



As the Version of Record of this article is going to be / has been published on a gold open access basis under a CC BY 4.0 licence, this Accepted Manuscript is available for reuse under a CC BY 4.0 licence immediately.

Everyone is permitted to use all or part of the original content in this article, provided that they adhere to all the terms of the licence <https://creativecommons.org/licenses/by/4.0>

Although reasonable endeavours have been taken to obtain all necessary permissions from third parties to include their copyrighted content within this article, their full citation and copyright line may not be present in this Accepted Manuscript version. Before using any content from this article, please refer to the Version of Record on IOPscience once published for full citation and copyright details, as permissions may be required. All third party content is fully copyright protected and is not published on a gold open access basis under a CC BY licence, unless that is specifically stated in the figure caption in the Version of Record.

View the [article online](#) for updates and enhancements.

## Roadmap

# Roadmap on Exsolution for Energy Applications

**Dragos Neagu**<sup>1,29,30</sup>, **J.T.S. Irvine**<sup>2,29,30</sup>, **Jiayue Wang**<sup>3</sup>, **Bilge Yildiz**<sup>3,4</sup>, **Alexander K. Opitz**<sup>5</sup>, **Jürgen Fleig**<sup>5</sup>, **Yuhao Wang**<sup>6</sup>, **Jiapeng Liu**<sup>6</sup>, **Longyun Shen**<sup>6</sup>, **Francesco Ciucci**<sup>6,7,8,9</sup>, **Brian A. Rosen**<sup>10</sup>, **Yongchun Xiao**<sup>11,12,13</sup>, **Kui Xie**<sup>11,12,13,14</sup>, **Guangming Yang**<sup>15</sup>, **Zongping Shao**<sup>15,16</sup>, **Yubo Zhang**<sup>17</sup>, **Jakob Reinke**<sup>17</sup>, **Travis A. Schmauss**<sup>17</sup>, **Scott A. Barnett**<sup>17</sup>, **Roelf Maring**<sup>18</sup>, **Vasileios Kyriakou**<sup>18</sup>, **Usman Mushtaq**<sup>19</sup>, **Mihalis N. Tsampas**<sup>19</sup>, **Youdong Kim**<sup>20</sup>, **Ryan O'Hayre**<sup>20</sup>, **Alfonso J. Carrillo**<sup>21</sup>, **Thomas Ruh**<sup>22</sup>, **Lorenz Lindenthal**<sup>22</sup>, **Florian Schrenk**<sup>22</sup>, **Christoph Rameshan**<sup>22</sup>, **Evangelos I. Papaioannou**<sup>23</sup>, **Kalliopi Kousi**<sup>24</sup>, **Ian S. Metcalfe**<sup>25</sup>, **Xiaoxiang Xu**<sup>26</sup>, **Gang Liu**<sup>27,28</sup>

<sup>1</sup> Department of Chemical and Process Engineering, University of Strathclyde, Glasgow, United Kingdom

<sup>2</sup> School of Chemistry, University of St Andrews, Fife, United Kingdom

<sup>3</sup> Department of Nuclear Science and Engineering, Massachusetts Institute of Technology, Cambridge, MA, USA

<sup>4</sup> Department of Materials Science and Engineering, Massachusetts Institute of Technology, Cambridge, MA, USA

<sup>5</sup> TU Wien, Institute of Chemical Technologies and Analytics, Vienna, Austria

<sup>6</sup> Department of Mechanical and Aerospace Engineering, HKUST, Hong Kong SAR, P. R. China

<sup>7</sup> Department of Chemical and Biological Engineering, HKUST, Hong Kong SAR, P. R. China

<sup>8</sup> HKUST Shenzhen-Hong Kong Collaborative Innovation Research Institute, Futian, Shenzhen, P. R. China

<sup>9</sup> HKUST Energy Institute, The Hong Kong University of Science and Technology, Hong Kong SAR, P. R. China

<sup>10</sup> Department of Materials Science and Engineering, Tel Aviv University, Ramat Aviv, 6997801, ISRAEL

<sup>11</sup> Key Laboratory of Optoelectronic Materials Chemistry and Physics, FJIRSM, CAS, Fujian 350002, China

<sup>12</sup> Key Laboratory of Design & Assembly of Functional Nanostructures, FJIRSM, CAS, Fujian 350002, China

<sup>13</sup> Advanced Energy Science and Technology Guangdong Laboratory, Guangdong 116023, China

<sup>14</sup> Fujian Science & Technology Innovation Laboratory for Optoelectronic Information of China, Fujian, China

<sup>15</sup> State Key Laboratory of Materials-Oriented Chemical Engineering, Nanjing Tech University, Nanjing, China

<sup>16</sup> WA School of Mines: Minerals, Energy and Chemical Engineering, Curtin University, Perth, WA, Australia

<sup>17</sup> Department of Materials Science and Engineering, Northwestern University, Evanston, IL, USA

<sup>18</sup> Engineering & Technology Institute Groningen, University of Groningen, 9747 AG Groningen, the Netherlands

<sup>19</sup> Dutch Institute for Fundamental Energy Research (DIFFER), 5612 AJ Eindhoven, the Netherlands

<sup>20</sup> Colorado School of Mines, Golden, CO, USA

<sup>21</sup> Instituto de Tecnología Química (Universitat Politècnica de València – CSIC) Valencia, Spain

<sup>22</sup> Chair of Physical Chemistry, Montanuniversität Leoben, 8700 Leoben, Austria

<sup>23</sup> School of Engineering, Newcastle University, Newcastle, United Kingdom

<sup>24</sup> Department of Chemical and Process Engineering, University of Surrey, United Kingdom

<sup>25</sup> Department of Chemical Engineering and Advanced Materials, Newcastle University, United Kingdom

<sup>26</sup> Shanghai Key Lab of Chemical Assessment and Sustainability, Tongji University, Shanghai, China

<sup>27</sup> Shenyang National Laboratory for Materials Science, Institute of Metal Research, CAS, Shenyang, China

<sup>28</sup> School of Materials Science and Engineering, University of Science and Technology of China, Shenyang, China

<sup>29</sup> Guest editors of the Roadmap.

<sup>30</sup> Author to whom any correspondence should be addressed.

E-mails: [dragos.neagu@strath.ac.uk](mailto:dragos.neagu@strath.ac.uk), [jtsi@st-andrews.ac.uk](mailto:jtsi@st-andrews.ac.uk)

## Abstract

Over the last decade, exsolution has emerged as a powerful new method for decorating oxide supports with uniformly dispersed nanoparticles for energy and catalytic applications. Due to their exceptional anchorage, resilience to various degradation mechanisms, as well as numerous ways in which they can be produced, transformed and applied, exsolved nanoparticles have set new standards for nanoparticles in terms of activity, durability and functionality. In conjunction with multifunctional supports such as perovskite oxides, exsolution becomes a powerful platform for the design of advanced energy materials. In the following sections, we review the current status of the exsolution approach, seeking to facilitate transfer of ideas between different fields of application. We also explore future directions of research, particularly noting the multi-scale development required to take the concept forward, from fundamentals through operando studies to pilot scale demonstrations.

## Contents

- **Introduction from the Guest Editors**  
Dragos Neagu and J.T.S. Irvine
- **Fundamental**
  1. **Understanding and tuning point defects in the host oxides to control exsolved nanoparticles**  
Jiayue Wang and Bilge Yildiz
  2. **Understanding electrochemical exsolution through *in-situ* studies**  
Alexander K. Opitz and Jürgen Fleig
  3. **Design and modelling of new alternative exsolution systems**  
Yuhao Wang, Jiapeng Liu, Longyun Shen and Francesco Ciucci
  4. **The effect of extended defects during exsolution and implications for activity**  
Brian A. Rosen
- **Electrochemical**
  5. **Exsolution for methane conversion to ethylene**  
Yongchun Xiao and Kui Xie
  6. **Exsolution for power generation from ammonia**  
Guangming Yang and Zongping Shao
  7. **Alloy exsolution for SOFC anodes**  
Yubo Zhang, Jakob Reinke, Travis A. Schmauss and Scott A. Barnett
  8. **Exsolution for solid oxide CO<sub>2</sub> and/or H<sub>2</sub>O co-electrolysis**  
Roelf Maring, Vasileios Kyriakou, Usman Mushtaq and Mihalis N. Tsampas
  9. **Exsolution in solid state protonic systems**  
Youdong Kim and Ryan O'Hayre
- **Catalytic**
  10. **Exsolution for methane reforming**  
Alfonso J. Carrillo
  11. **Exsolution for CO<sub>2</sub> utilization applications**  
Thomas Ruh, Lorenz Lindenthal, Florian Schrenk, and Christoph Rameshan
  12. **Exsolution for CO Oxidation**  
Evangelos I. Papaioannou
- **Looping**
  13. **Exsolution for chemical looping hydrogen production**  
Kalliopi Kousi and Ian S. Metcalfe
- **Photocatalysis**
  14. **Exsolving functional nanoparticles from semiconductor matrix to expedite efficient photocatalysis**  
Xiaoxiang Xu and Gang Liu

## Introduction

Dragos Neagu<sup>1</sup> and John Irvine<sup>2</sup>

<sup>1</sup> Department of Chemical and Process Engineering, University of Strathclyde, Glasgow, United Kingdom

<sup>2</sup> School of Chemistry, University of St Andrews, Fife, United Kingdom

Exsolution generally refers to a process through which an initially homogenous solid solution separates into at least two different crystalline phases. This process has been long been known to geologists, with various rock formations exhibiting it at different scales, as exemplified in Figure 1a. However, a decade ago exsolution has transitioned from the 'stone age' to the 'nano age', as shown in Figure 1b. This was made possible through control of crystal defect chemistry of the support from which nanoparticles exsolve, and has advanced exsolution from a naturally-occurring curiosity to a powerful nano-structuring tool.

In this new capacity, exsolution has addressed many key challenges related to deployability, durability, and activity of nanoparticles that other preparation methods had been struggling to deliver. For example, as compared to chemical or physical deposition methods, exsolved nanoparticles are significantly more uniformly dispersed and sized over the support, and much better anchored, being socketed (partly immersed) within the surface of the support with stronger support interactions. This greatly enhances nanoparticle stability against agglomeration and deactivation through various mechanisms, most notably coking in hydrocarbon environments, a longstanding challenge in hydrocarbon catalysis. Additionally, exsolution has opened completely new ways to deploy nanoparticles, for example electrochemically within seconds at electrodes, or to reshape and boost their activity, while preserving their arrangement. Depending on the defect chemistry of the support exsolved nanoparticles can also be re-dissolved in the parent support and subsequently re-exsolved to rejuvenate the structure.

These functionalities, uniquely brought about by exsolution become even more diverse and useful technologically when considering them in tandem with the support. One of the most extensively used families of supports for exsolution have been perovskites oxides, owing to flexibility with which they can accommodate various element substitution, as well as types of crystal defects required to control exsolution. At the same time, perovskites provide an avenue to electron and ion conductivity, often key requirements in energy materials and applications, which, together with the catalytic activity introduced through exsolution constitutes a powerful and versatile platform for designing advanced, multifunctional materials for a range of technologies. Current areas of application include fuel cells for power generation, electrolyzers for hydrogen and syngas production, as well as various catalytic or photo-catalytic materials for carbon dioxide utilisation, methane reforming, or chemical looping.

In this review, we examine the current status of exsolution, identify opportunities for cross-exchange of ideas between fields of application, new directions of research, as well as key milestones for advancing the concept to the next level and transitioning to more widespread application in relevant industries. Challenges identified span multiple scales, from formulating and formalising material design, to better tools for in situ or operando observation of the process and the resulting materials and devices during operation, to larger scale demonstrations in respective industries.

Since its inception, a decade ago, exsolution has advanced at an incredible pace, with a cadence of major breakthroughs in understanding, control or application demonstrations, every 1-2 years. This trend is expected to continue as it benefits from a rapidly growing researcher base, currently covering five continents, from very diverse career stage and research backgrounds, some of which we have the pleasure of enclosing in this review.

The last decade marked the transition of exsolved materials from the ‘stone age’ to the ‘nano age’ consolidating its position as a powerful nano-structuring platform. The next decade is likely to see a substantial drive to its application in clean energy solutions and net zero, thus probably the next decade in exsolution research will likely be the ‘energy age’.

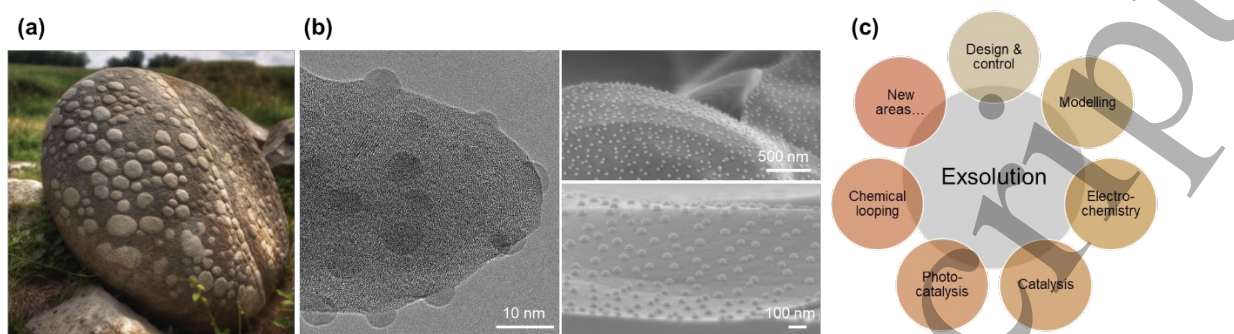


Figure 1 - Exsolution from the ‘stone age’ to the ‘nano age’.

(a) Example of exsolution process occurring naturally in rock formations (Copyright: Dragos Neagu). (b) Examples of exsolution at the nanoscale enabled by control of support crystal defect chemistry (Copyright: Dragos Neagu and John Irvine). (c) Overview of the main topics of the current Roadmap, from design, control and modelling to multiple areas of application in electrochemical and catalytic energy conversion.

## Section 1 - Understanding and tuning point defects in the host oxides to control exsolved nanoparticles

Jiayue Wang<sup>1</sup> and Bilge Yildiz<sup>1,2</sup>

<sup>1</sup>Dept. of Nuclear Science and Engineering, Massachusetts Institute of Technology, Cambridge, MA, USA

<sup>2</sup>Dept. of Materials Science and Engineering, Massachusetts Institute of Technology, Cambridge, MA, USA

### 1.1 Status

A recent advance in materials for electrochemical energy and fuels conversion is to synthesize self-assembled metal nanoparticle catalysts via “exsolution”<sup>1-4</sup>. While exsolution is an exciting and promising method, precise control over the exsolved particles has yet to be achieved. Therefore, an ability to control the morphology and composition of the exsolution particles is critical to implement this technique for the design of nanostructured catalysts. Recent studies have suggested that point defects in the host oxide can be a fundamental knob to tailor exsolution both thermodynamically and kinetically. In this paper, we review the recent studies in elucidating the role of point defects in tailoring exsolution, and also the efforts thus far to engineer material’s defect chemistry to rationally engineer the exsolution process.

### 1.2 Current and Future Challenges

In heterogeneous catalysis, it has been generally observed that the catalytic performance of metal particles increases with decreasing particle sizes<sup>5</sup>. For example, the intrinsic catalytic activities of Au nanoparticles towards CO oxidation were observed to be greatly enhanced at sub-10nm particle sizes<sup>6</sup>. Therefore, exsolving nanoparticles with ever smaller sizes and higher densities is desirable. However, as the exsolution process often requires long-time reduction at elevated temperatures, it typically produces 10s nm metal nanoparticles<sup>7-10</sup>. While the obtained improvement in reaction kinetics is already promising, we believe that “there is plenty of room at the bottom”. To realize the few atom

1  
2  
3 cluster limits for the exsolved catalysts, one has to be able to control the nucleation process in  
4 exsolution<sup>11</sup>, through the underlying mechanisms.

5  
6 Point defect formation in the host oxide has been recently proposed as an effective approach to  
7 tailor exsolution, both thermodynamically and kinetically<sup>12,13</sup>. First, since exsolution is a partial  
8 decomposition process, it is associated with the formation of point defects in the host oxide (such as  
9 oxygen and cation vacancies, see **Figure 1a**). Therefore, facilitating point defect formation in the host  
10 oxide should promote exsolution thermodynamically. For example, both anion and cation deficiencies  
11 in the host oxide have been observed to assist nanoparticle exsolution<sup>13-15</sup>. Second, based on previous  
12 studies on metal particle nucleation on binary oxides<sup>16,17</sup>, point defects (such as oxygen vacancies) on  
13 oxide surfaces may serve as preferential nucleation sites for the exsolved metal nanoparticles.  
14 Therefore, by carefully tuning the defect chemistry of the host oxide, one might be able to increase  
15 the nanoparticle density and dispersion<sup>18</sup> by modulating the process nucleation process.

16  
17  
18  
19  
20 One major challenge thus far in applying defect engineering in exsolution is to link the microscopic  
21 point defect formation and the macroscopic nanoparticle exsolution. Experimentally, it has been  
22 challenging to isolate point defect contributions from other experimental parameters. Most studies  
23 to date focused on screening host oxides with different compositions to examine the exsolution  
24 process as a function of defect concentration<sup>13,15</sup>. However, variation in the host oxide compositions  
25 may also introduce other degrees of uncertainties, such as the solubility difference<sup>19,20</sup>. This  
26 complexity thus requires carefully designed experiments to decouple point defect formation from  
27 other compositional effects on exsolution. Computationally, it has been challenging to identify the key  
28 defect structure that facilitates the nucleation of the exsolved nanoparticles. Today, a majority of  
29 studies have used the surface cation segregation energy as a descriptor to understand the exsolution  
30 mechanism as well as to screen optimal materials for exsolution<sup>15,21-23</sup>. Nevertheless, it remains  
31 unclear as to how the defect structure and concentration affect the nucleation process in exsolution.  
32 To make things more complicated, recent studies have revealed that the host oxide surface can  
33 undergo drastic structural evolution during exsolution<sup>11,24</sup>. The challenges described above thus call  
34 for novel experimental and computational approaches in understanding and tuning the defect-  
35 mediated exsolution process.

### 41 42 **1.3 Advances in Science and Technology to Meet Challenges**

#### 43 **Combining theory and experiment to uncover point-defect-mediated nucleation in exsolution.**

44  
45 As discussed earlier, gaining a deeper understanding of the nucleation process in exsolution is critical  
46 for precise control over the size and density of exsolved nanoparticles toward optimal catalytic activity.  
47 For exsolution on polycrystalline samples, the resulting nanoparticle density is often in the range of  
48  $10^9 - 10^{10} \text{ cm}^{-2}$  (**Figure 1b**)<sup>25-27</sup>. Intriguingly, recent studies found that exsolution on single-crystalline  
49 thin films can generate nanoparticles with densities larger than  $10^{11} \text{ cm}^{-2}$  (**Figure 1c**)<sup>12,28</sup>, which is more  
50 desirable for (electro)catalysis. Therefore, there is a huge motivation for researchers to understand  
51 the nucleation mechanism on single-crystalline materials that can produce a higher particle density,  
52 and come up with rational design principles to boost exsolution on polycrystalline materials.

53  
54  
55  
56  
57 In a recent effort, Wang and Yildiz et al. investigated the Fe<sup>0</sup> nanoparticle nucleation process on  
58 an atomically smooth, (001)-oriented epitaxial La<sub>0.6</sub>Sr<sub>0.4</sub>FeO<sub>3</sub> (LSF) thin film and found that the high  
59 density of exsolved nanoparticles on single-crystalline thin films is due to point-defect-mediated  
60

1  
2  
3 nucleation. As shown in **Figure 1c**, the exsolved Fe<sup>0</sup> nanoparticles on the LSF surface are uniformly  
4 distributed on the terraces, with no preference for the step edges. This characteristic suggests that  
5 point defects at the surface are more favorable for nanoparticle nucleation and growth than step  
6 edges<sup>16,17</sup>. To identify the critical surface defect structure that governs the nanoparticle nucleation,  
7 Monte Carlo (MC) simulations were used to model the surface concentrations of isolated oxygen  
8 vacancies, oxygen vacancy pairs, and large oxygen vacancy clusters on the (001)-oriented LSF surface.  
9 As shown in **Figure 1d**, the surface Fe<sup>0</sup> nanoparticle density agrees well within the range of the surface  
10 oxygen vacancy pairs. On the other hand, the calculated density of both the isolated oxygen vacancy  
11 and large vacancy clusters are around three orders of magnitude off compared to the particle density.  
12 This comparison delivers strong evidence that the surface oxygen vacancy pairs are the likely  
13 nucleation center for Fe<sup>0</sup> nanoparticle exsolution. In support of this mechanism, density functional  
14 theory (DFT) calculation further confirms that surface oxygen vacancy pairs are the more favorable  
15 sites for Fe adatoms and Fe dimers on the LSF surface, compared to the isolated oxygen vacancy sites<sup>12</sup>.  
16 These findings thus suggest that promoting point-defect-mediated nucleation can be the key to  
17 realizing high particle density in the exsolution process, which calls for approaches to effectively tailor  
18 the defect chemistry in host oxides. We will discuss this topic in the next section.  
19  
20  
21  
22  
23  
24  
25  
26  
27  
28  
29  
30  
31  
32  
33  
34  
35  
36  
37  
38  
39  
40  
41  
42  
43  
44  
45  
46  
47  
48  
49  
50  
51  
52  
53  
54  
55  
56  
57  
58  
59  
60

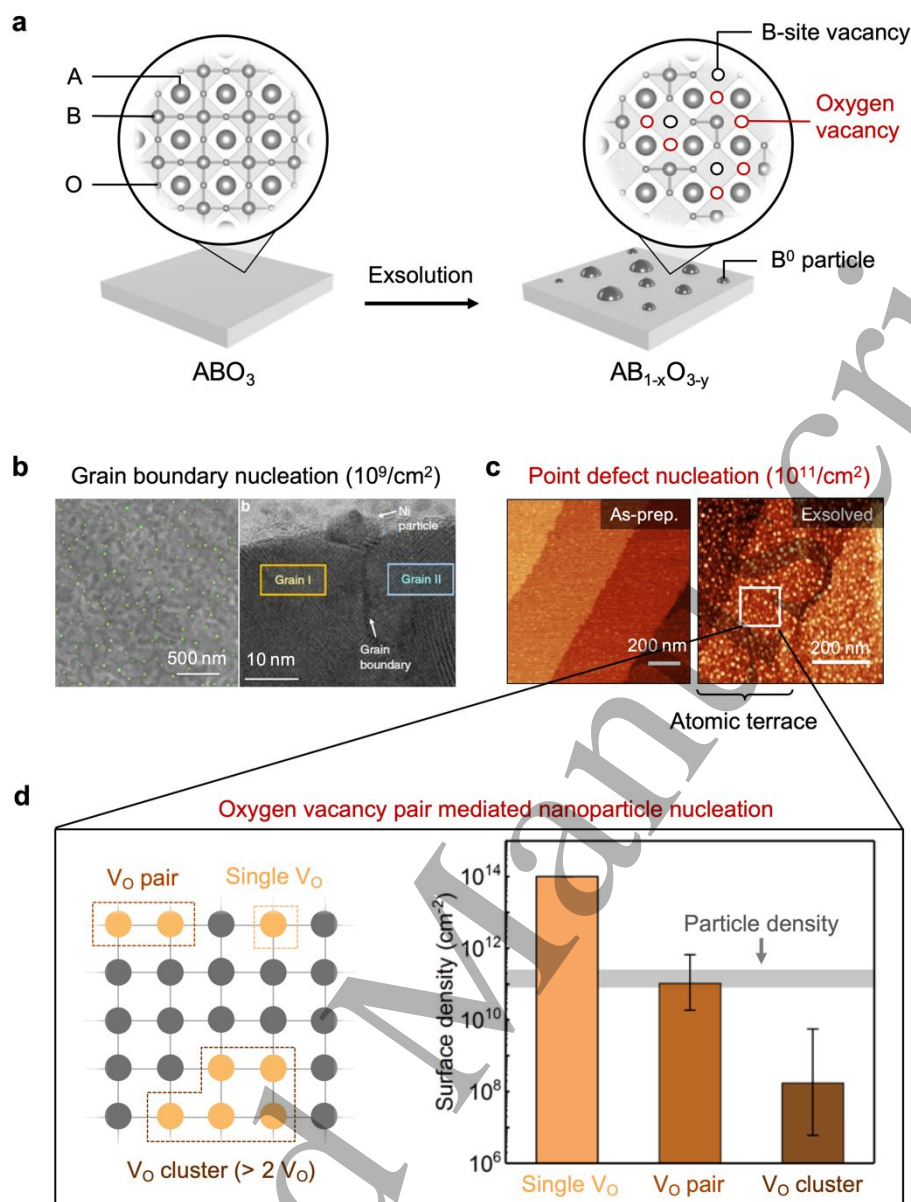


**Figure 1 Identifying the role of point defects in nanoparticle exsolution.** (a) Schematics of the exsolution process on the surface of perovskite (ABO<sub>3</sub>) materials. Besides the formation of B<sup>0</sup> nanoparticles, exsolution also generates both B-site and oxygen vacancies in perovskites. (b-c) Comparison between the exsolved nanoparticles that are exsolved (b) at grain boundaries of Sm-doped CeO<sub>2</sub><sup>26</sup> and (c) at point defects on the surface of atomic-flat La<sub>0.6</sub>Sr<sub>0.4</sub>FeO<sub>3</sub> (LSF) thin films<sup>12</sup>. Note that the point-defect-mediated nucleation results in much higher particle density. (d) Monte Carlo simulation showing the correlation between the surface density of oxygen vacancy pairs and that of the exsolved nanoparticles on the LSF surface<sup>12</sup>. These results suggest surface oxygen vacancy pairs are the likely nucleation center for the exsolved nanoparticles. Figure 1b is reproduced with permission from ref. <sup>26</sup>, Copyright 2018, Nature Publishing Group. Figures c,d are adapted with permission from ref. <sup>12</sup>. Copyright 2021 American Chemical Society.



1  
2  
3  
4 **Tuning defect chemistry with external stimuli to control exsolution.** One recent advance in  
5 exsolution is to use external stimuli (such as lattice strain<sup>29</sup>, oxygen chemical potential<sup>30</sup>, electrical  
6 polarization<sup>31</sup>, and photo-illumination<sup>32</sup>) to tailor the concentration and stability of point defects in  
7 the host oxide, and thus control the morphology of the exsolved nanoparticles. The major advantage  
8 of using external stimuli is that it provides another degree of freedom in tailoring the defect chemistry  
9 in materials, beyond the nominal host oxide composition. As such, one can tailor the defect chemistry  
10 after the materials/devices have already been synthesized, and introduce dynamic modulation under  
11 operational conditions<sup>33,34</sup>. Moreover, as discussed earlier, such dopant-free method is also ideal for  
12 fundamental studies in elucidating the role of point defects in modulating exsolution.  
13  
14

15  
16 Elastic lattice strain has been widely explored to tailor exsolution<sup>12,28,35</sup>. For example, Wang *et al.*<sup>12</sup>  
17 and Kim *et al.*<sup>35</sup> reported tensile strain to promote metal exsolution in  $\text{La}_{0.6}\text{Sr}_{0.4}\text{FeO}_3$  (LSF) and  
18  $\text{SrTi}_{0.75}\text{Co}_{0.25}\text{O}_3$  (STC), respectively. On the contrary, Han *et al.*<sup>28</sup> found that compressive strain is  
19 favorable for Ni exsolution in  $\text{La}_{0.2}\text{Sr}_{0.7}\text{Ti}_{0.9}\text{Ni}_{0.1}\text{O}_3$  (LSTN). These seemingly contradictory observations  
20 can be reconciled in terms of strain-mediated point defect formation. That is, the favored strain  
21 direction to promote nanoparticle exsolution is the one that favors the formation of point defects in  
22 the host oxides<sup>12</sup>. Take LSF as an example (**Figure 2c**), first principles calculation shows that biaxial  
23 tensile strain facilitates the formation of both oxygen vacancy and Schottky defects (i.e., the two  
24 primary point defects associated with exsolution) in LSF<sup>12</sup>. In accordance with the strain-dependent  
25 defect formation, it was also found that the tensile-strained LSF demonstrated enhanced exsolution  
26 phenomena, with an increased amount of total exsolved  $\text{Fe}^0$ , smaller particle size, and higher particle  
27 density<sup>12</sup>. On the other hand, the exsolution on the compressive-strained LSF surface is suppressed  
28 (**Figure 2c**).  
29  
30  
31  
32

33  
34 In addition to strain, researchers have also explored other types of external stimuli to promote  
35 and control exsolution via defect engineering, such as electrochemical polarization<sup>36</sup>, radiation<sup>37</sup>, and  
36 thermal shock<sup>38</sup> (**Figure 2c**). For electrochemical methods, Myung *et al.* have shown that by using  
37 electrochemical reduction, the voltage-exsolved nanoparticles can have higher particle densities,  
38 smaller particle sizes, and hence higher catalytic activities than the conventional thermally exsolved  
39 nanoparticles<sup>36</sup>. Opitz *et al.* have furthered used electrochemical biasing to realize reversible control  
40 of exsolution, which has implications on controllably tailoring materials'  $\text{H}_2\text{O}$  splitting kinetics<sup>33</sup>.  
41 Regarding irradiation, Kyriakou *et al.* employed  $\text{N}_2$  plasma treatment to facilitate exsolution, and  
42 found that the plasma-assisted exsolution can generate Ni nanoparticles that have up to ten times  
43 higher particle density compared to thermal chemical exsolution<sup>37</sup>. Recently, Khalid *et al.* have  
44 leveraged argon plasma treatment to promote Ni exsolution out of  $\text{La}_{0.43}\text{Ca}_{0.37}\text{Ti}_{0.94}\text{Ni}_{0.06}\text{O}_{2.955}$  (LCTN)  
45 at room temperature<sup>39</sup>. Finally, in terms of thermal control of exsolution, Sun *et al.* have utilized  
46 ultrafast thermal annealing (i.e., thermal shock) to promote exsolution<sup>38</sup>. As a result, they found that  
47 the exsolved nanoparticles produced by thermal shock have significantly higher particle density and  
48 reduced particle size, as compared to the conventional furnace-based exsolution. The aforementioned  
49 exciting phenomena clearly demonstrate that modulating defect chemistry from external stimuli can  
50 play a critical role in enabling novel exsolution modulation.  
51  
52  
53  
54  
55  
56  
57  
58  
59  
60

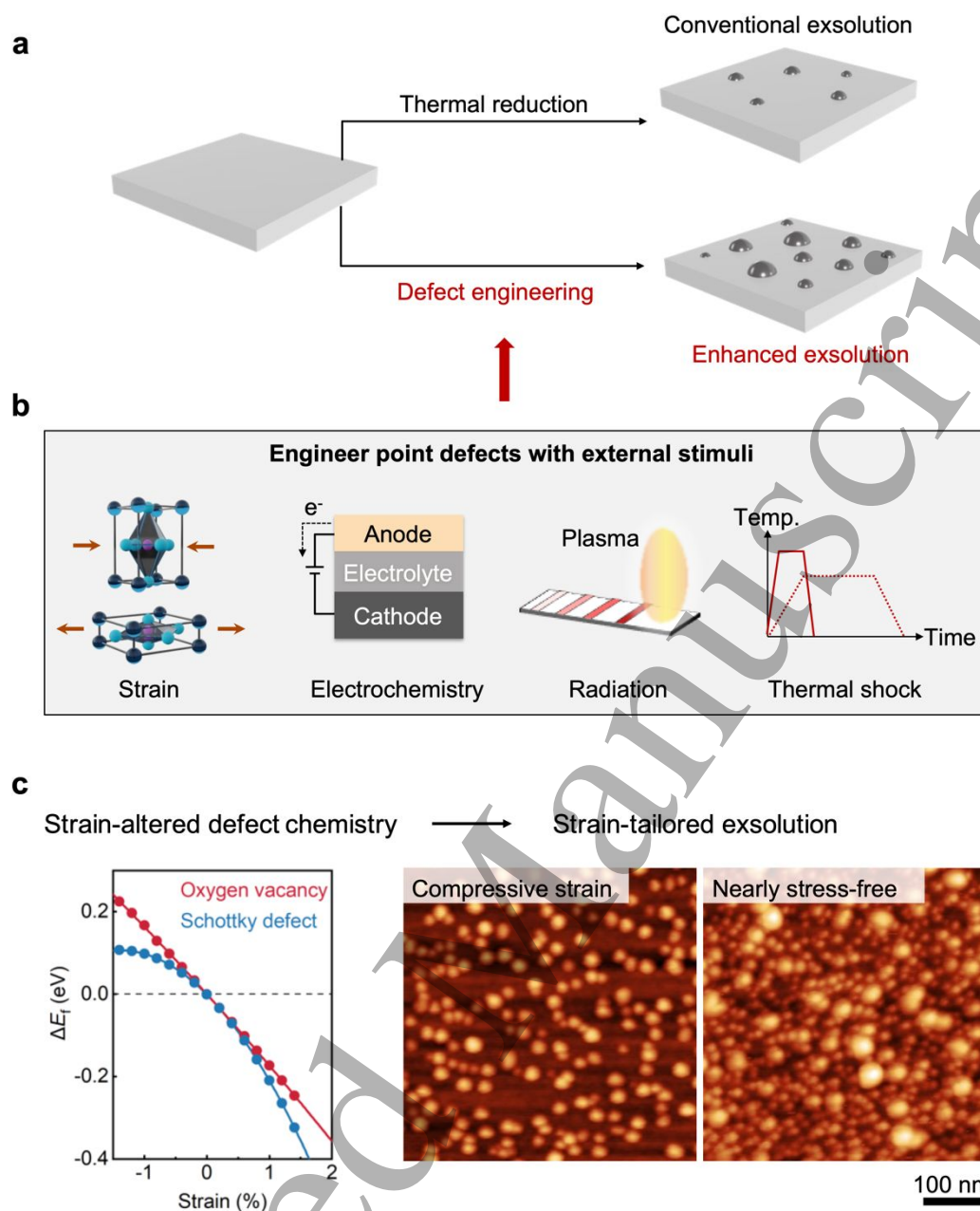


**Figure 2 - Tailoring exsolution via external stimuli mediated defect formation.** (a) Schematics of promoting nanoparticle exsolution via defect engineering. (b) Schematics of external stimuli that have been used in literature to promote exsolution, which include lattice strain, electrochemical polarization, plasma treatment, and thermal shock. (c) Example of using lattice strain to tailor nanoparticle exsolution in LSF. Left figure: Density functional theory calculation showing the strain-dependent point defect formation, where tensile strain promotes both oxygen vacancy and Schottky defect formation in LSF. Right figure: AFM images showing the strain-dependent exsolution, where compressive strain suppresses  $\text{Fe}^3$  exsolution in LSF. The figures are adapted with permission from ref. <sup>12</sup>. Copyright 2021 American Chemical Society.

#### 1.4 Concluding Remarks

In summary, point defects play a crucial role in determining the exsolution products both thermodynamically and kinetically. As a result, tuning point defects in the host oxide via external

stimuli (such as strain, electric field, oxygen chemical potential, and radiation) can be an effective approach to optimize the size and density of the exsolved nano-catalysts. To enable rational defect engineering, further studies are required to illustrate the detailed exsolution mechanism. Therefore, a combination of *in-situ/operando* characterization (such as near ambient pressure XPS<sup>34</sup>, environmental TEM<sup>40</sup>, and grazing incident X-ray scattering<sup>33</sup>) and multiscale modeling (such as first-principles calculation<sup>41</sup>, Monte Carlo simulation<sup>12</sup>, and phase-field modeling<sup>42</sup>) are suggested for the future studies to establish the precise defect structure-property relationship in exsolution.

### 1.5 Acknowledgements

The authors thank the OxEon Corporation for supporting this work.

### 1.6 References

- 1 Nishihata, Y. *et al.* Self-regeneration of a Pd-perovskite catalyst for automotive emissions control. *Nature* **418**, 164-167 (2002). <https://doi.org:10.1038/nature00893>
- 2 Neagu, D. *et al.* Nano-socketed nickel particles with enhanced coking resistance grown in situ by redox exsolution. *Nature Communications* **6**, 8120 (2015). <https://doi.org:10.1038/ncomms9120>
- 3 Kousi, K., Tang, C., Metcalfe, I. S. & Neagu, D. Emergence and Future of Exsolved Materials. *Small* **17**, 2006479 (2021). <https://doi.org:https://doi.org/10.1002/sml.202006479>
- 4 Kim, J. H. *et al.* Nanoparticle Ex-solution for Supported Catalysts: Materials Design, Mechanism and Future Perspectives. *ACS Nano* **15**, 81-110 (2021). <https://doi.org:10.1021/acsnano.0c07105>
- 5 Yang, X.-F. *et al.* Single-Atom Catalysts: A New Frontier in Heterogeneous Catalysis. *Accounts of Chemical Research* **46**, 1740-1748 (2013). <https://doi.org:10.1021/ar300361m>
- 6 Haruta, M. Size- and support-dependency in the catalysis of gold. *Catalysis Today* **36**, 153-166 (1997). [https://doi.org:https://doi.org/10.1016/S0920-5861\(96\)00208-8](https://doi.org:https://doi.org/10.1016/S0920-5861(96)00208-8)
- 7 Jo, Y.-R. *et al.* Growth Kinetics of Individual Co Particles Ex-solved on SrTi<sub>0.75</sub>Co<sub>0.25</sub>O<sub>3-δ</sub> Polycrystalline Perovskite Thin Films. *Journal of the American Chemical Society* **141**, 6690-6697 (2019). <https://doi.org:10.1021/jacs.9b01882>
- 8 Kobsiriphat, W. *et al.* Nickel- and Ruthenium-Doped Lanthanum Chromite Anodes: Effects of Nanoscale Metal Precipitation on Solid Oxide Fuel Cell Performance. *Journal of The Electrochemical Society* **157**, B279 (2010). <https://doi.org:10.1149/1.3269993>

- 1  
2  
3  
4 9 Wang, Y. *et al.* Exsolved Fe–Ni nano-particles from Sr<sub>2</sub>Fe<sub>1.3</sub>Ni<sub>0.2</sub>Mo<sub>0.5</sub>O<sub>6</sub>  
5 perovskite oxide as a cathode for solid oxide steam electrolysis cells. *Journal of*  
6 *Materials Chemistry A* **4**, 14163-14169 (2016). <https://doi.org:10.1039/C6TA06078A>  
7  
8  
9 10 Götsch, T. *et al.* Crystallographic and electronic evolution of lanthanum strontium  
11 ferrite (La<sub>0.6</sub>Sr<sub>0.4</sub>FeO<sub>3-δ</sub>) thin film and bulk model systems during iron exsolution.  
12 *Physical Chemistry Chemical Physics* **21**, 3781-3794 (2019).  
13 <https://doi.org:10.1039/C8CP07743F>  
14  
15 11 Neagu, D. *et al.* In Situ Observation of Nanoparticle Exsolution from Perovskite  
16 Oxides: From Atomic Scale Mechanistic Insight to Nanostructure Tailoring. *ACS Nano*  
17 **13**, 12996-13005 (2019). <https://doi.org:10.1021/acsnano.9b05652>  
18  
19 12 Wang, J. *et al.* Tuning Point Defects by Elastic Strain Modulates Nanoparticle  
20 Exsolution on Perovskite Oxides. *Chemistry of Materials* **33**, 5021-5034 (2021).  
21 <https://doi.org:10.1021/acs.chemmater.1c00821>  
22  
23 13 Neagu, D., Tsekouras, G., Miller, D. N., Ménard, H. & Irvine, J. T. S. In situ growth of  
24 nanoparticles through control of non-stoichiometry. *Nature Chemistry* **5**, 916-923  
25 (2013). <https://doi.org:10.1038/nchem.1773>  
26  
27 14 Sun, Y.-F. *et al.* New Opportunity for in Situ Exsolution of Metallic Nanoparticles on  
28 Perovskite Parent. *Nano Letters* **16**, 5303-5309 (2016).  
29 <https://doi.org:10.1021/acs.nanolett.6b02757>  
30  
31 15 Kwon, O. *et al.* Exsolution trends and co-segregation aspects of self-grown catalyst  
32 nanoparticles in perovskites. *Nature Communications* **8**, 15967 (2017).  
33 <https://doi.org:10.1038/ncomms15967>  
34  
35 16 Bäumer, M. *et al.* Nucleation and growth of transition metals on a thin alumina film.  
36 *Surface Science* **454-456**, 957-962 (2000).  
37 [https://doi.org:https://doi.org/10.1016/S0039-6028\(00\)00255-7](https://doi.org:https://doi.org/10.1016/S0039-6028(00)00255-7)  
38  
39 17 Haas, G. *et al.* Nucleation and growth of supported clusters at defect sites:  
40 Pd/MgO(001). *Physical Review B* **61**, 11105-11108 (2000).  
41 <https://doi.org:10.1103/physrevb.61.11105>  
42  
43 18 Thanh, N. T. K., Maclean, N. & Mahiddine, S. Mechanisms of Nucleation and Growth  
44 of Nanoparticles in Solution. *Chemical Reviews* **114**, 7610-7630 (2014).  
45 <https://doi.org:10.1021/cr400544s>  
46  
47 19 Yanagisawa, S., Uozumi, A., Hamada, I. & Morikawa, Y. Search for a Self-  
48 Regenerating Perovskite Catalyst Using ab Initio Thermodynamics Calculations. *The*  
49  
50  
51  
52  
53  
54  
55  
56  
57  
58  
59  
60

- 1  
2  
3  
4 *Journal of Physical Chemistry C* **117**, 1278-1286 (2013).  
5 <https://doi.org:10.1021/jp305392x>  
6
- 7 20 Tanaka, H. *et al.* Self-Regenerating Rh- and Pt-Based Perovskite Catalysts for  
8 Automotive-Emissions Control. *Angewandte Chemie International Edition* **45**, 5998-  
9 6002 (2006). <https://doi.org:https://doi.org/10.1002/anie.200503938>  
10
- 11 21 Hamada, I., Uozumi, A., Morikawa, Y., Yanase, A. & Katayama-Yoshida, H. A  
12 Density Functional Theory Study of Self-Regenerating Catalysts  $\text{LaFe}_{1-x}\text{M}_x\text{O}_{3-y}$  (M  
13 = Pd, Rh, Pt). *Journal of the American Chemical Society* **133**, 18506-18509 (2011).  
14 <https://doi.org:10.1021/ja110302t>  
15
- 16 22 Tian, Z.-x. *et al.* First-principles investigation on the segregation of Pd at  $\text{LaFe}_{1-x}\text{Pd}_x\text{O}_{3-y}$   
17 surfaces. *Nanoscale Research Letters* **8**, 203 (2013).  
18 <https://doi.org:10.1186/1556-276X-8-203>  
19
- 20 23 Gao, Y. *et al.* Energetics of Nanoparticle Exsolution from Perovskite Oxides. *The*  
21 *Journal of Physical Chemistry Letters* **9**, 3772-3778 (2018).  
22 <https://doi.org:10.1021/acs.jpcllett.8b01380>  
23
- 24 24 Wang, J. *et al.* Exsolution-Driven Surface Transformation in the Host Oxide. *Nano*  
25 *Letters* **22**, 5401-5408 (2022). <https://doi.org:10.1021/acs.nanolett.2c01439>  
26
- 27 25 Nenning, A. *et al.* The Electrochemical Properties of  $\text{Sr}(\text{Ti,Fe})\text{O}_{3-\delta}$  for Anodes in Solid  
28 Oxide Fuel Cells. *Journal of The Electrochemical Society* **164**, F364-F371 (2017).  
29 <https://doi.org:10.1149/2.1271704jes>  
30
- 31 26 Kwak, N. W. *et al.* In situ synthesis of supported metal nanocatalysts through  
32 heterogeneous doping. *Nature Communications* **9**, 4829 (2018).  
33 <https://doi.org:10.1038/s41467-018-07050-y>  
34
- 35 27 Zhu, T., Troiani, H. E., Moggi, L. V., Han, M. & Barnett, S. A. Ni-Substituted  
36  $\text{Sr}(\text{Ti,Fe})\text{O}_3$  SOFC Anodes: Achieving High Performance via Metal Alloy  
37 Nanoparticle Exsolution. *Joule* **2**, 478-496 (2018).  
38 <https://doi.org:10.1016/j.joule.2018.02.006>  
39
- 40 28 Han, H. *et al.* Lattice strain-enhanced exsolution of nanoparticles in thin films. *Nature*  
41 *Communications* **10**, 1471 (2019). <https://doi.org:10.1038/s41467-019-09395-4>  
42
- 43 29 Aschauer, U., Pfenninger, R., Selbach, S. M., Grande, T. & Spaldin, N. A. Strain-  
44 controlled oxygen vacancy formation and ordering in  $\text{CaMnO}_3$ . *Physical Review B* **88**,  
45 054111 (2013). <https://doi.org:10.1103/PhysRevB.88.054111>  
46  
47  
48  
49  
50  
51  
52  
53  
54  
55  
56  
57  
58  
59  
60

- 1  
2  
3  
4 30 Chen, D. & Tuller, H. L. Voltage-Controlled Nonstoichiometry in Oxide Thin Films:  
5 Pr<sub>0.1</sub>Ce<sub>0.9</sub>O<sub>2-δ</sub> Case Study. *Advanced Functional Materials* **24**, 7638-7644 (2014).  
6 [https://doi.org:https://doi.org/10.1002/adfm.201402050](https://doi.org/https://doi.org/10.1002/adfm.201402050)  
7  
8  
9 31 Youssef, M., Van Vliet, K. J. & Yildiz, B. Polarizing Oxygen Vacancies in Insulating  
10 Metal Oxides under a High Electric Field. *Physical Review Letters* **119**, 126002 (2017).  
11 <https://doi.org/10.1103/PhysRevLett.119.126002>  
12  
13 32 Chen, Z. *et al.* Organic Photochemistry-Assisted Nanoparticle Segregation on  
14 Perovskites. *Cell Reports Physical Science*, 100243 (2020).  
15 [https://doi.org:https://doi.org/10.1016/j.xcrp.2020.100243](https://doi.org/https://doi.org/10.1016/j.xcrp.2020.100243)  
16  
17 33 Opitz, A. K. *et al.* Understanding electrochemical switchability of perovskite-type  
18 exsolution catalysts. *Nature Communications* **11**, 4801 (2020).  
19 <https://doi.org/10.1038/s41467-020-18563-w>  
20  
21 34 Opitz, A. K. *et al.* Enhancing Electrochemical Water-Splitting Kinetics by Polarization-  
22 Driven Formation of Near-Surface Iron(0): An In Situ XPS Study on Perovskite-Type  
23 Electrodes. *Angewandte Chemie International Edition* **54**, 2628-2632 (2015).  
24 <https://doi.org/10.1002/anie.201409527>  
25  
26 35 Kim, K. *et al.* Control of transition metal–oxygen bond strength boosts the redox ex-  
27 solution in a perovskite oxide surface. *Energy & Environmental Science* (2020).  
28 <https://doi.org/10.1039/D0EE01308K>  
29  
30 36 Myung, J.-h., Neagu, D., Miller, D. N. & Irvine, J. T. S. Switching on electrocatalytic  
31 activity in solid oxide cells. *Nature* **537**, 528-531 (2016).  
32 <https://doi.org/10.1038/nature19090>  
33  
34 37 Kyriakou, V. *et al.* Plasma Driven Exsolution for Nanoscale Functionalization of  
35 Perovskite Oxides. *Small Methods* **5**, 2100868 (2021).  
36 [https://doi.org:https://doi.org/10.1002/smt.202100868](https://doi.org/https://doi.org/10.1002/smt.202100868)  
37  
38 38 Sun, Z., Fan, W. & Bai, Y. A Flexible Method to Fabricate Exsolution-Based  
39 Nanoparticle-Decorated Materials in Seconds. *Advanced Science* **9**, 2200250 (2022).  
40 [https://doi.org:https://doi.org/10.1002/advs.202200250](https://doi.org/https://doi.org/10.1002/advs.202200250)  
41  
42 39 Khalid, H. *et al.* Rapid Plasma Exsolution from an A-site Deficient Perovskite Oxide at  
43 Room Temperature. *Advanced Energy Materials* **12**, 2201131 (2022).  
44 [https://doi.org:https://doi.org/10.1002/aenm.202201131](https://doi.org/https://doi.org/10.1002/aenm.202201131)  
45  
46 40 Lv, H. *et al.* In Situ Investigation of Reversible Exsolution/Dissolution of CoFe Alloy  
47 Nanoparticles in a Co-Doped Sr<sub>2</sub>Fe<sub>1.5</sub>Mo<sub>0.5</sub>O<sub>6-δ</sub> Cathode for CO<sub>2</sub> Electrolysis.  
48 *Advanced Materials* **32**, 1906193 (2020). <https://doi.org/10.1002/adma.201906193>  
49  
50  
51  
52  
53  
54  
55  
56  
57  
58  
59  
60

- 1  
2  
3  
4 41 Raman, A. S. & Vojvodic, A. Modeling Exsolution of Pt from ATiO<sub>3</sub> Perovskites (A  
5 = Ca/Sr/Ba) Using First-Principles Methods. *Chemistry of Materials* **32**, 9642-9649  
6 (2020). <https://doi.org:10.1021/acs.chemmater.0c03260>  
7  
8 42 Jiang, G., Yan, F., Wan, S., Zhang, Y. & Yan, M. Microstructure evolution and kinetics  
9 of B-site nanoparticle exsolution from an A-site-deficient perovskite surface: a phase-  
10 field modeling and simulation study. *Physical Chemistry Chemical Physics* **21**, 10902-  
11 10907 (2019). <https://doi.org:10.1039/C8CP07883A>  
12  
13  
14  
15  
16  
17  
18  
19  
20  
21  
22  
23  
24

## Section 2 - Understanding electrochemical exsolution through *in-situ* studies

Alexander K. Opitz and Jürgen Fleig

TU Wien, Institute of Chemical Technologies and Analytics, Vienna, Austria

### 2.1 Status

When exsolution of reducible transition metals from perovskite-type oxides was discovered as a novel way for preparing oxide supported metal particles, the obtained catalysts were typically studied by *ex-situ* techniques. With the growing interest for a basic understanding of the exsolution processes and of materials changes during operation, this highly promising catalyst type was more and more investigated also under *in-situ* conditions. This is particularly important because the particles obtained *via* an exsolution process are commonly very small (some nm) and in case of non-noble metals also highly prone to oxidation. Transfer of an exsolution catalyst from the gas phase and temperature where formation has taken place to any *ex-situ* analytical instrument can thus irreversibly alter the metal particles. *In-situ* characterization allows avoiding this problem and, moreover, can reveal time dependent changes of the catalyst. However, the term "*in-situ*" refers to different characterization approaches that should be distinguished here.

On the one hand, the catalytic performance increase upon exsolution can be monitored *in-situ*, which means that the rate of a reaction proceeding on the surface of the respective perovskite-type catalyst is tracked while the exsolution process itself occurs. This can be done either by measuring the amount of an expected product in a gas stream<sup>[1-4]</sup>, or – if the exsolution catalyst was employed as an electrode in a solid oxide electrochemical cell – by recording the current passing through this cell upon applying a bias voltage (see Fig. 1)<sup>[5-12]</sup>.

On the other hand, the chemical, crystallographic, compositional, and morphological state of the exsolution particles (as well as of the parent matrix) can be tracked during particle formation and during catalyst operation. Here, different tools come into play as also illustrated in Fig. 1. First, the

appearance of metal particles and their changes can be studied *in-situ* with X-ray diffraction (XRD) during the abovementioned chemical or electrochemical reactions<sup>[1,2,7,13–15]</sup>. Second, spectroscopic approaches such as X-ray photoelectron spectroscopy (AP-XPS) and X-ray absorption spectroscopy (XAS) are used to study the exsolution of metal particles from their perovskite-type host oxide<sup>[6,16–20]</sup>. With both methods not only the formation of metal particles but also their reversible switching between reduced and oxidized state can be investigated<sup>[6,7]</sup>. The third and latest development visualizes the exsolution process from the very first moment of nucleation by *in-situ* transmission electron microscopy (TEM)<sup>[13,21]</sup>. This helped gaining deep insights into the very first seconds of an exsolution particle's life.

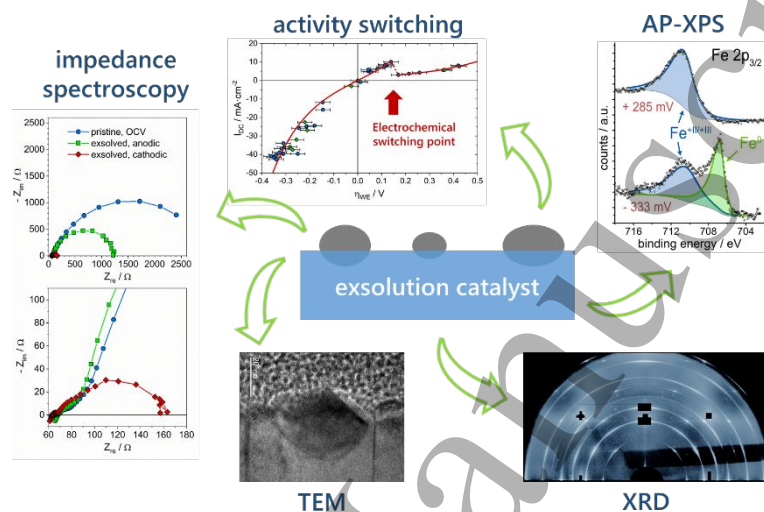


Figure 1 - Illustration of different results obtained by *in-situ* measurements on the model type exsolution catalyst  $\text{La}_{0.6}\text{Sr}_{0.4}\text{FeO}_{3-\delta}$  with exsolved iron particles decorating its surface.

## 2.2 Current and Future Challenges

Some challenges for *in-situ* characterization of exsolved particles arise from an extension of the scope in this field. Initially, exsolution was used as a method to prepare catalyst particles with superior properties on oxide surfaces. More recently, the possibility of preparing bulk exsolutions (also called endo-particles) came into focus. This allows obtaining self-assembled nano-composites with unprecedented structure and properties<sup>[18,22,23]</sup>. *In-situ* studying the evolution of these buried particles and the associated surrounding nanostructures, however, is still rather difficult.

For surface exsolution catalysts, the current research activities go into several directions. Reduction of particle size is desired and low temperature exsolution is a possible strategy to achieve this goal. In addition, alloy and dual phase exsolution is in the focus of interest. In those cases it is very important to know the achievable particle size, composition, oxidation state, and crystallographic phase under the operating conditions of the catalyzed reaction. Especially for catalysis on bimetallic particles, such a knowledge is crucial, as the catalytic activity or selectivity for a particular product can depend sensitively on the composition of the exsolved alloy particles, and the same applies to changes in the crystallographic phase.



Another important topic to be understood is the mechanism of the electrochemical switching process of exsolution particles, which is particularly interesting, since it allows catalytic properties to be switched on and off by applying a voltage. The complexity of this question arises from the fact that two independent driving forces affect the oxidation state of the exsolved particles – the oxygen chemical potential  $\mu_{\text{O}}$  in the gas phase and  $\mu_{\text{O}}$  in the supporting oxide. In conventional exsolution catalysts these two chemical potentials are the same. However, in polarized oxides used as electrodes of electrochemical cells, the electrode overpotential can strongly shift  $\mu_{\text{O}}$  from its (gas) equilibrium value<sup>[24]</sup>, as oxide ions and electrons from the mixed conducting parent oxide are electrochemically pumped into or out of the particle. It is a mostly unknown interplay of kinetic steps (transport, reactions at surfaces and interfaces) that finally determine whether the gas or the oxide “wins” that game and how fast the corresponding changes take place. Achieving a fundamental understanding of this switching kinetics would enable tailored catalytic properties and could expand the application field of exsolution catalysts in electrochemical cells also to non-faradaic reactions. There, the reaction rate is no longer coupled to the current, and a voltage would only be needed to keep the particle in its desired (active or inactive) state.

### 2.3 Advances in Science and Technology to Meet Challenges

For at least three of the abovementioned challenges – endo-particle formation, alloy and dual-phase exsolution, as well as understanding the mechanism of electrochemical activity switching – *in-situ* TEM is expected to provide decisive insights for their deeper understanding, similar to heterogeneous catalysis, where this technique has been successfully contributing to a deeper understanding for some time.<sup>[25–28]</sup> In endo-particle, alloy, and dual-phase exsolution, *in-situ* TEM is essentially the logical continuation of previous efforts, as it is capable of virtually simultaneously providing information on morphology, chemical composition, and crystallographic phase. The combination of several other *in-situ* techniques may be an alternative or at least a very good supplement to *in-situ* TEM studies.

The goal of studying the mechanism of electrochemical activity switching raises the bar even higher. Here, not only a parent oxide with its exsolved particles needs to be studied, but an entire solid oxide electrochemical cell is required for being able to pump oxygen in and out of the surface particles. It is probably most promising to use thin film cells in current state-of-the-art *in-situ* TEM sample holders, though many challenges remain, such as performing the TEM experiments under defined atmosphere, elevated temperature and with applied electrochemical bias voltage. Expanding the limitations of other *in-situ* methods is also important. For example, *in-situ* XRD and XPS measurements with optimized time resolution can provide highly valuable additional information on the kinetics of electrochemical activity switching and on the origin of its hysteresis-like behavior<sup>[7]</sup>.

Substantial improvements could also be expected from adding other measurement techniques to the toolbox of *in-situ* studies, such as *in-situ* gravimetric measurements<sup>[29]</sup> under polarization or mapping phase changes by chemical capacitance changes during impedance studies. In addition to such sophisticated *in-situ* experiments, a better understanding of electrochemical switching also requires progress in modelling these processes. So far even the concepts for describing the kinetics of the electrochemical activity switching are not fully developed yet.

### 2.4 Concluding Remarks

With the growing interest in understanding the exsolution process on an atomistic level, the demand for analytical methods has strongly increased in recent years. Methods such as *in-situ* AP-XPS, XRD, and TEM have been successfully applied to reveal highly valuable insights into this topic. Among these methods *in-situ* TEM with all its analytical capabilities appears to be the most powerful, but also the most challenging characterization technique, to address the currently most important questions in the field of exsolutions. It is still a highly non-trivial task to apply these analytical tools also to the very small feature sizes of exsolved metal particles. Moreover, studying switchable exsolutions on electrodes of solid oxide cells requires implementation of model cells into current *in-situ* TEM sample holders and their operation during TEM experiments. Together with developing and implementing additional *in-situ* characterization tools this should lead to a major leap forward in understanding the redox behavior of switchable exsolution particles.

## 2.5 References

- [1] L. Lindenthal, R. Rameshan, H. Summerer, T. Ruh, J. Popovic, A. Nenning, S. Löffler, A. K. Opitz, P. Blaha, C. Rameshan, *Catalysts* **2020**, *10*, 268.
- [2] L. Lindenthal, J. Popovic, R. Rameshan, J. Huber, F. Schrenk, T. Ruh, A. Nenning, S. Löffler, A. K. Opitz, C. Rameshan, *Applied Catalysis B: Environmental* **2021**, *292*, 120183.
- [3] G. Dimitrakopoulos, A. F. Ghoniem, B. Yildiz, *Sustainable Energy Fuels* **2019**, *3*, 2347.
- [4] J. Oh, S. Joo, C. Lim, H. J. Kim, F. Ciucci, J.-Q. Wang, J. W. Han, G. Kim, *Angewandte Chemie International Edition* **2022**, *61*, e202204990.
- [5] L. Adjianto, V. B. Padmanabhan, R. J. Gorte, J. M. Vohs, *J. Electrochem. Soc.* **2012**, *159*, F751.
- [6] A. K. Opitz, A. Nenning, C. Rameshan, R. Rameshan, R. Blume, M. Hävecker, A. Knop-Gericke, G. Rupprechter, J. Fleig, B. Klötzer, *Angewandte Chemie International Edition* **2015**, *54*, 2628.
- [7] A. K. Opitz, A. Nenning, V. Vonk, S. Volkov, F. Bertram, H. Summerer, S. Schwarz, A. Steiger-Thirsfeld, J. Bernardi, A. Stierle, J. Fleig, *Nat Commun* **2020**, *11*, 4801.
- [8] J. Myung, D. Neagu, D. N. Miller, J. T. S. Irvine, *Nature* **2016**, *537*, 528.
- [9] G. Tsekouras, D. Neagu, J. T. S. Irvine, *Energy Environ. Sci.* **2013**, *6*, 256.
- [10] W. Kobsiriphat, B. D. Madsen, Y. Wang, M. Shah, L. D. Marks, S. A. Barnett, *J. Electrochem. Soc.* **2010**, *157*, B279.
- [11] T. Cao, O. Kwon, R. J. Gorte, J. M. Vohs, *Nanomaterials* **2020**, *10*, 2445.
- [12] T. Zhu, H. Troiani, L. V. Moggi, M. Santaya, M. Han, S. A. Barnett, *Journal of Power Sources* **2019**, *439*, 227077.
- [13] H. Lv, L. Lin, X. Zhang, Y. Song, H. Matsumoto, C. Zeng, N. Ta, W. Liu, D. Gao, G. Wang, X. Bao, *Advanced Materials* **2020**, *32*, 1906193.
- [14] O. Kwon, K. Kim, S. Joo, H. Y. Jeong, J. Shin, J. W. Han, S. Sengodan, G. Kim, *J. Mater. Chem. A* **2018**, *6*, 15947.
- [15] T. Götsch, L. Schlicker, M. F. Bekheet, A. Doran, M. Grünbacher, C. Praty, M. Tada, H. Matsui, N. Ishiguro, A. Gurlo, B. Klötzer, S. Penner, *RSC Advances* **2018**, *8*, 3120.
- [16] A. Nenning, A. K. Opitz, C. Rameshan, R. Rameshan, R. Blume, M. Hävecker, A. Knop-Gericke, G. Rupprechter, B. Klötzer, J. Fleig, *J. Phys. Chem. C* **2016**, *120*, 1461.
- [17] J. Wang, J. Yang, A. K. Opitz, W. Bowman, R. Bliem, G. Dimitrakopoulos, A. Nenning, I. Waluyo, A. Hunt, J.-J. Gallet, B. Yildiz, *Chem. Mater.* **2021**, *33*, 5021.
- [18] J. Wang, K. Syed, S. Ning, I. Waluyo, A. Hunt, E. J. Crumlin, A. K. Opitz, C. A. Ross, W. J. Bowman, B. Yildiz, *Advanced Functional Materials* **2022**, *32*, 2108005.
- [19] T. Götsch, N. Köpfle, M. Grünbacher, J. Bernardi, E. A. Carbonio, M. Hävecker, A. Knop-Gericke, M. F. Bekheet, L. Schlicker, A. Doran, A. Gurlo, A. Franz, B. Klötzer, S. Penner, *Phys. Chem. Chem. Phys.* **2019**, *21*, 3781.
- [20] J. Wang, A. Kumar, J. L. Wardini, Z. Zhang, H. Zhou, E. J. Crumlin, J. T. Sadowski, K. B. Woller, W. J. Bowman, J. M. LeBeau, B. Yildiz, *Nano Lett.* **2022**, *22*, 5401.
- [21] D. Neagu, V. Kyriakou, I.-L. Roiban, M. Aouine, C. Tang, A. Caravaca, K. Kousi, I. Schreur-Piet, I. S. Metcalfe, P. Vernoux, M. C. M. van de Sanden, M. N. Tsampas, *ACS Nano* **2019**, *13*, 12996.

- [22] K. Kousi, C. Tang, I. S. Metcalfe, D. Neagu, *Small* **2021**, *17*, 2006479.
- [23] J. Spring, E. Sediva, Z. D. Hood, J. C. Gonzalez-Rosillo, W. O'Leary, K. J. Kim, A. J. Carrillo, J. L. M. Rupp, *Small* **2020**, *16*, 2003224.
- [24] A. Schmid, G. M. Rupp, J. Fleig, *Phys. Chem. Chem. Phys.* **2018**, *20*, 12016.
- [25] J. F. Creemer, S. Helveg, G. H. Hoveling, S. Ullmann, A. M. Molenbroek, P. M. Sarro, H. W. Zandbergen, *Ultramicroscopy* **2008**, *108*, 993.
- [26] S. B. Vendelbo, C. F. Elkjær, H. Falsig, I. Puspitasari, P. Dona, L. Mele, B. Morana, B. J. Nelissen, R. van Rijn, J. F. Creemer, P. J. Kooyman, S. Helveg, *Nature Mater* **2014**, *13*, 884.
- [27] J. Cao, A. Rinaldi, M. Plodinec, X. Huang, E. Willinger, A. Hammud, S. Hieke, S. Beeg, L. Gregoratti, C. Colbea, R. Schlögl, M. Antonietti, M. Greiner, M. Willinger, *Nat Commun* **2020**, *11*, 3554.
- [28] L. I. van der Wal, S. J. Turner, J. Zečević, *Catal. Sci. Technol.* **2021**, *11*, 3634.
- [29] P. Simons, H.-I. Ji, T. C. Davenport, S. M. Haile, *Journal of the American Ceramic Society* **2017**, *100*, 1161.

### Section 3 - Modelling and design of new, alternative exsolution systems

Yuhao Wang<sup>1</sup>, Jiapeng Liu<sup>1</sup>, Longyun Shen<sup>1</sup> and Francesco Ciucci<sup>1,2,3,4</sup>

<sup>1</sup> Department of Mechanical and Aerospace Engineering, HKUST, Hong Kong SAR, P. R. China

<sup>2</sup> Department of Chemical and Biological Engineering, HKUST, Hong Kong SAR, P. R. China

<sup>3</sup> HKUST Shenzhen-Hong Kong Collaborative Innovation Research Institute, Futian, Shenzhen, P. R. China

<sup>4</sup> HKUST Energy Institute, The Hong Kong University of Science and Technology, Hong Kong SAR, P. R. China

#### 3.1 Status

Metal nanoparticles are widely used to achieve high levels of activity in catalytic systems. However, these nanoparticles tend to degrade and agglomerate over time, leading to poor device durability. Since its discovery in 2002,<sup>1</sup> exsolution has emerged as a simple method to generate highly effective nanoparticles from perovskite supports.<sup>2,3</sup> Thanks to their tight anchoring, these nanoparticles show good stability with respect to agglomeration and poisoning. There are multiple applications of exsolutions that include catalysis, fuel cells, electrolysis, and rechargeable batteries.<sup>4-6</sup> New materials with enhanced characteristics, e.g., improved durability and electrokinetic activity, can be designed via exsolution and, in that context, modeling will play a pivotal role.

Exsolution is a phase decomposition process controlled by external conditions (such as hydrogen partial pressure or electric fields) and facilitated by the presence of certain defects.<sup>6</sup> Certain A-site-deficient perovskite materials when exposed to reducing conditions, fabricate nanoparticle exsolution through several interacting sub steps, as shown in **Figure 1**.<sup>7,8</sup> These include 1) migration of easily reducible transition metal cations towards the material's surface; 2) reduction of these cations into metal atoms; 3) clustering and nucleation of nanoparticles; and 4) nanoparticle growth. An important factor to consider is the Gibbs free energy of defects and nanoparticles because these energies are also drivers for nanoparticle nucleation and growth. In classical nucleation theory, a change in volume before after exsolution will decrease the Gibbs free energy, which is compensated by an increasing surface energy.<sup>9</sup> If a critical radius can be obtained, the nanoparticle is stabilized and can grow further. This understanding of the physical dynamics has been confirmed by several high-quality experiments, which have shown that nanoparticles do exsolve quickly, epitaxially, and isotropically from their original nucleation site.<sup>10,11</sup>

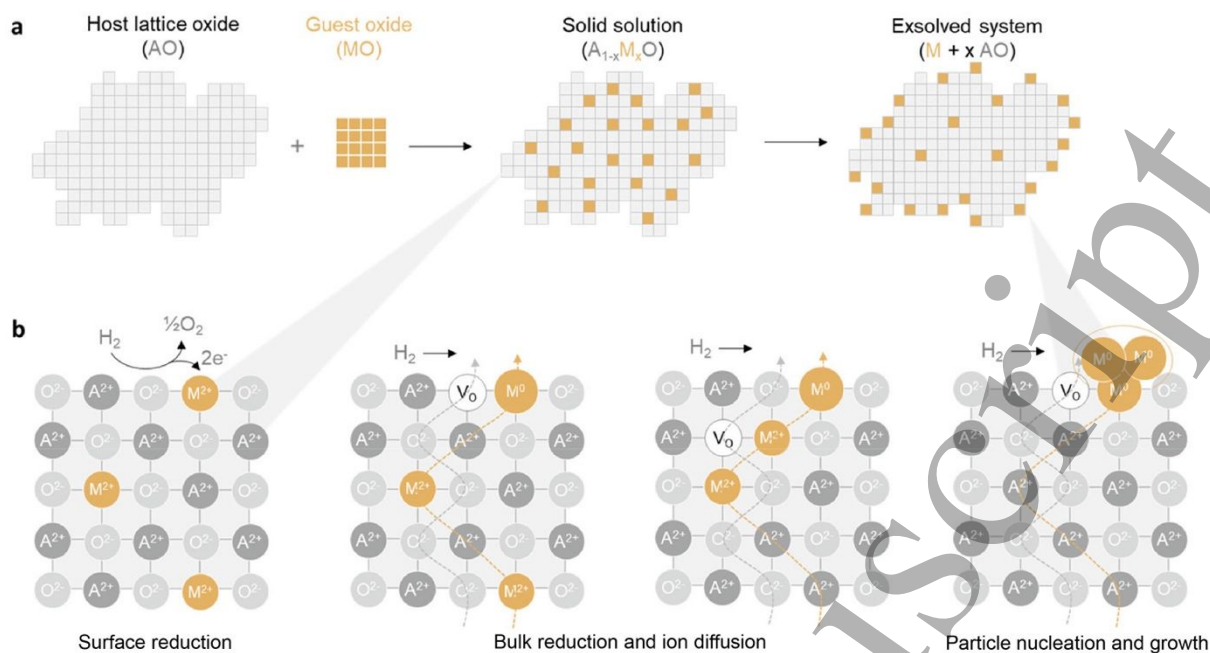


Figure 1 - A schematic illustration of a) exsolution and b) its key physical processes.<sup>7</sup>

Used with permission of 2021, Wiley-VCH

### 3.2 Current and Future Challenges

The exsolution mechanism has been studied both experimentally and computationally for several perovskites. It was found that the reduction-induced crystal reconstruction of a simple cubic, Co-doped  $Pr_{0.5}Ba_{0.5}MnO_3$  to form a layered orthorhombic perovskite-type,  $PrBaMn_2O_5$ , is the driving force for Co segregation. In addition, reducing atmospheres create oxygen vacancies which lower the Co-O bond energy and provide transition metal diffusive pathways, ultimately promoting exsolution.<sup>12</sup> Oxygen vacancies are also necessary to exsolve bimetallic nanoparticles where the reduction of a transition metal oxide is facilitated by oxygen vacancies near the surface.<sup>13</sup> Ab initio simulations have been instrumental in confirming the experimental evidence that specific crystal surface orientations and terminations produce exsolved nanoparticles.<sup>2</sup> For instance, exsolution from  $La_{0.2}Sr_{0.7}Ti_{0.9}Ni_{0.1}O_{3-\delta}$  (LSTN) thin films depends on surface termination.<sup>14,15</sup> Density functional theory calculations have also been used to study these mechanisms by leveraging small ( $\sim 100$  atoms) and idealized slab models,<sup>16-18</sup> which allowed the computation of transition metal segregation energies and the formation energies of defects. Most studies in the area concur that A-site deficiency and the presence of oxygen vacancies are key factors controlling metals segregation.<sup>6,16</sup>

Density functional theory cannot explain more complex experimental conditions in which exsolution is carried out. Moreover, with conventional atomistic calculations, it remains challenging to model the strain, interfacial and intrinsic defects, alongside applied external conditions, such as atmospheric and electrical-field switching.<sup>19,3,8,15,14</sup> Fortunately, a handful of continuum models<sup>8,20,21</sup> have been proposed to study these factors. Nonetheless, expanding these models is necessary to gain a deeper insight into exsolution mechanisms, control nanoparticle characteristics, and minimize their degradation.

### 3.3 Advances in Science and Technology to Meet Challenges

As illustrated above, several simulation works have focused on elucidating the energetics of metal segregation towards perovskite surfaces. However, there has been only limited success in the search for new perovskite compositions of enhanced electrochemical activity and exsolution capability. To optimize these two properties, validated experiments and easily computable descriptors are needed.<sup>22</sup> These descriptors could be linked to mechanisms such as segregation energetics, crystal stability, and electrokinetic reactivity. For compositional search and descriptor development to take place, extensive materials databases are required.<sup>23</sup> It should be noted that first-principle atomistic methods are poorly suited to searching for optimal materials over large compositional spaces. These methods are typically computationally expensive and can handle only a few hundred atoms. Realistic models (i.e., those involving defects such as grain boundaries and large supercells) may contain thousands of atoms, causing a considerable bottleneck for computational resources. To tackle this challenge, artificial intelligence will likely play a key role as appropriately trained graph neural networks<sup>24,25</sup> could be used to relax structures and predict materials properties (i.e., exsolution energies) with an accuracy comparable to that achieved by density functional theory.<sup>26</sup> Consequently, the search for materials could be accomplished directly by optimizing a descriptor evaluated using easily computable neural networks. This procedure would allow the probing of large compositional spaces at a fraction of the cost of conventional density functional theory simulations.

While density functional theory is only capable of producing ground-state energies (at 0 K), exsolution is a process that typically requires between 400-1000 °C. However, *Ab initio* molecular dynamics simulations can overcome this discrepancy as these simulations depend on pressure as well as temperature. Although *ab initio* molecular dynamics simulations are computationally demanding and limited to small atomic systems with short simulation times (below a fraction of a nanosecond),<sup>27</sup> these constraints could be alleviated by artificial intelligence as machine-learning-based force fields. Such can achieve force evaluations with quantum mechanical accuracy at high computational speeds. In turn, larger atomic systems could be used to capture the dynamics of transition metal atom migration and surface clustering more realistically (e.g., at grain boundaries as a function of temperature and pressure, etc.).<sup>28</sup>

From the discussion above, it becomes apparent that the next generation of exsolution models will need to be matched with a range of experiments that accurately represent atomic scales (~1 nm) and microscale-level (~10 nm) processes.<sup>29</sup> The phase-field crystal method, which can bridge atomic and mesoscopic scales, could be used to simulate the nucleation and growth of exsolved nanoparticles. By combining non-equilibrium thermodynamics and phase transformation dynamics, the phase-field crystal approach can, in principle, handle the characteristic time and length scales of diffusional, nucleation, and growth processes that underpin exsolution.<sup>30</sup> However, for larger three-dimensional systems, computational scaling remains a significant challenge.<sup>31</sup> These issues can be overcome by using modern scale-bridging multiscale modeling. Multiscale modeling requires a cascade of models tailored to specific length scales (e.g., quantum mechanics of metal atom diffusion and reaction energetics at the <1 nm scale, molecular dynamics to capture metal atom clustering at the 10 nm scale, and continuum models to simulate particle growth and strain above that).<sup>33</sup> These could then be linked rigorously through a heterogeneous multiscale method.<sup>34</sup> In addition, physics-informed neural networks have emerged as a unique approach for learning structures and defects in

1  
2  
3 materials.<sup>35</sup> Using these advanced models on time-resolved, environmental, and transmission electron  
4 microscopy data could help determine physical models for exsolution automatically.  
5

6  
7 Finally, it is important to stress that many potential applications, including the prediction of  
8 electrocatalytic activity degradation and the optimal control of nanoparticle properties during  
9 operation and synthesis, require models that are far less computationally demanding than those  
10 described above. Therefore, future research should also be focused on reduced-order models<sup>37</sup> that  
11 can capture the physics and chemistry of the exsolution process and the degradation of nanoparticles.  
12  
13

### 14 **3.4 Concluding Remarks**

15  
16 Exsolution has emerged as a major strategy to produce nanoparticles that are stable and highly  
17 active. However, as the details of the mechanism by which nanoparticles exsolve are still not fully  
18 understood, opportunities for designing and optimizing new electrocatalysts remain limited. To  
19 overcome this challenge, models will play a key role. Due to the complexity of the exsolution  
20 mechanism, which involves multiple time/length scales and physical processes, multiscale models are  
21 needed. In parallel, optimal compositions should be obtained by optimizing suitable descriptors. In  
22 this context, acceleration through artificial networks would allow for the probing of large  
23 compositional spaces, ultimately realizing the application of high-performance materials with  
24 optimized nanoparticles.  
25  
26  
27  
28

### 29 **3.5 Acknowledgements**

30  
31 The authors gratefully acknowledge the financial support from the Research Grants Council of  
32 Hong Kong (RGC Ref No. 16201820 and 16206019). This work was supported in part by the Project of  
33 Hetao Shenzhen-Hong Kong Science and Technology Innovation Cooperation Zone (HZQB-KCZYB-  
34 2020083).  
35  
36

### 37 **3.6 References**

- 38  
39 [1] Nishihata, Y.; Mizuki, J.; Akao, T.; Tanaka, H.; Uenishi, M.; Kimura, M.; Okamoto, T.; Hamada, N.  
40 Self-Regeneration of a Pd-Perovskite Catalyst for Automotive Emissions Control. *Nature* **2002**,  
41 418 (6894), 164–167. <https://doi.org/10.1038/nature00893>.  
42  
43 [2] Neagu, D.; Oh, T.-S.; Miller, D. N.; Ménard, H.; Bukhari, S. M.; Gamble, S. R.; Gorte, R. J.; Vohs, J.  
44 M.; Irvine, J. T. S. Nano-Socketed Nickel Particles with Enhanced Coking Resistance Grown in Situ  
45 by Redox Exsolution. *Nature Communications* **2015**, 6 (1), 8120.  
46 <https://doi.org/10.1038/ncomms9120>.  
47  
48 [3] Myung, J.; Neagu, D.; Miller, D. N.; Irvine, J. T. S. Switching on Electrocatalytic Activity in Solid  
49 Oxide Cells. *Nature* **2016**, 537 (7621), 528–531. <https://doi.org/10.1038/nature19090>.  
50  
51 [4] Cong, Y.; Geng, Z.; Zhu, Q.; Hou, H.; Wu, X.; Wang, X.; Huang, K.; Feng, S. Cation-Exchange-  
52 Induced Metal and Alloy Dual-Exsolution in Perovskite Ferrite Oxides Boosting the Performance  
53 of Li-O<sub>2</sub> Battery. *Angewandte Chemie International Edition* **2021**, 60 (43), 23380–23387.  
54 <https://doi.org/10.1002/anie.202110116>.  
55  
56 [5] Ren, X.; Yu, D.; Yuan, L.; Bai, Y.; Huang, K.; Liu, J.; Feng, S. In Situ Exsolution of Ag from AgBiS<sub>2</sub>  
57 Nanocrystal Anode Boosting High-Performance Potassium-Ion Batteries. *J. Mater. Chem. A* **2020**,  
58 8 (30), 15058–15065. <https://doi.org/10.1039/D0TA03964K>.  
59  
60 [6] Kim, J. H.; Kim, J. K.; Liu, J.; Curcio, A.; Jang, J.-S.; Kim, I.-D.; Ciucci, F.; Jung, W. Nanoparticle Ex-  
Solution for Supported Catalysts: Materials Design, Mechanism and Future Perspectives. *ACS*  
*Nano* **2021**, 15 (1), 81–110. <https://doi.org/10.1021/acsnano.0c07105>.

- 1  
2  
3 [7] Kousi, K.; Tang, C.; Metcalfe, I. S.; Neagu, D. Emergence and Future of Exsolved Materials. *Small* **2021**, 17 (21), 2006479. <https://doi.org/10.1002/sml.202006479>.
- 4  
5 [8] Gao, Y.; Chen, D.; Saccoccio, M.; Lu, Z.; Ciucci, F. From Material Design to Mechanism Study:  
6 Nanoscale Ni Exsolution on a Highly Active A-Site Deficient Anode Material for Solid Oxide Fuel  
7 Cells. *Nano Energy* **2016**, 27, 499–508. <https://doi.org/10.1016/j.nanoen.2016.07.013>.
- 8  
9 [9] Zhang, J.; Gao, M.-R.; Luo, J.-L. In Situ Exsolved Metal Nanoparticles: A Smart Approach for  
10 Optimization of Catalysts. *Chem. Mater.* **2020**, 32 (13), 5424–5441.  
11 <https://doi.org/10.1021/acs.chemmater.0c00721>.
- 12  
13 [10] Neagu, D.; Kyriakou, V.; Roiban, I.-L.; Aouine, M.; Tang, C.; Caravaca, A.; Kousi, K.; Schreur-Piet,  
14 I.; Metcalfe, I. S.; Vernoux, P.; van de Sanden, M. C. M.; Tsampas, M. N. In Situ Observation of  
15 Nanoparticle Exsolution from Perovskite Oxides: From Atomic Scale Mechanistic Insight to  
16 Nanostructure Tailoring. *ACS Nano* **2019**, 13 (11), 12996–13005.  
17 <https://doi.org/10.1021/acsnano.9b05652>.
- 18  
19 [11] Jo, Y.-R.; Koo, B.; Seo, M.-J.; Kim, J. K.; Lee, S.; Kim, K.; Han, J. W.; Jung, W.; Kim, B.-J. Growth  
20 Kinetics of Individual Co Particles Ex-Solved on SrTi<sub>0.75</sub>Co<sub>0.25</sub>O<sub>3-δ</sub> Polycrystalline Perovskite  
21 Thin Films. *J. Am. Chem. Soc.* **2019**, 141 (16), 6690–6697. <https://doi.org/10.1021/jacs.9b01882>.
- 22  
23 [12] Sun, Y.-F.; Zhang, Y.-Q.; Chen, J.; Li, J.-H.; Zhu, Y.-T.; Zeng, Y.-M.; Amirkhiz, B. S.; Li, J.; Hua, B.;  
24 Luo, J.-L. New Opportunity for in Situ Exsolution of Metallic Nanoparticles on Perovskite Parent.  
25 *Nano Lett.* **2016**, 16 (8), 5303–5309. <https://doi.org/10.1021/acs.nanolett.6b02757>.
- 26  
27 [13] Kwon, O.; Sengodan, S.; Kim, K.; Kim, G.; Jeong, H. Y.; Shin, J.; Ju, Y.-W.; Han, J. W.; Kim, G.  
28 Exsolution Trends and Co-Segregation Aspects of Self-Grown Catalyst Nanoparticles in  
29 Perovskites. *Nature Communications* **2017**, 8 (1), 15967.  
30 <https://doi.org/10.1038/ncomms15967>.
- 31  
32 [14] Han, H.; Park, J.; Nam, S. Y.; Kim, K. J.; Choi, G. M.; Parkin, S. S. P.; Jang, H. M.; Irvine, J. T. S.  
33 Lattice Strain-Enhanced Exsolution of Nanoparticles in Thin Films. *Nature Communications* **2019**,  
34 10 (1), 1471. <https://doi.org/10.1038/s41467-019-09395-4>.
- 35  
36 [15] Kim, K. J.; Han, H.; Defferriere, T.; Yoon, D.; Na, S.; Kim, S. J.; Dayaghi, A. M.; Son, J.; Oh, T.-S.;  
37 Jang, H. M.; Choi, G. M. Facet-Dependent in Situ Growth of Nanoparticles in Epitaxial Thin Films:  
38 The Role of Interfacial Energy. *J. Am. Chem. Soc.* **2019**, 141 (18), 7509–7517.  
39 <https://doi.org/10.1021/jacs.9b02283>.
- 40  
41 [16] Gao, Y.; Lu, Z.; You, T. L.; Wang, J.; Xie, L.; He, J.; Ciucci, F. Energetics of Nanoparticle Exsolution  
42 from Perovskite Oxides. *J. Phys. Chem. Lett.* **2018**, 9 (13), 3772–3778.  
43 <https://doi.org/10.1021/acs.jpcllett.8b01380>.
- 44  
45 [17] Hamada, I.; Uozumi, A.; Morikawa, Y.; Yanase, A.; Katayama-Yoshida, H. A Density Functional  
46 Theory Study of Self-Regenerating Catalysts LaFe<sub>1-x</sub>MxO<sub>3-y</sub> (M = Pd, Rh, Pt). *J. Am. Chem. Soc.*  
47 **2011**, 133 (46), 18506–18509. <https://doi.org/10.1021/ja110302t>.
- 48  
49 [18] Tian, Z.; Inagaki, K.; Morikawa, Y. Density Functional Theory on the Comparison of the Pd  
50 Segregation Behavior at LaO- and FeO<sub>2</sub>-Terminated Surfaces of LaFe<sub>1-x</sub>PdxO<sub>3-y</sub>. *Current*  
51 *Applied Physics* **2012**, 12, S105–S109. <https://doi.org/10.1016/j.cap.2012.06.007>.
- 52  
53 [19] Neagu, D.; Tsekouras, G.; Miller, D. N.; Ménard, H.; Irvine, J. T. S. In Situ Growth of Nanoparticles  
54 through Control of Non-Stoichiometry. *Nature Chemistry* **2013**, 5 (11), 916–923.  
55 <https://doi.org/10.1038/nchem.1773>.
- 56  
57 [20] Oh, T.-S.; Rahani, E. K.; Neagu, D.; Irvine, J. T. S.; Shenoy, V. B.; Gorte, R. J.; Vohs, J. M. Evidence  
58 and Model for Strain-Driven Release of Metal Nanocatalysts from Perovskites during Exsolution.  
59 *J. Phys. Chem. Lett.* **2015**, 6 (24), 5106–5110. <https://doi.org/10.1021/acs.jpcllett.5b02292>.
- 60 [21] Jiang, G.; Yan, F.; Wan, S.; Zhang, Y.; Yan, M. Microstructure Evolution and Kinetics of B-Site  
Nanoparticle Exsolution from an A-Site-Deficient Perovskite Surface: A Phase-Field Modeling and  
Simulation Study. *Phys. Chem. Chem. Phys.* **2019**, 21 (21), 10902–10907.  
<https://doi.org/10.1039/C8CP07883A>.

- 1  
2  
3 [22] Jacobs, R.; Hwang, J.; Shao-Horn, Y.; Morgan, D. Assessing Correlations of Perovskite Catalytic  
4 Performance with Electronic Structure Descriptors. *Chem. Mater.* **2019**, 31 (3), 785–797.  
5 <https://doi.org/10.1021/acs.chemmater.8b03840>.  
6  
7 [23] Jain, A.; Ong, S. P.; Hautier, G.; Chen, W.; Richards, W. D.; Dacek, S.; Cholia, S.; Gunter, D.;  
8 Skinner, D.; Ceder, G.; Persson, K. A. Commentary: The Materials Project: A Materials Genome  
9 Approach to Accelerating Materials Innovation. *APL Materials* **2013**, 1 (1), 011002.  
10 <https://doi.org/10.1063/1.4812323>.  
11  
12 [24] Xie, T.; Grossman, J. C. Crystal Graph Convolutional Neural Networks for an Accurate and  
13 Interpretable Prediction of Material Properties. *Phys. Rev. Lett.* **2018**, 120 (14), 145301.  
14 <https://doi.org/10.1103/PhysRevLett.120.145301>.  
15  
16 [25] Chen, C.; Ye, W.; Zuo, Y.; Zheng, C.; Ong, S. P. Graph Networks as a Universal Machine Learning  
17 Framework for Molecules and Crystals. *Chem. Mater.* **2019**, 31 (9), 3564–3572.  
18 <https://doi.org/10.1021/acs.chemmater.9b01294>.  
19  
20 [26] Chen, C.; Ong, S. P. A Universal Graph Deep Learning Interatomic Potential for the Periodic  
21 Table, 2022. <https://doi.org/10.48550/ARXIV.2202.02450>.  
22  
23 [27] He, X.; Zhu, Y.; Epstein, A.; Mo, Y. Statistical Variances of Diffusional Properties from Ab Initio  
24 Molecular Dynamics Simulations. *npj Computational Materials* **2018**, 4 (1), 18.  
25 <https://doi.org/10.1038/s41524-018-0074-y>.  
26  
27 [28] Park, C. W.; Kornbluth, M.; Vandermause, J.; Wolverton, C.; Kozinsky, B.; Mailoa, J. P. Accurate  
28 and Scalable Graph Neural Network Force Field and Molecular Dynamics with Direct Force  
29 Architecture. *npj Computational Materials* **2021**, 7 (1), 73. [https://doi.org/10.1038/s41524-021-](https://doi.org/10.1038/s41524-021-00543-3)  
30 [00543-3](https://doi.org/10.1038/s41524-021-00543-3).  
31  
32 [29] Salvalaglio, M. and E., Ken R. Coarse-Grained Modeling of Crystals by the Amplitude Expansion of  
33 the Phase-Field Crystal Model: An Overview. *Modelling and Simulation in Materials Science and*  
34 *Engineering* **2022**.  
35  
36 [30] Provatas, N.; Dantzig, J. A.; Athreya, B.; Chan, P.; Stefanovic, P.; Goldenfeld, N.; Elder, K. R. Using  
37 the Phase-Field Crystal Method in the Multi-Scale Modeling of Microstructure Evolution. *JOM*  
38 **2007**, 59 (7), 83–90. <https://doi.org/10.1007/s11837-007-0095-3>.  
39  
40 [31] Cheng, M.; Warren, J. A. An Efficient Algorithm for Solving the Phase Field Crystal Model. *Journal*  
41 *of Computational Physics* **2008**, 227 (12), 6241–6248. <https://doi.org/10.1016/j.jcp.2008.03.012>.  
42  
43 [32] Geers, M. G. D.; Kouznetsova, V. G.; Brekelmans, W. A. M. Multi-Scale Computational  
44 Homogenization: Trends and Challenges. *Journal of Computational and Applied Mathematics*  
45 **2010**, 234 (7), 2175–2182. <https://doi.org/10.1016/j.cam.2009.08.077>.  
46  
47 [33] Bruix, A.; Margraf, J. T.; Andersen, M.; Reuter, K. First-Principles-Based Multiscale Modelling of  
48 Heterogeneous Catalysis. *Nature Catalysis* **2019**, 2 (8), 659–670.  
49 <https://doi.org/10.1038/s41929-019-0298-3>.  
50  
51 [34] Abdulle, A.; Weinan, E.; Engquist, B.; Vanden-Eijnden, E. The Heterogeneous Multiscale Method.  
52 *Acta Numerica* **2012**, 21, 1–87. <https://doi.org/10.1017/S0962492912000025>.  
53  
54 [35] Zhang Enrui; Dao Ming; Karniadakis George Em; Suresh Subra. Analyses of Internal Structures  
55 and Defects in Materials Using Physics-Informed Neural Networks. *Science Advances* 8 (7),  
56 eabk0644. <https://doi.org/10.1126/sciadv.abk0644>.  
57  
58 [36] Raissi Maziar; Yazdani Alireza; Karniadakis George Em. Hidden Fluid Mechanics: Learning  
59 Velocity and Pressure Fields from Flow Visualizations. *Science* **2020**, 367 (6481), 1026–1030.  
60 <https://doi.org/10.1126/science.aaw4741>.  
[37] Tran, A.; Wildey, T.; Sun, J.; Liu, D.; Wang, Y. A Stochastic Reduced-Order Model for Statistical  
Microstructure Descriptors Evolution. *Journal of Computing and Information Science in*  
*Engineering* **2022**, 1–18. <https://doi.org/10.1115/1.4054237>.



## Section 4 – The effect of extended defects during exsolution and implications for activity

Brian A. Rosen

Department of Materials Science and Engineering, Tel Aviv University, Ramat Aviv, ISRAEL

### 4.1 Status

Heterogeneous catalysis is regarded as a surface-specific process; therefore, the majority of research related to defect engineering of catalysts relates to point defects which influence the surface chemistry. With the rise in popularity of defect engineering came an explosion of work on how 0D point crystalline defects (e.g., atomic substitutions, vacancies, and interstitials) impacts surface adsorption, kinetics, and phase stability.[1] By comparison, the impact of extended (1D and 2D) defects such as dislocations, grain boundaries, twin boundaries, and stacking faults on catalysis are far less studied since these types of defects are thought to influence bulk rather than the surface.[2]

Recent work has shown that the presence of extended defects in a catalyst or its precursor can influence the exsolution mechanism and resulting catalytic properties. 2D crystalline defects have been shown to act as nucleation points for the exsolution process. For example, in-situ TEM under an  $H_2$  atmosphere at  $350^\circ C$  shown in **Figure 1** shows 1-nm Ni particles forming specifically on the Ruddlesden-Popper (RP) stacking faults of the  $LaNiO_3$  backbone, as opposed to the defect-free regions where no Ni nanoparticles are found.[3] In fact, the exsolution process started nearly  $150^\circ C$  higher when the  $LaNiO_3$  was free of RP defects. Similar results have been shown for exsolution at grain boundaries, another type of 2D defect.[4] Interestingly, the impact of 2D defects for exsolution goes beyond the growth mechanism, and extends to the performance of the resultant catalyst. As an example, Ni particles grown on Ruddlesden-Popper stacking faults in  $LaNiO_3$  showed enhanced stability against coking during methane dry reforming compared to Ni particles grown from the pristine backbone.[5]

Additionally, there is experimental and computational evidence that the presence of sub-surface stacking faults in the oxide support can influence the adsorption energy of atoms and molecules, whereby modulating catalyst performance via Sabatier's principle.[6] These findings underscore the potential importance of multi-dimensional defect engineering, particularly in the design of catalysts prepared by exsolution. Further advances in this field can lead to materials where these two effects are simultaneously exploited. In such a material, 2D defects are inserted in pre-determined positions and/or at predetermined densities, whereby modulating the electronic and adsorption properties of the catalyst. When exsolution begins, metal particle growth would initiate at those same locales, allowing for the active site to be planted near the region of enhanced transport or adsorption.

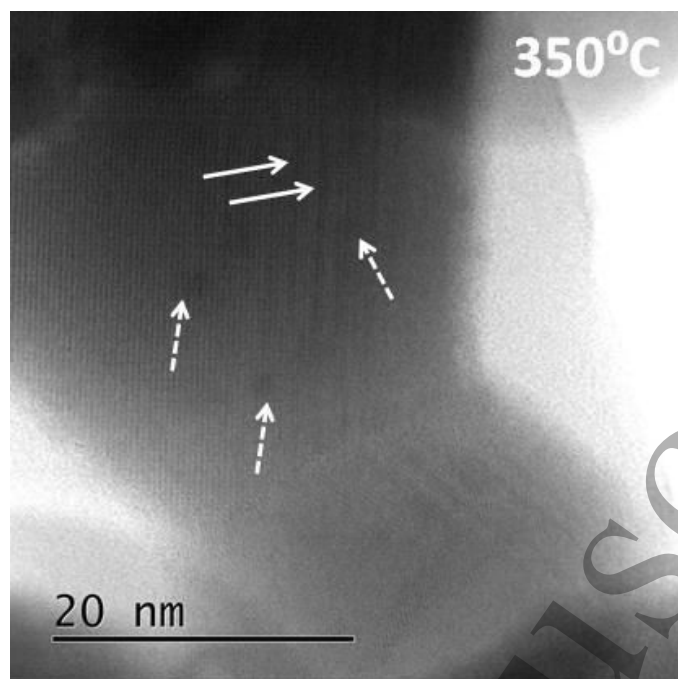


Figure 1 - In-situ TEM under 20 mbar H<sub>2</sub> at 350°C showing the growth of Ni nanoparticles on Ruddlesden-Popper stacking faults in LaNiO<sub>3</sub>. Dashed arrows indicate the location of Ni nanoparticles (dark contrast circles), solid arrows indicate the position of stacking faults (dark contrast vertical lines). Adapted from [3] with permission (CC-BY).

## 4.2 Current and Future Challenges

The primary reason why extended defects are not frequently reported in exsolution studies is that controlling the density of such defects is highly challenging.[7] 0D crystalline defects such as vacancies and substitutions can be systematically and confidently studied as controlling such defects only requires changing the metal stoichiometry.[8] By comparison, inducing a known amount of growth mistakes in multiple dimensions is more complex. Typically, the parameters of the synthesis itself must be modulated in order to significantly change the extended defect structure of a material. Perovskite oxides represent an excellent platform for studying this phenomenon, as most of them can be synthesized using a wide variety of techniques including aqueous co-precipitation, non-aqueous co-precipitation, sol-gel, combustion, hydrothermal, flame spray pyrolysis, co-deflagration, solid-state, and gas-phase condensation (e.g. CVD, ALD) techniques. Since the formation of a pristine single crystal generally requires a steady and controlled growth process, it may be said that the probability for forming multi-dimensional defects increases by triggering a dramatic environmental change during the crystallization process (e.g. a rapid temperature or pH swing). Indeed, out of all the synthesis techniques mentioned above, the density of stacking faults in La-based perovskite oxides was found to be highest during co-precipitation, where the pH of the solvent is rapidly increased.

These challenges are amplified when trying to explain enhanced catalytic activity through computational modelling (e.g. DFT) of materials with extended defects. Even in the case where the experimentalist has coarse control over the density of stacking faults or grain boundaries in the catalyst, the exact locations of these defects cannot yet be determined ab-initio, meaning there will be significant discrepancies between defect structure of the real catalyst and the simulated one.[6] A

possible solution to this problem is the use of the PLD (or similar) technique to precisely decide where the stacking fault will occur [9, 10]; however, this strategy is typically limited to fundamental rather than practical catalyst design.

The final challenge stems from the fact that there is not a standardized way to describe the density of extended defects for the sake of modulating catalytic action. A simple proposal for stacking faults is to count the number of faults per nanometer in a particular crystallographic direction, however this technique erases information about the nature of the fault (Ruddlesden Popper  $n=2$  vs. 3), the effect of faults appearing in bunches, and the proximity of the fault to the free surface.

### 4.3 Advances in Science and Technology to Meet Challenges

Solution-based oxide synthesis, while theoretically simple, comes with a myriad of free variables which can impact the growth of oxides destined for nanoparticles growth by exsolution. The development of synthesis-defect-structure relationships for oxides using solution-based methods requires careful experimental control and tuning. Well-planned studies can often yield clear results about how subtle changes such as the stirring rate, pH ramp, temperature ramp, or annealing temperature can influence the formation of extended defects.[11] In this context, a rigorous study which utilizes design of experiments (DoE)[12] together with a quantitative descriptor of stacking faults in the resultant oxide may yield significant advancements.

The number of techniques available to identify, quantify, and characterize extended defects has also grown beyond ex-situ S/TEM and AFM[13] to include atom probe tomography (APT) [14] and in-situ TEM.[15] The increased availability of in-situ holders allows for more studies on the exsolution process itself, particularly allowing for pinpointing the influence of temperature ramp on the growth mechanism. XRD is an under-utilized but important technique that may show promise for the global quantification of stacking faults in certain samples by line-shape analysis. The peak shape of highly faulted perovskites have been shown to have increased Lorentzian character.[16] This technique requires further study, but if successful can easily be applied under in-situ conditions using an in-situ XRD chamber (e.g. XRK-900 by AntonParr) or a synchrotron, the latter providing time resolution on the order of seconds. Techniques which characterize the electrical properties of microstructural defects and interfaces have also seen advancement in recent years; for example, nanometric four-point probe experiments have been shown to allow for resistivity-structure relationships in the vicinity of a grain boundary or stacking fault.[17]

The increased computing resources available to researchers allows for the study of more complex systems. Calculating the kinetic barriers for adsorption of gasses on faulted perovskite surfaces can often have lower numerical stability and present as highly nonconvex problems. The effect of electronic correlation and magnetism in certain backbones used in exsolution (such as  $\text{LaFeO}_3$ ) can make barrier calculations prohibitive, and yet, as defect engineering gains more attention and computing power is improved, the computational contributions to this field will rapidly increase. **Figure 2** shows an example where the adsorption energies of CO, CO+O and CO+O<sub>2</sub> (co)-adsorption on defective  $\text{LaFeO}_3$  were calculated using the nudged elastic band (NEB) method, however the barrier heights were not able to be calculated.

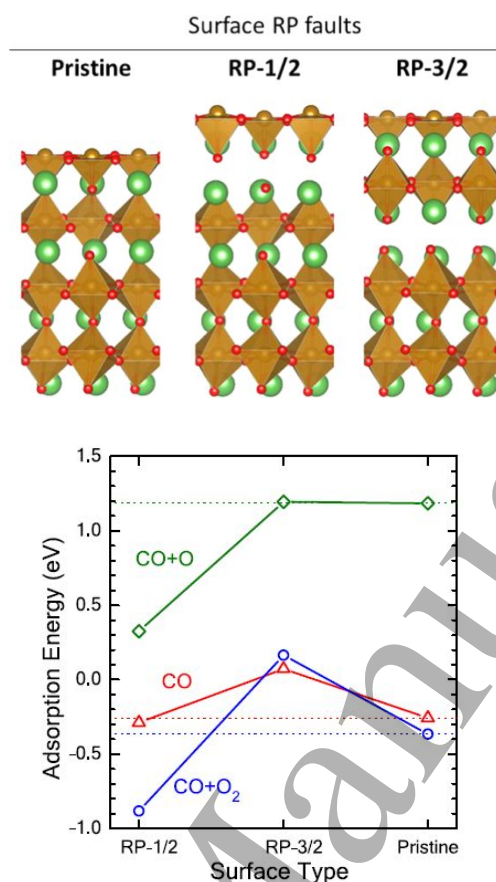


Figure 2 - DFT-calculated (co-)adsorption energies for CO, CO+O<sub>2</sub>, and CO+O on pristine and defective LaFeO<sub>3</sub> where the stacking fault is placed 1/2 and 3/2 unit cells below the surface (RP-1/2 and RP-3/2 respectively).

Reproduced from [6] with permission.

#### 4.4 Concluding Remarks

Exploiting the defect structure for exsolution catalysts requires a multi-pronged approach with improved control, identification, classification, and simulation of extended defects during the exsolution process and subsequent reaction. Significant improvements in in-situ microscopy, tomography, and computing power have already allowed for advancement, but clever techniques for ab-initio placement of extended defects in nanomaterials are still in its nascent stages. With these improved capabilities and initial reports, however, there must also come an expansion of research in the field of catalyst defect engineering to include multi-dimensional defects.

#### 4.5 References

- [1] C. Xie, D. Yan, H. Li, S. Du, W. Chen, Y. Wang, *et al.*, "Defect Chemistry in Heterogeneous Catalysis: Recognition, Understanding, and Utilization," *ACS Catalysis*, vol. 10, pp. 11082-11098, 2020/10/02 2020.
- [2] P. L. Gai-Boyes, "Defects in Oxide Catalysts: Fundamental Studies of Catalysis in Action," *Catalysis Reviews*, vol. 34, pp. 1-54, 1992/02/01 1992.

- 1  
2  
3 [3] S. Singh, E. Prestat, L.-F. Huang, J. M. Rondinelli, S. J. Haigh, and B. A. Rosen, "Role of 2D and 3D  
4 Defects on the Reduction of LaNiO<sub>3</sub> Nanoparticles for Catalysis," *Scientific reports*, vol. 7, pp. 1-  
5 7, 2017.
- 6 [4] Y.-R. Jo, B. Koo, M.-J. Seo, J. K. Kim, S. Lee, K. Kim, *et al.*, "Growth Kinetics of Individual Co  
7 Particles Ex-solved on SrTi<sub>0.75</sub>Co<sub>0.25</sub>O<sub>3-δ</sub> Polycrystalline Perovskite Thin Films," *Journal of the*  
8 *American Chemical Society*, vol. 141, pp. 6690-6697, 2019/04/24 2019.
- 9 [5] S. Singh, D. Zubenko, and B. A. Rosen, "Influence of LaNiO<sub>3</sub> shape on its solid-phase  
10 crystallization into coke-free reforming catalysts," *ACS Catalysis*, vol. 6, pp. 4199-4205, 2016.
- 11 [6] R. Bornovski, L.-F. Huang, E. P. Komarala, J. M. Rondinelli, and B. A. Rosen, "Catalytic  
12 Enhancement of CO Oxidation on LaFeO<sub>3</sub> Regulated by Ruddlesden–Popper Stacking Faults,"  
13 *ACS applied materials & interfaces*, vol. 11, pp. 33850-33858, 2019.
- 14 [7] T. Horide, M. Ishimaru, K. Sato, and K. Matsumoto, "Combined effect of nanorod and stacking  
15 fault for improving nanorod interface in YBa<sub>2</sub>Cu<sub>3</sub>O<sub>7-δ</sub> nanocomposite films," *Superconductor*  
16 *Science and Technology*, vol. 33, p. 115001, 2020.
- 17 [8] D. Neagu, G. Tsekouras, D. N. Miller, H. Ménard, and J. T. Irvine, "In situ growth of nanoparticles  
18 through control of non-stoichiometry," *Nature chemistry*, vol. 5, pp. 916-923, 2013.
- 19 [9] W. Wunderlich, M. Fujimoto, and H. Ohsato, "Formation of stacking faults from misfit  
20 dislocations at the BaTiO<sub>3</sub>/SrTiO<sub>3</sub> interface simulated by molecular dynamics," *Materials Science*  
21 *and Engineering: A*, vol. 309-310, pp. 148-151, 2001/07/15/ 2001.
- 22 [10] W. Y. Wang, Y. L. Tang, Y. L. Zhu, J. Suriyaprakash, Y. B. Xu, Y. Liu, *et al.*, "Atomic mapping of  
23 Ruddlesden–Popper faults in transparent conducting BaSnO<sub>3</sub>-based thin films," *Scientific*  
24 *Reports*, vol. 5, p. 16097, 2015/11/03 2015.
- 25 [11] A. S. Menon, S. Khalil, D. O. Ojwang, K. Edström, C. P. Gomez, and W. R. Brant, "Synthesis–  
26 structure relationships in Li- and Mn-rich layered oxides: phase evolution, superstructure  
27 ordering and stacking faults," *Dalton Transactions*, vol. 51, pp. 4435-4446, 2022.
- 28 [12] "Design of Experiments," in *Analytic Methods for Design Practice*, G.-J. Park, Ed., ed London:  
29 Springer London, 2007, pp. 309-391.
- 30 [13] T.-S. Oh, E. K. Rahani, D. Neagu, J. T. S. Irvine, V. B. Shenoy, R. J. Gorte, *et al.*, "Evidence and  
31 Model for Strain-Driven Release of Metal Nanocatalysts from Perovskites during Exsolution," *The*  
32 *Journal of Physical Chemistry Letters*, vol. 6, pp. 5106-5110, 2015/12/17 2015.
- 33 [14] N. Volz, F. Xue, C. H. Zenk, A. Bezold, S. Gabel, A. Subramanyam, *et al.*, "Understanding creep of  
34 a single-crystalline Co-Al-W-Ta superalloy by studying the deformation mechanism, segregation  
35 tendency and stacking fault energy," *Acta Materialia*, vol. 214, p. 117019, 2021.
- 36 [15] P. Cao, P. Tang, M. F. Bekheet, H. Du, L. Yang, L. Haug, *et al.*, "Atomic-Scale Insights into Nickel  
37 Exsolution on LaNiO<sub>3</sub> Catalysts via In Situ Electron Microscopy," *The Journal of Physical*  
38 *Chemistry C*, vol. 126, pp. 786-796, 2022/01/13 2022.
- 39 [16] A. Boulle, C. Legrand, R. Guinebretiere, J. Mercurio, and A. Dauger, "X-Ray diffraction line  
40 broadening by stacking faults in SrBi<sub>2</sub>Nb<sub>2</sub>O<sub>9</sub>/SrTiO<sub>3</sub> epitaxial thin films," *Thin Solid Films*, vol.  
41 391, pp. 42-46, 2001.
- 42 [17] H. Bishara, M. Ghidelli, and G. Dehm, "Approaches to Measure the Resistivity of Grain  
43 Boundaries in Metals with High Sensitivity and Spatial Resolution: A Case Study Employing Cu,"  
44 *ACS Applied Electronic Materials*, vol. 2, pp. 2049-2056, 2020/07/28 2020.
- 45  
46  
47  
48  
49  
50  
51  
52  
53  
54  
55  
56  
57  
58  
59  
60

## Section 5 – Exsolution for methane conversion to ethylene

Yongchun Xiao<sup>1,2,3</sup> and Kui Xie<sup>1,2,3,4</sup>

<sup>1</sup> Key Laboratory of Optoelectronic Materials Chemistry and Physics, FJIRSM, CAS, Fujian 350002, China

<sup>2</sup> Key Laboratory of Design & Assembly of Functional Nanostructures, FJIRSM, CAS, Fujian 350002, China

<sup>3</sup> Advanced Energy Science and Technology Guangdong Laboratory, Guangdong 116023, China

<sup>4</sup> Fujian Science & Technology Innovation Laboratory for Optoelectronic Information of China, Fujian, China

### 5.1 Status

Converting methane, the main component of natural gas and biogas, whose reserves are pretty vast in the world, into value-added chemicals, such as ethylene, has been driven for several decades by the demands in renewable energy along with the long-term decline in petroleum and coal reserves. The development of cost-effective, high conversion, high selectivity and stable catalysts remains a fundamental challenge. The recent several years have seen a revival in the popularity of metal exsolution as an *in situ* synthesis method to create highly active metal anchored in the surface of an oxide scaffold [1]. Exsolution materials are proposed as quite effective catalysts to enhance catalytic performance for the conversion of small molecules, such as  $\text{CH}_4 \rightarrow \text{C}_2\text{H}_4$  [2],  $\text{C}_2\text{H}_6 \rightarrow \text{C}_2\text{H}_4$  [3]  $\text{CH}_4 \rightarrow \text{CO}$  [4], due to the strong interactions between the exsolved metal and oxide interface, which would facilitate electron and ion transport at hetero-interfaces (Figure 1) [5].

The oxidative coupling of methane (OCM) reaction ( $2\text{CH}_4 + 2\text{O}^{2-} \rightleftharpoons \text{C}_2\text{H}_4 + 2\text{H}_2\text{O} + 4\text{e}^-$ ) and non-oxidative coupling of methane (NOCM) process ( $2\text{CH}_4 \rightleftharpoons \text{C}_2\text{H}_4 + 4\text{H}^+ + 4\text{e}^-$ ) could be ideally accomplished efficiently in electrochemical processes. Moreover, green/sustainable electrochemical processes could be promoted through synergistically controlling electrochemical redox reactions and advanced catalysis on the porous electrodes. The solid oxide electrolyzers (SOEs) have gained much interest from both academics and industry in the electrochemical conversion of  $\text{CH}_4$  to  $\text{C}_2\text{H}_4$  at high efficiency using renewable electrical energy, which involves the cracking of the C–H bond in  $\text{CH}_4$  and the alternative coupling of the C–C bond to generate  $\text{C}_2\text{H}_4$ .

The OCM reaction has been extensively studied, while the problem of methane over-oxidation needs to be addressed. In our previous work [2], we utilized  $\text{Sr}_2\text{Fe}_{1.5+x}\text{Mo}_{0.5}\text{O}_{6-\delta}$  ( $x=0-0.1$ ) anode with different distribution of exsolved Fe nanoparticles on the perovskite scaffold ( $x\text{Fe-SFMO}$ ) to realize OCM reaction in an oxide-ion-conducting SOEs. It shows that the highest  $\text{C}_2$  product yields are 16.7% (11.5%  $\text{C}_2\text{H}_4$  + 5.2%  $\text{C}_2\text{H}_6$ ) with the  $\text{C}_2$  selectivity of 82.2%, and that even after 100 h of high temperature (850 °C) operation, it still shows the efficient conversion (Figure 2). Exsolution catalyst offers an efficient method to generate  $\text{C}_2$  chemicals from methane through the OCM process using a SOEs reactor. The NOCM process using exsolution materials prevents excessive oxidation of methane and ethylene product, however, its thermodynamics is limited in a large range of temperatures and only beneficial at temperatures above 950 °C [6].

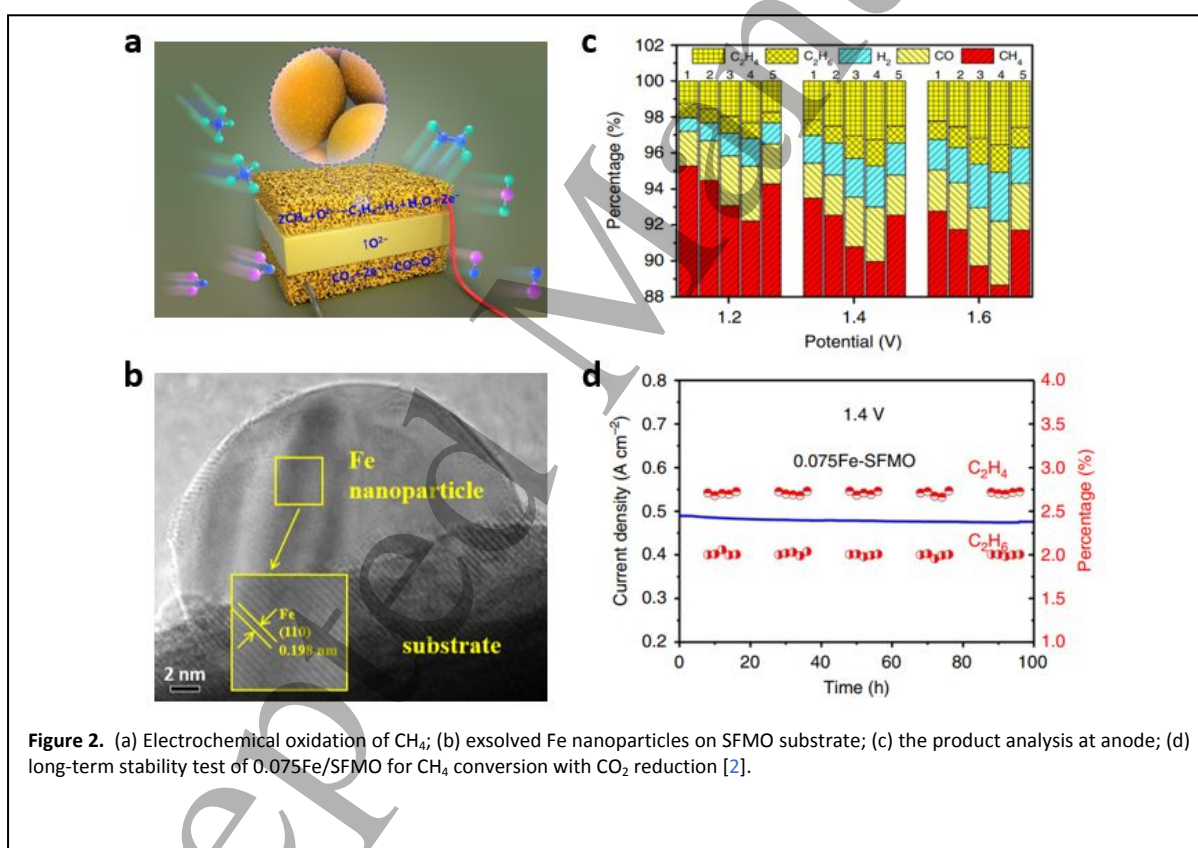
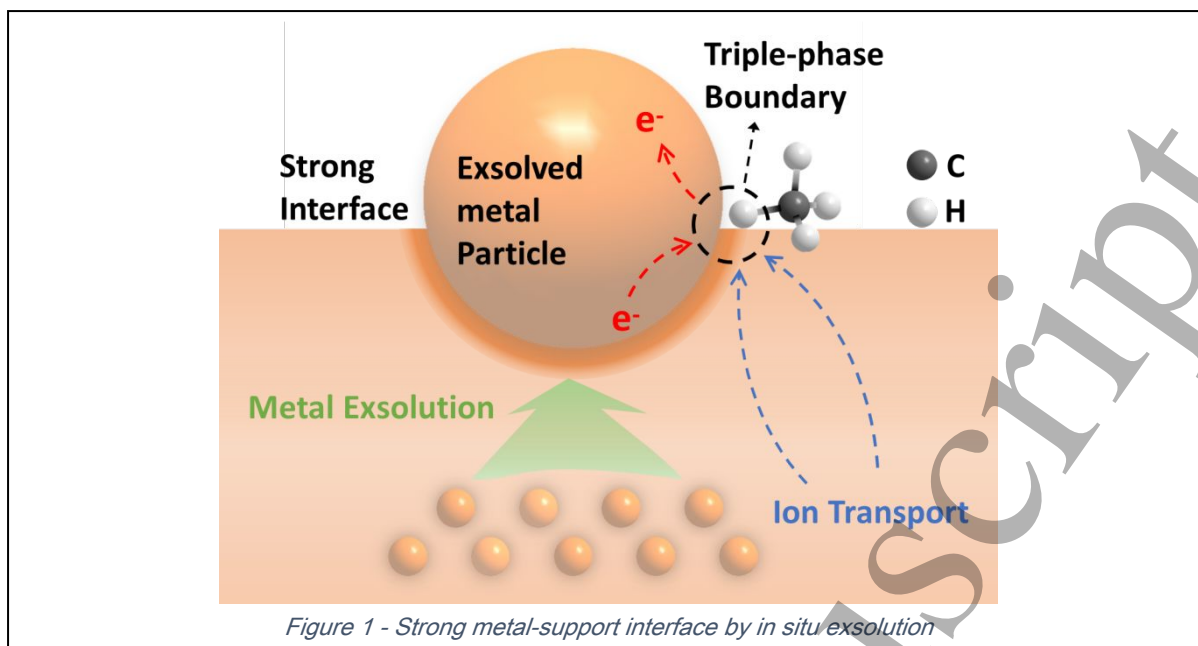


Figure 2. (a) Electrochemical oxidation of  $\text{CH}_4$ ; (b) exsolved Fe nanoparticles on SFMO substrate; (c) the product analysis at anode; (d) long-term stability test of 0.075Fe/SFMO for  $\text{CH}_4$  conversion with  $\text{CO}_2$  reduction [2].

## 5.2 Current and Future Challenges

The exsolution catalysts used in the SOEs reactor for the OCM/NOCM reaction have advanced the impressive performance; however, disruptive advances are still necessary to make such technology commercially available. Several challenges remain for it to become a competitive

1  
2  
3 technological process for obtaining desired products such as ethylene directly from natural gas or  
4 biogas.  
5

6  
7 In order to obtain exsolution catalysts for high activity and excellent durability in the  
8 conversion of  $\text{CH}_4$ , a set of complex designs is required, resulting in relatively complex oxide  
9 formulations, often incorporating multiple elements with various defects chemistries. Such diversity  
10 facilitates the output of new compositions tailored for high-temperature applications of methane  
11 conversion and more systematic characterization of a reference system, which controls crucial  
12 parameters including components, size, distribution or amount, thus consolidating properties of  
13 resistance to amalgamation and surface area loss at high operation temperature, and strong  
14 interactions and increased triple-phase boundaries between the electron-conducting nanoparticles  
15 and the oxide supports. The lack of detailed compositional, structural, thermodynamic and kinetic  
16 information for such systems, together with the difficulties of theoretically modeling systems with  
17 multi-defects/dopants, have made it difficult to establish a set of commonly used rational design  
18 principles that are still largely empirical.  
19  
20  
21  
22

23 The influence of local interface structure of exsolution catalysts on activity and stability for  
24 methane conversion is still not clear. For example, in the oxide-ion conducting SOEs, the  
25 electrochemical transport of  $\text{O}^{2-}$  ions from the cathode to the anode is indeed a step to generate active  
26 species for  $\text{CH}_4$  activation with the existence of exsolution catalysts. The mechanism and kinetics of  
27 the conversion of  $\text{O}^{2-}$  ions to different types of active oxygen species, which is considered to be one of  
28 the key radicals initiating oxidation of  $\text{CH}_4$  and selective coupling to ethylene at the anodic confined  
29 active metal-oxide interface, are still required to further in-depth investigate, thus guiding the advance  
30 of a novel active exsolved catalyst for the electro-thermal synergistic conversion of  $\text{CH}_4$  to  $\text{C}_2\text{H}_4$ .  
31  
32  
33

34 In addition to exsolution catalyst optimization and reaction mechanism investigation, ideal  
35 operating conditions for conversion of  $\text{CH}_4$  to  $\text{C}_2$  in SOEs, such as flow rate, temperature, and  
36 concentration of oxygen-containing feed gas at the cathode,  $\text{CH}_4$  concentration at the anode, applied  
37 current, etc., together with more stable SOEs component materials and microstructural engineering  
38 of electrolyzer, need to be further optimized to achieve an optimized SOEs system for the coupling  
39 pprocess of methane to  $\text{C}_2$  hydrocarbons.  
40  
41  
42  
43  
44

### 45 **5.3 Advances in Science and Technology to Meet Challenges**

46  
47 In the face of the challenges and issues discussed above, the significant efforts of researchers  
48 in exsolution and SOEs have allowed us to point out some possible approaches to accelerate the  
49 industrial processes of  $\text{CH}_4$  conversion into  $\text{C}_2$  hydrocarbons using such reactor system.  
50  
51

52 Many parameters to design and control the structure of exsolution materials with the  
53 conversion, selectivity, and stability necessary for a commercial application are yet to be explored,  
54 including different oxide crystal structures and defect chemistries, less-explored anion sublattice,  
55 active elements (e.g. Fe, Ni, Co, FeCo, or NiCu) [4,7]. These could help improve bulk and surface  
56 transport of ions, reducing the exsolution temperature and providing new opportunities in methane  
57 electrochemical coupling under milder conditions. It is also crucial to diversify the microstructures of  
58  
59  
60



oxide perovskites such as thin-film, hierarchical, and porous. In addition to the material itself, more methods to trigger the exsolution of the material should be explored, including but not limited to chemical, electrochemical and light driving forces [6]. For instance, reduction temperature and time determine particle size and amount; the oxygen partial pressure and the nature of reducing atmosphere control the shape and composition of the nanoparticles. But more efforts are needed to exsolve single atoms (one of the ultimate frontiers in catalyst design), such as single iron sites, which show the highest methane conversion (48.1%) and ethylene selectivity (48.4%) at 1090 °C [8].

The development of advanced *in situ* characterization techniques, such as *in situ* XRD, *in situ* XPS, *in situ* DRIFTS, *in situ* Raman, *in situ* x-ray absorption spectroscopy, *in situ* TEM, enable probing the elusive, rapidly changing reaction intermediates and morphology of the exsolved interface. Thus, it helps us better understand the mechanism of methane coupling and the relationship between exsolution materials and their catalytic performance. In addition, through computational simulation and modeling, machine learning, high throughput computation, the transport of heat and mass and the degradation mechanisms in electrochemical systems could be understood, providing theoretical guidance for the synthesis of *in situ* exsolution catalysts and the design of OCM/NOCM systems in SOEs reactors [9, 10].

#### 5.4 Concluding Remarks

In summary, the direct conversion of methane to ethylene through an electro-/thermo-catalyzing process with exsolution materials is an important research topic that would bring significant changes to the traditional petroleum-based ethylene industry, while more efficient and sustainable technologies are still required. With substantial efforts focused on the study of the design of innovative exsolution materials, the mechanism of methane coupling with and an effective combination of advanced *in situ* characterizations, computational simulation, and machine learning techniques to overcome the challenges in the field, the C<sub>2</sub> production via OCM/NOCM process using SOEs reactors system with exsolved metal-oxide materials is likely to become feasible. Utilizing exsolution materials as a class of highly efficient catalysts for methane conversion to ethylene could be a key technology in future decarbonization of massive petrochemical industrial processes.

#### 5.5 Acknowledgements

We acknowledge the National Key Research and Development, Program of China (2017YFA0700102), Natural Science Foundation of China (91845202) and Strategic Priority Research Program of Chinese Academy of Sciences (XDB2000000).

#### 5.6 References

- [1] Xiao Y C and Xie K 2022 Active exsolved metal-oxide interfaces in porous single-crystalline ceria monoliths for efficient and durable CH<sub>4</sub>/CO<sub>2</sub> reforming. *Angew. Chem. Int. Edit.* **61**
- [2] Zhu C L, Hou S S, Hu X L, Lu J H, Chen F L and Xie K 2019 Electrochemical conversion of methane to ethylene in a solid oxide electrolyzer *Nat. Commun.* **10** 1173

- 1  
2  
3 [3] Zhang X R, Ye L T, Li H, Chen F L and Xie K 2020 Electrochemical dehydrogenation of ethane to  
4 ethylene in a solid oxide electrolyzer *ACS Catal.* **10** 3505-13  
5 [4] Lu J H, Zhu C L, Pan C C, Lin W L, Lemmon J P, Chen F L, Li C S and Xie K 2018 Highly efficient  
6 electrochemical reforming of CH<sub>4</sub>/CO<sub>2</sub> in a solid oxide electrolyser. *Sci. Adv.* **4** eaar5100  
7 [5] Sun X, Chen H J, Yin Y M, T. Curnan M, Han J W, Chen Y and Ma Z F 2021 Progress of exsolved  
8 metal nanoparticles on oxides as high performance (electro)catalysts for the conversion of small  
9 molecules *Small* **17** 2005383-419  
10 [6] Liu Y, Yuan S Z and Xie K 2021 Conversion of methane to ethylene with BaCe<sub>0.9</sub>Y<sub>0.1</sub>Co<sub>x</sub>O<sub>3-delta</sub>  
11 hydrogen permeation membrane *Chinese J Struct. Chem.* **40** 901-7  
12 [7] Rosen B A 2020 Progress and opportunities for exsolution in electrochemistry *Electrochem* **1** 32-  
13 43.  
14 [8] Guo X G, Fang G Z, Li G, Ma H, Fan H J, Yu L, Ma C, Wu X, Deng D H, Wei M M, Tan D L, S R,  
15 Zhang S, Li J Q, Sun L T, Tang Z C, Pan X L and Bao X H 2014 Direct, nonoxidative conversion of  
16 methane to ethylene, aromatics, and hydrogen *Science* **344** 616-19  
17 [9] Ghareghashi A, Ghader S and Hashemipour H 2013 Theoretical analysis of oxidative coupling of  
18 methane and fischer tropesch synthesis in two consecutive reactors: comparison of fixed bed and  
19 membrane reactor. *J Ind. Eng. Chem.* **19** 1811-26  
20 [10] Fouty N J, Carrasco J C and Lima F V 2017 Modeling and design optimization of multifunctional  
21 membrane reactors for direct methane aromatization. *Membranes-Basel* **7** 48  
22  
23  
24  
25  
26  
27

## 28 Section 6 – Exsolution for power generation from ammonia

29 Guangming Yang<sup>1</sup> and Zongping Shao<sup>1,2</sup>

30 <sup>1</sup>State Key Laboratory of Materials-Oriented Chemical Engineering, Nanjing Tech University, Nanjing, China

31 <sup>2</sup>WA School of Mines: Minerals, Energy and Chemical Engineering, Curtin University, Perth, WA, Australia

### 32 33 34 35 36 37 38 39 40 41 42 43 44 45 46 47 48 49 50 51 52 53 54 55 56 57 58 59 60

### 34 6.1 Status

Ammonia (NH<sub>3</sub>) is a carbon-free and hydrogen-rich energy source that is widely used in many fields, such as nitrogen fertilizers, refrigerants, and fiber production. In addition to the advantages of green environmental protection, NH<sub>3</sub> energy also has the following unique advantages as a future alternative to hydrogen energy: (1) high energy density; (2) easy storage and transportation; (3) high safety; (4) mature large-scale production process.<sup>[1]</sup> It can also be directly used in fuel cells, especially solid oxide fuel cells (SOFCs). Compared with other types of fuel cells, SOFCs have the advantages of high electrode reaction rate, high ionic conductivity, high energy efficiency, and a wide range of available fuels. Meanwhile, high temperature can significantly promote the thermal decomposition of NH<sub>3</sub>, thus allowing NH<sub>3</sub> to be used directly as a fuel in SOFCs. According to the type of electrolyte, SOFCs can be divided into two categories: oxygen anion conducting electrolyte-based SOFCs (O-SOFCs) and proton conducting electrolyte-based SOFCs (H-SOFCs). Compared to O-SOFCs, H-SOFCs based on proton conductor electrolytes have unique advantages: firstly, the generation of nitrogen oxides (such as NO) can be effectively avoided; secondly, the reaction-product water will generate at the air electrode, which can avoid the dilution of the fuel and improve the conversion efficiency of the system; in addition, the proton conductor exhibits good ionic conductivity at medium and low temperatures, which can reduce the operating temperature of SOFCs.<sup>[2]</sup> **Figure 1** shows the working principle of ammonia-fueled O-SOFCs and ammonia-fueled H-SOFCs.

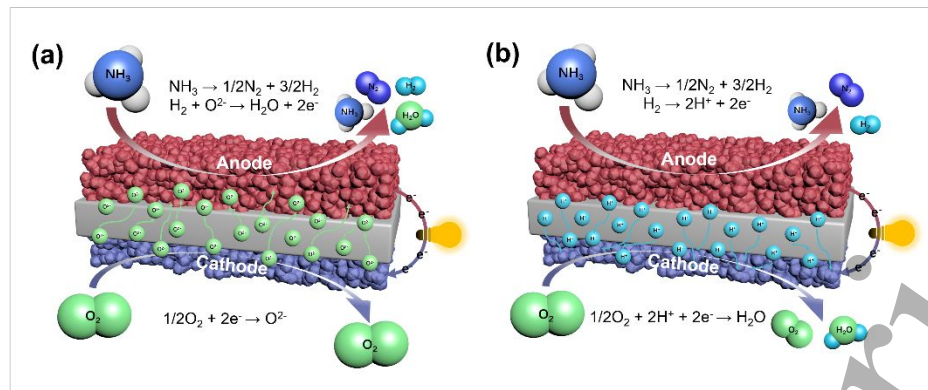


Figure 1 - Schematic illustration of (a) ammonia-fueled O-SOFC, and (b) ammonia-fueled H-SOFC.

In direct-ammonia SOFCs (DA-SOFCs), ammonia is first thermally decomposed to generate  $\text{N}_2$  and  $\text{H}_2$ , and then  $\text{H}_2$  undergoes electrochemical oxidation to complete the ammonia electrode reaction. Therefore, ammonia electrodes have an important impact on the performance of DA-SOFCs. Ammonia electrodes generally can be divided into two categories: one is non-precious metal materials (such as Ni-based electrodes); the other is noble metal materials (Ru, Pd, Pt, etc.). Past studies have proved that precious metal catalysts have a high decomposition efficiency of  $\text{NH}_3$ , which can still reach more than 90% at 450 °C, but its expensive price limits its large-scale application.<sup>[3]</sup> Since Ni-based electrodes also have excellent catalytic properties against  $\text{NH}_3$  at 550 °C, the most commonly used DA-SOFCs electrode is the traditional composite electrode of Ni and electrolyte ceramic materials. Another method to promote the catalytic activity of electrodes is to introduce nano catalysts into the electrodes. At present, the preparation methods of nanoparticle-modified electrodes that have been more studied in SOFCs are mainly composed of two steps of solution impregnation and low temperature sintering.<sup>[4]</sup> Although the electrodes prepared by the impregnation method have high catalytic activity, the nanoparticles have some disadvantages such as large particle size, uneven distribution, complex preparation process, easy sintering, and reduced electrode porosity, which are difficult to operate in practical applications. Recently, Irvine et al. improved the activity of catalysts by enabling *in-situ* growth of nanoscale phases from non-stoichiometric perovskite surfaces in a reducing environment.<sup>[5]</sup> Owing to the small size of the exsolved nanoparticles, the uniform distribution on the electrode surface, and the good exsolution-dissolution repeatability of the nanoparticles, they have been widely used in SOFC anodes. In this topic, we summarize the recent reports on a series of nanocatalysts prepared by the exsolution method for the application of DA-SOFCs, and propose the challenges that the exsolution method will face in the application of DA-SOFCs.

## 6.2 Current and Future Challenges

Among non-precious metal materials, Ni has the highest catalytic activity for ammonia decomposition and owns the lower cost. Therefore, the current research on ammonia electrode materials mainly focuses on Ni-based electrodes.<sup>[2]</sup> However, related studies have shown that high concentrations of  $\text{NH}_3$  can cause Ni coarsening and destroy the microstructure of ammonia electrodes, thereby reducing the performance and stability of DA-SOFCs.<sup>[6]</sup> Therefore, improving the anti-coarsening ability of Ni-based ammonia electrodes is the key to enhancing the stability and catalytic activity of ammonia electrodes. In order to improve the catalytic activity and durability of DA-SOFC anodes, the ammonia catalytic activity and reaction sites can be effectively improved by using nanoparticle catalysts to modify the anode surface. Recently, Zhang et al. reported a Fe-modified Ni-

1  
2  
3 based ceramic anode, which effectively enhanced the activity and stability for ammonia conversion.<sup>[7]</sup>  
4 Meanwhile, Fe-modified electrode can effectively improve the surface adsorption of NH<sub>3</sub> and reduce  
5 the desorption barrier of N<sub>2</sub>, which was also confirmed by first-principles calculations. In addition, the  
6 Ni nano-modified anode also showed obvious advantages in ammonia decomposition reaction. A Ni-  
7 doped Ba(Zr<sub>0.1</sub>Ce<sub>0.7</sub>Y<sub>0.1</sub>Yb<sub>0.1</sub>)<sub>0.95</sub>Ni<sub>0.05</sub>O<sub>3-δ</sub> (BZCYbN) strategy was proposed by Song *et al.* to promote  
8 electrolyte sintering and alleviate the detrimental reaction between NiO and BaZr<sub>0.1</sub>Ce<sub>0.7</sub>Y<sub>0.1</sub>Yb<sub>0.1</sub>O<sub>3-δ</sub>  
9 (BZCYb) in the anode, while Ni nanoparticles were exsolved onto the anode surface to improve  
10 ammonia catalytic activity and hydrogen surface exchange rate.<sup>[8]</sup> Therefore, the BZCYbN-based  
11 single cell using ammonia as fuel produces a PPD of 523 mW cm<sup>-2</sup> at 650 °C, which is increased by  
12 36.6% compared with un-modified BZCYb-based single cell. Cavazzani *et al.* also confirmed that the  
13 dissolution of Ni also significantly promotes hydrogen oxidation process.<sup>[9]</sup>  
14  
15  
16  
17  
18

19 Noble metals usually have high electronic conductivity and catalytic activity, among which Ru-  
20 based materials have the highest catalytic activity for ammonia decomposition. Zhu *et al.* reported a  
21 high-performance ammonia catalyst Ru-(BaO)<sub>2</sub>(CaO)(Al<sub>2</sub>O<sub>3</sub>) (Ru-B<sub>2</sub>CA) and combined it with H-SOFC to  
22 obtain a PPD of h of 877 mW cm<sup>-2</sup> at 650 °C under NH<sub>3</sub> fuel.<sup>[10]</sup> The degradation rate of H-SOFCs was  
23 significantly decreased by using Ru-B<sub>2</sub>CA catalyst for the pre-catalysis of ammonia gas. Ultimately, the  
24 DA-SOFCs of this structure operated stably for 1200 hours under test conditions. In addition,  
25 ruthenium not only provides excellent catalytic activity for the anode, but trace amounts of ruthenium  
26 doping can also promote the exsolution of metals in the perovskite in the form of alloys, which can  
27 greatly enhance the catalytic activity of DA-SOFC anode. Xiong *et al.* treated the synthesized  
28 Pr<sub>0.6</sub>Sr<sub>0.4</sub>Co<sub>0.2</sub>Fe<sub>0.75</sub>Ru<sub>0.05</sub>O<sub>3-δ</sub> (PSCFRu) and Pr<sub>0.6</sub>Sr<sub>0.4</sub>Co<sub>0.2</sub>Fe<sub>0.8</sub>O<sub>3-δ</sub> (PSCF) perovskites under H<sub>2</sub>  
29 atmosphere, compared with reduced PSCF (r-PSCF), a large amount of CoFeRu-based alloy  
30 nanoparticles was exsolved from the reduced PSCFRu (r-PSCFRu) (100 vs. 400 particles μm<sup>-2</sup>) with  
31 smaller particles (50 vs. 20 nm), which led to a significant increase in the catalytic activity of r-PSCFRu  
32 for the ammonia decomposition reaction.<sup>[11]</sup> The experimental results also show that the DA-SOFC  
33 with r-PSCFRu anode has a PPD of 374 mW cm<sup>-2</sup> at 800 °C, which is nearly 30 % higher than that of the  
34 cell with r-PSCF anode, and the operational durability is also improved. This shows the catalytic activity  
35 of ammonia electrodes can be significantly improved by doping Ru in perovskite materials. Besides  
36 ruthenium, the noble metal palladium also exhibits excellent catalytic activity in DA-SOFCs. The  
37 catalytic activity of palladium for NH<sub>3</sub> at intermediate temperatures was investigated by Aoki *et al.*<sup>[12]</sup>  
38 Their BZCY-Pd oxide-metal-based ammonia DA-SOFCs achieved a stable power output of 0.58 W cm<sup>-2</sup>  
39 at 600 °C.  
40  
41  
42  
43  
44  
45  
46  
47

### 48 **6.3 Advances in Science and Technology to Meet Challenges**

49  
50  
51 The current research on surface exsolution catalysts for ammonia fuel cell anodes has  
52 numerous hurdles. Although it is well recognized that surface exsolution of some metals can  
53 dramatically improve ammonia catalytic activity, the appropriate temperature, particle size, nanoalloy  
54 formation process, and surface electrochemical reaction mechanism of nanoparticle exsolution are  
55 still cannot be analyzed exactly. Probing using *in-situ* transmission electron microscopy (*in-situ* TEM)  
56 and *in-situ* X-ray absorption fine structure (XAFS) spectroscopy are anticipated to provide decisive  
57 insights into these challenges. It is possible to adjust the ideal circumstances for nanoparticle  
58 exsolution by combining these two types of *in situ* characterization, which can simultaneously provide  
59  
60

information on the morphology, composition, and diffraction of the crystal phase of exsolved particles with temperature and time. Additionally, the microkinetic modeling and density functional theory (DFT) calculations can more clearly explain the reaction mechanism of the  $\text{NH}_3$ -catalyzed process on the surface of exsolved nanoparticles. The optimal reaction sites for the surface activity of the desolated nanoparticles were theoretically predicted using the DFT simulations. To calculate the surface kinetic rates of desolation of various elements, the  $\text{NH}_3$  adsorption energy and  $\text{N}_2$  desorption energy on the surface of various metal particles could be estimated. The DFT calculation can also accurately determine the reaction energy barriers of ammonia dehydrogenation and its intermediates ( $\text{H}_3\text{N}^* \rightarrow \text{H}_2\text{N}^* + \text{H}^* \rightarrow \text{HN}^* + 2\text{H}^* \rightarrow \text{N}^* + 3\text{H}^*$ ) at various active sites, which offers an accurate theoretical foundation for further investigation of the catalytic effect of nanoparticles out of solution on ammonia decomposition.

The stability of in-situ growth nanoparticles also meets great challenge in DA-SOFCs, since nanoparticles usually undergo agglomeration at high temperatures and reducing atmosphere. Especially, traditional nickel-based ceramics can be easily pulverized when suffer from high  $\text{NH}_3$  concentration, leading to a serious degradation in long-term operation. Bimetal exsolution, such as Co-Mo, Ni-Fe, Ni-Ru, have been investigated in thermally  $\text{NH}_3$  decomposition, which can not only improve the decomposition activity, but also hinder metallic nanoparticles agglomeration, sintering, and poisoning. [13, 14] Song *et al.* prepared a high-performance DA-SOFC via the *in-situ* exsolved NiCo alloy nanoparticles modified  $\text{La}_{0.55}\text{Sr}_{0.30}\text{TiO}_{3-\delta}$  (LST) anode substrate, which is proved to have a fast ammonia decomposition reaction dynamic rate because it effectively balances the process of adsorption and disconnection of the  $\text{NH}_3$  and  $\text{N}_2$ . [15] The intense interaction between NiCo alloy and LST perovskite as well as the inherent sintering resistance make DA-SOFC show a good stability at 700 °C. Therefore, bimetallic exsolution strategy serves as the essential candidates applied in DA-SOFCs anodes.

Although the exsolved nano-catalyst has excellent electrochemical performance and stability in DAFC anode, its mechanism is not well understood, especially whether the exsolved nano-particles also play other roles in the reaction? Recently, a new  $\text{Ba}(\text{Zr}_{0.1}\text{Ce}_{0.7}\text{Y}_{0.1}\text{Yb}_{0.1})_{0.95}\text{Pd}_{0.05}\text{O}_{3-\delta}$  (BZCYYbPd) perovskite and used Ni-BZCYYbPd was reported as an anode for H-SOFCs. [16] The catalytic activity and chemical stability of the anode for ammonia decomposition were successfully enhanced by doping 5 mol% palladium into a conventional proton conductor metal-ceramic material. This is due to the Pd nanoparticles exsolved from BZCYYbPd in a reducing atmosphere can provide additional active sites for ammonia electrode catalysis. Meanwhile, the strong hydrogen adsorption ability of Pd metal keeps the ammonia electrode surface with a high hydrogen concentration, which inhibits the coarsening effect of  $\text{NH}_3$  on the Ni-based ammonia electrode, thus enhancing the chemical stability of the ammonia electrode. Finally, the H-SOFCs with Ni-BZCYYbPd as the ammonia electrode exhibit superior performance ( $724 \text{ mW cm}^{-2}$  @ 650 °C) and good stability for 350 h. Therefore, the exsolved Pd nanoparticles not only improve the catalytic activity of ammonia, but also play a key role in the stability of the electrode.

## 6.4 Conclusions and Challenges

The nanoparticle-modified hydrogen electrode material prepared by the exsolution method has excellent catalytic activity for  $\text{NH}_3$  splitting and  $\text{H}_2$  oxidating performance, which makes the performance of DC-SOFCs comparable to SOFCs fueled by  $\text{H}_2$ . However, there are still some challenges in the DA-SOFCs prepared by the exsolution method, such as the long-term stability of the exsolved nanoparticles and the influence on the overall structure of the electrode when the

nanoparticles are re-exsolved. At the same time, the mechanism of the exsolved nanoparticles in the operation of DA-SOFCs is not yet clear, and further *in-situ* characterizations such as Raman spectroscopy, synchrotron radiation photoelectron spectroscopy/absorption spectroscopy, and scanning tunneling microscopy are needed, thus providing a theoretical basis for the design and development of electrodes for the exsolution of highly active nanoparticles.

## 6.5 Acknowledgements

The authors acknowledge the financial support from the National Key R&D Program of China (2022YFB4004000)

## 6.6 References

- [1] D. T. Tran, T. H. Nguyen, H. Jeong, P. K. L. Tran, D. Malhotra, K. U. Jeong, N. H. Kim, J. H. Lee. Recent engineering advances in nanocatalysts for NH<sub>3</sub>-to-H<sub>2</sub> conversion technologies. *Nano Energy*, 2022, 94, 106929.
- [2] G. Jeerh, M. Zhang, S. Tao. Recent progress in ammonia fuel cells and their potential applications. *J. Mater. Chem. A*, 2021, 9(2): 727-752.
- [3] F. Schüth, R. Palkovits, R. Schlögl, D. S. Su. Ammonia as a possible element in an energy infrastructure: catalysts for ammonia decomposition. *Energy Environ. Sci.*, 2012, 5(4): 6278-6289.
- [4] J.M. Vohs, R.J. Gorte. High-performance SOFC cathodes prepared by infiltration. *Adv. Mater.* 2009, 21(9), 943-956.
- [5] J.H. Myung, D. Neagu, D.N. Miller, J.T.S. Irvine. Switching on electrocatalytic activity in solid oxide cells. *Nature* 2016, 537(7621), 528-531.
- [6] J. Yang, A. Molouk, T. Okanishi, H. Muroyama, T. Matsui, K. Eguchi. A stability study of Ni/Yttria-stabilized zirconia anode for direct ammonia solid oxide fuel cells. *ACS Appl. Mater. Interfaces* 2015, 7(51), 28701.
- [7] H. Zhang, Y. Zhou, K. Pei, Y. Pan, K. Xu, Y. Ding, B. Zhao, K. Sasaki, Y. Choi, Y. Chen, M. Liu. An efficient and durable anode for ammonia protonic ceramic fuel cells. *Energy Environ. Sci.*, 2022, 15, 287-295.
- [8] Y. Song, J. Chen, M. Yang, M. Xu, D. Liu, M. Liang, Y. Wang, R. Ran, W. Wang, F. Ciucci, Z. Shao. Realizing simultaneous detrimental reactions suppression and multiple benefits generation from nickel doping toward improved protonic ceramic fuel cell performance. *Small*, 2022, 2200450.
- [9] J. Cavazzani, E. Squizzato, E. Brusamarello, A. Glisenti. Exsolution in La and Ni co-doped strontium titanate: a suitable anode for running SOFCs on ammonia as alternative fuel. *E3S Web of Conferences*, 2022, 334.
- [10] L. Zhu, C. Cadigan, C. Duan, J. Huang, L. Bian, L. Le, C. H. Hernandez, V. Avance, R. O'Hayre, N. P. Sullivan. Ammonia-fed reversible protonic ceramic fuel cells with Ru-based catalyst. *Commun. Chem.*, 2021, 4, 121.
- [11] X. Xiong, J. Yu, X. Huang, D. Zou, Y. Song, M. Xu, R. Ran, W. Wang, W. Zhou, Z. Shao. Slightly ruthenium doping enables better alloy nanoparticle exsolution of perovskite anode for high-performance direct-ammonia solid oxide fuel cells. *J. Mater. Sci. Technol.*, 2022, 125, 51-58.
- [12] Y. Aoki, T. Yamaguchi, S. Kobayashi, D. Kowalski, C. Zhu, H. Habazaki. High-efficiency direct ammonia fuel cells based on BaZr<sub>0.1</sub>Ce<sub>0.7</sub>Y<sub>0.2</sub>O<sub>3-δ</sub>/Pd oxide-metal junctions. *Glob. Chall.*, 2018, 2(1), 1700088.
- [13] X. Duan, G. Qian, X. Zhou, D. Chen, W. Yuan, MCM-41 supported CoMo bimetallic catalysts for enhanced hydrogen production by ammonia decomposition. *Chem. Eng. J.*, 2012, 207, 103.
- [14] C. Chen, Y. Chen, A. M. Ali, W. Luo, J. Wen, L. Zhang, H. Zhang, Bimetallic Ru-Fe nanoparticles supported on carbon nanotubes for ammonia decomposition and synthesis. *Chem. Eng. Technol.*, 2020, 43(4), 719-730.
- [15] Y. Song, H. Li, M. Xu, G. Yang, W. Wang, R. Ran, W. Zhou, Z. Shao. Infiltrated NiCo alloy nanoparticle decorated perovskite oxide: a highly active, stable, and antisintering anode for direct-ammonia solid oxide fuel cells. *Small*, 2020, 16(28), 2001859.
- [16] F. He, Q. Gao, Z. Liu, M. Yang, R. Ran, G. Yang, W. Wang, W. Zhou, Z. Shao, A new Pd doped proton conducting perovskite oxide with multiple functionalities for efficient and stable power generation from ammonia at reduced temperatures. *Adv. Energy Mater.*, 2021, 11, 2003916.

## Section 7 – Alloy Exsolution for SOFC Anodes

Yubo Zhang, Jakob Reinke, Travis A. Schmauss and Scott A. Barnett

Department of Materials Science and Engineering, Northwestern University, Evanston, IL, USA

### 7.1 Status

Solid oxide fuel cells (SOFCs) have shown great potential to fulfil today's requirement in energy generation and storage due to their high efficiency, fuel flexibility, and low emissions [1]. While conventional cermet SOFC anodes such as Ni-YSZ have shown good electrochemical performance, they suffer from poor redox stability, coking in C-containing fuels, and poor sulfur tolerance [2]. Although extrinsic addition of catalytic nanoparticles via methods like precursor solution infiltration has been reported to alleviate these problems and enhance anode catalytic activity, these nanoparticles usually suffer from coarsening resulting in poor durability [3].

Accepted Manuscript

Exsolution in SOFC anodes was first demonstrated in 2007 by Madsen et al. in  $\text{La}_{0.8}\text{Sr}_{0.2}\text{Cr}_{0.82}\text{Ru}_{0.18}\text{O}_{3-6}$  (LSCrRu) [4], where nano-sized Ru particles were observed on anode surfaces during cell operation and significantly improved the electrochemical performance. Since then exsolution has been extensively studied for SOFC perovskite anodes where metal nanoparticles of Ni,

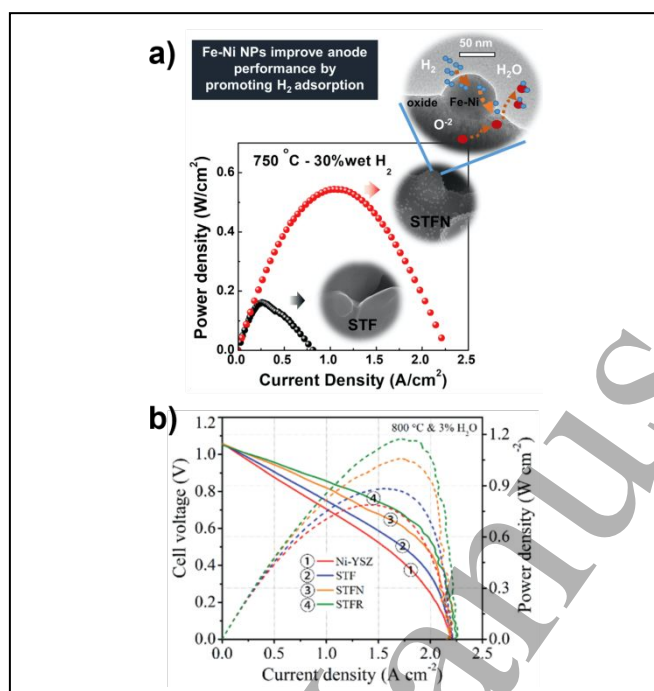


Figure 1 - a) Exsolved Fe-Ni nanoparticles observed for  $\text{Sr}_{0.95}\text{Ti}_{0.3}\text{Fe}_{0.63}\text{Ni}_{0.07}\text{O}_3$  (STFN) SOFC anodes upon reduction; the nanoparticles enhance H<sub>2</sub> adsorption and lead to superior electrochemical performance compared to un-exsolved  $\text{SrTi}_{0.3}\text{Fe}_{0.7}\text{O}_3$  (STF) anodes. Figure reprinted from Ref. [6] with permission from Elsevier, 2018. b) Comparison of performance results for SOFCs with different fuel electrodes – the exsolution anodes STF-Ni and  $\text{Sr}_{0.95}(\text{Ti}_{0.3}\text{Fe}_{0.63}\text{Ru}_{0.07})\text{O}_3$  (STFR) show superior performance compared to Ni-YSZ and STF. Measurements were conducted at 800 °C in air and 3% H<sub>2</sub>O humidified hydrogen. Figure reproduced from Ref [7] with permission from The Royal Society of Chemistry

Co, Fe, Ru have been reported as well as bimetallic alloys of these elements [5]. One example is shown in Figure 1a, where Fe-Ni exsolved particles in  $\text{Sr}_{0.95}\text{Ti}_{0.3}\text{Fe}_{0.63}\text{Ni}_{0.07}\text{O}_3$  (STFN) anodes resulted in higher SOFC power density compared with  $\text{SrTi}_{0.3}\text{Fe}_{0.7}\text{O}_3$  (STF) anodes with no metal exsolution, explained by enhanced H<sub>2</sub> adsorption [6]. With large surface area and good catalytic capability, perovskite anodes with exsolved nanoparticles have often shown similar or sometimes even superior electrochemical performance than un-exsolved perovskite anodes and conventional cermet anodes. For example, a recent study comparing different anodes in otherwise similar SOFCs showed superior performance of STF-Ni and  $\text{Sr}_{0.95}(\text{Ti}_{0.3}\text{Fe}_{0.63}\text{Ru}_{0.07})\text{O}_3$  (STFR), the latter with Fe-Ru nanoparticles, compared to Ni-YSZ or STF (Figure 1b) [7]. Different from infiltrated nanoparticles, exsolved nanoparticles have been shown to be socketed into the parent perovskite surface, making them more resistant to sintering and thereby offering better long-term stability [8]. Exsolution anodes general provide good redox cycling capability due to the low metal content compared to Ni-YSZ, and it may be possible to regenerate such anodes by redox cycling [9]. Moreover, exsolved anodes are more resistant than conventional cermet anodes to carbon coking [8] and sulfur poisoning [10].

## 7.2 Current and Future Challenges



1  
2  
3  
4  
5  
6  
7  
8  
9  
10  
11  
12  
13  
14  
15  
16  
17  
18  
19  
20  
21  
22  
23  
24  
25  
26  
27  
28  
29  
30  
31  
32  
33  
34  
35  
36  
37  
38  
39  
40  
41  
42  
43  
44  
45  
46  
47  
48  
49  
50  
51  
52  
53  
54  
55  
56  
57  
58  
59  
60

Despite the development over the last 15 years, challenges remain for the application of SOFC exsolution anodes. Exsolution is usually induced by high temperature reduction of SOFC anodes, and it has been reported that reduction temperature [11], time [12] and atmosphere ( $pO_2$ ) [13] can all affect the morphology, size and density of the exsolved nanoparticles, leading to different electrochemical properties. Thus, it is still unclear how to tailor the exsolution process to optimize the performance. Moreover, given the fact that exsolution is the result of decomposition, phase transformation of the parent perovskite may occur simultaneously with exsolution. Both positive [14] and negative [15] effects have been reported for the conductivity and electrochemical activity of the exsolved anode due to a phase change, suggesting a complicated synergy between exsolved particles and their parent oxide structure. Furthermore, the optimization and tailoring of the composition of exsolved particles remain challenging, especially for materials with multiple cations on B sites where bi-metallic exsolution happens upon reduction. A model has been proposed to predict the composition of the exsolved bi-metallic nanoparticles [6], but it needs further validation. It is also unclear how the alloy composition affects the electrochemical performance of the SOFC anodes.

In addition to electrochemical performance, operational durability of the exsolved SOFC anodes is also of great importance. Different from SOFCs with conventional cermet anodes, durability tests for SOFCs with exsolved perovskite anodes have only been in the range of hundreds of hours [6], [16]; there is no consensus as to the main degradation mechanisms for these anodes. Moreover, there is a lack of long-term stability studies of exsolved SOFC anodes under different real-life fuel conditions (e.g. different steam contents, carbon and sulfur-containing fuels, and different redox cycles).

Finally, due to the operating conditions of SOFC anodes (high temperature, reducing atmosphere), it is challenging to study exsolved nanoparticle formation and oxide phase changes *in operando*, limiting our understanding of the exsolution process. Measurements made after cell operation and cooling to ambient temperature may introduce significant artifacts that obfuscate the true structure.

### 7.3 Advances in Science and Technology to Meet Challenges

To meet the challenges noted above, a better fundamental understanding of the exsolution process during SOFC operation is needed. *In situ* characterization methods such as *in situ* X-ray Diffraction (XRD) [15], thermogravimetric analysis [6], and environmental transmission electron microscopy (TEM) [13] have all been used to elucidate the exsolution process (examples shown in Figure 2), but the number of studies focusing on the fundamental understanding of exsolution is limited. Developing and utilizing advanced characterization in the SOFC anode environment (high temperature, reducing atmosphere) will help reveal the anode morphological and compositional evolution including exsolved particle size, composition, and density as well as oxide phase changes, improving the mechanistic understanding of exsolution and leading to better control of the exsolution process.

Moreover, theory and modeling will complement the experimental studies to better understand exsolution. Beyond the density functional theory (DFT) studies on phase reconstruction and nanoparticle formation during metal exsolution [14], [17], the scientific community would benefit from more modeling work to investigate the relationship between

exsolution conditions, the microstructure and composition of exsolved anodes, and resulting electrochemical properties. *Finite modeling analysis could help investigate the change of electrochemical properties of the material during exsolution and phase-field modeling could also provide a powerful tool to simulate the formation and evolution of exsolved particles.*

Finally, while some studies have shown that exsolved nanoparticles can enhance the electronic conductivity of the anode [18], [19], perovskite-based SOFC anodes generally suffer from low electronic conductivity compared with their cermet counterparts. This could lead to significant resistance losses when exsolved anode materials are scaled up from the button cell to the stack level. Although this could be minimized via optimized interconnect designs, it will likely be important to develop higher conductive exsolution anodes and related oxide current collector materials.

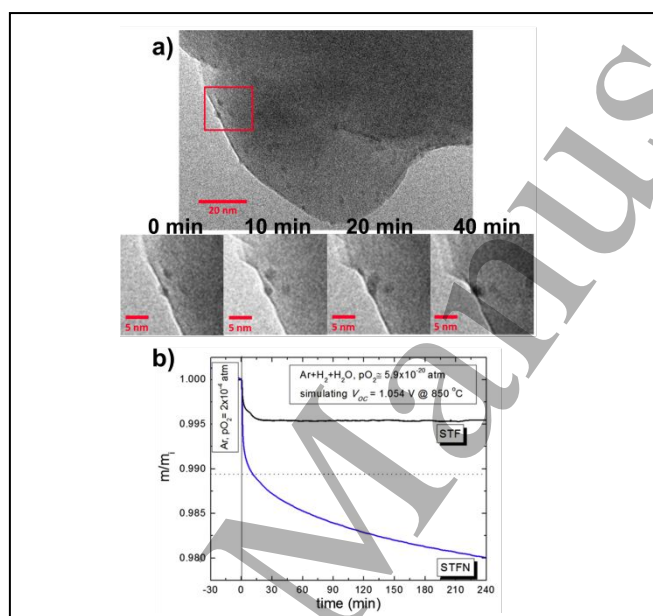


Figure 2 - Examples of in situ exsolution characterization: a) transmission electron microscopy (TEM) images of Ru exsolution from  $(La,Sr)(Cr,Fe,Ru)O_3$  after exposure to vacuum for 0, 10, 20 and 40 mins at 750°C, showing coalescence of two exsolved Ru particles; b) thermogravimetric analyses of  $SrTi_{0.3}Fe_{0.7}O_3$  (STF) and  $Sr_{0.95}Ti_{0.3}Fe_{0.63}Ni_{0.07}O_3$  (STFN) after exposure to a reducing atmosphere at 850°C, where the Ni exsolution from STF results in a much larger mass loss compared to STF. Data in a) provided courtesy of Elizabeth C. Miller [20]; b) reprinted from Ref. [6] with permission from Elsevier, 2018.

#### 7.4 Concluding Remarks

Alloy exsolution on SOFC anodes has been a fast-growing research field over the past 15 years. The enhanced electrochemical performance and stability against coking, impurity poisoning, and redox cycling have made exsolved perovskite materials a promising alternative to the incumbent cermet anodes. Despite the progress that has been made, there are great opportunities for further R&D, e.g., to improve the fundamental understanding of the exsolution process, study long-term stability, and develop new compositions with improved electronic conductivity, with the goal of developing highly active, durable exsolved SOFC perovskite anodes. Further development should also include implementation of exsolved materials in large-area SOFCs and stacks.

#### 7.5 Acknowledgements

The authors gratefully acknowledge financial support from Department of Energy grant # DE-SC0016965, and Department of Energy grant # DE-FE0031986, which equally supported the authors in writing this review.

## 7.6 References

- [1] E. D. Wachsman and K. T. Lee, "Lowering the Temperature of Solid Oxide Fuel Cells," *Science*, vol. 334, no. 6058, pp. 935–939, Nov. 2011, doi: 10.1126/science.1204090.
- [2] Z. Gao, L. V. Mogni, E. C. Miller, J. G. Railsback, and S. A. Barnett, "A Perspective On Low-Temperature Solid Oxide Fuel Cells," *Energy Environ. Sci.*, vol. 9, no. 5, pp. 1602–1644, 2016, doi: 10.1039/C5EE03858H.
- [3] T. Klemensø, K. Thydén, M. Chen, and H.-J. Wang, "Stability of Ni–Yttria Stabilized Zirconia Anodes Based on Ni-Impregnation," *J. Power Sources*, vol. 195, no. 21, pp. 7295–7301, Nov. 2010, doi: 10.1016/j.jpowsour.2010.05.047.
- [4] B. D. Madsen, W. Kobsiriphat, Y. Wang, L. D. Marks, and S. A. Barnett, "Nucleation of Nanometer-Scale Electrocatalyst Particles in Solid Oxide Fuel Cell Anodes," *J. Power Sources*, vol. 166, no. 1, pp. 64–67, Mar. 2007, doi: 10.1016/j.jpowsour.2006.12.080.
- [5] T. Cao, O. Kwon, R. J. Gorte, and J. M. Vohs, "Metal Exsolution to Enhance the Catalytic Activity of Electrodes in Solid Oxide Fuel Cells," *Nanomaterials*, vol. 10, no. 12, pp. 1–23, 2020, doi: 10.3390/nano10122445.
- [6] T. Zhu, H. E. Troiani, L. V. Mogni, M. Han, and S. A. Barnett, "Ni-Substituted Sr(Ti,Fe)O<sub>3</sub> SOFC Anodes: Achieving High Performance via Metal Alloy Nanoparticle Exsolution," *Joule*, vol. 2, no. 3, pp. 478–496, Mar. 2018, doi: 10.1016/j.joule.2018.02.006.
- [7] S.-L. Zhang *et al.*, "Advanced Oxygen-Electrode-Supported Solid Oxide Electrochemical Cells with Sr(Ti,Fe)O<sub>3-δ</sub>-Based Fuel Electrodes for Electricity Generation and Hydrogen Production," *J. Mater. Chem. A*, vol. 8, no. 48, pp. 25867–25879, 2020, doi: 10.1039/D0TA06678H.
- [8] D. Neagu *et al.*, "Nano-Socketed Nickel Particles with Enhanced Coking Resistance Grown In Situ by Redox Exsolution," *Nat. Commun.*, vol. 6, no. 1, p. 8120, Nov. 2015, doi: 10.1038/ncomms9120.
- [9] D. M. Bierschenk *et al.*, "Pd-substituted (La,Sr)CrO<sub>3-δ</sub>-Ce<sub>0.9</sub>Gd<sub>0.1</sub>O<sub>2-δ</sub> Solid Oxide Fuel Cell Anodes Exhibiting Regenerative Behavior," *J. Power Sources*, vol. 196, no. 6, pp. 3089–3094, Mar. 2011, doi: 10.1016/j.jpowsour.2010.12.050.
- [10] H. Li *et al.*, "Exsolved Alloy Nanoparticles Decorated Ruddlesden–Popper Perovskite as Sulfur-Tolerant Anodes for Solid Oxide Fuel Cells," *Energy & Fuels*, vol. 34, no. 9, pp. 11449–11457, Sep. 2020, doi: 10.1021/acs.energyfuels.0c02228.
- [11] W. Kobsiriphat, B. D. Madsen, Y. Wang, L. D. Marks, and S. A. Barnett, "La<sub>0.8</sub>Sr<sub>0.2</sub>Cr<sub>1-x</sub>Ru<sub>x</sub>O<sub>3-δ</sub>-Gd<sub>0.1</sub>Ce<sub>0.9</sub>O<sub>1.95</sub> Solid Oxide Fuel Cell Anodes: Ru Precipitation and Electrochemical Performance," *Solid State Ionics*, vol. 180, no. 2–3, pp. 257–264, Mar. 2009, doi: 10.1016/j.ssi.2008.12.022.
- [12] S. A. Horlick, Y.-L. Huang, I. A. Robinson, and E. D. Wachsman, "Controlling Exsolution with a Charge-Balanced Doping Approach," *Nano Energy*, vol. 87, no. March, p. 106193, Sep. 2021, doi: 10.1016/j.nanoen.2021.106193.
- [13] D. Neagu *et al.*, "In Situ Observation of Nanoparticle Exsolution from Perovskite Oxides: From

- Atomic Scale Mechanistic Insight to Nanostructure Tailoring,” *ACS Nano*, vol. 13, no. 11, pp. 12996–13005, 2019, doi: 10.1021/acsnano.9b05652.
- [14] Y. Sun *et al.*, “New Opportunity for In Situ Exsolution of Metallic Nanoparticles on Perovskite Parent,” *Nano Lett.*, vol. 16, no. 8, pp. 5303–5309, Aug. 2016, doi: 10.1021/acs.nanolett.6b02757.
- [15] X. Chen, W. Ni, J. Wang, Q. Zhong, M. Han, and T. Zhu, “Exploration of Co-Fe Alloy Precipitation and Electrochemical Behavior Hysteresis Using Lanthanum and Cobalt Co-Substituted  $\text{SrFeO}_{3.6}$  SOFC Anode,” *Electrochim. Acta*, vol. 277, pp. 226–234, Jul. 2018, doi: 10.1016/j.electacta.2018.05.019.
- [16] H. Lv *et al.*, “In Situ Investigation of Reversible Exsolution/Dissolution of CoFe Alloy Nanoparticles in a Co-Doped  $\text{Sr}_2\text{Fe}_{1.5}\text{Mo}_{0.5}\text{O}_{6-\delta}$  Cathode for  $\text{CO}_2$  Electrolysis,” *Adv. Mater.*, vol. 32, no. 6, p. 1906193, Feb. 2020, doi: 10.1002/adma.201906193.
- [17] I. Hamada, A. Uozumi, Y. Morikawa, A. Yanase, and H. Katayama-Yoshida, “A Density Functional Theory Study of Self-Regenerating Catalysts  $\text{LaFe}_{1-x}\text{M}_x\text{O}_{3-y}$  ( $\text{M} = \text{Pd}, \text{Rh}, \text{Pt}$ ),” *J. Am. Chem. Soc.*, vol. 133, no. 46, pp. 18506–18509, Nov. 2011, doi: 10.1021/ja110302t.
- [18] B. Hua, M. Li, Y.-F. Sun, J.-H. Li, and J.-L. Luo, “Enhancing Perovskite Electrocatalysis of Solid Oxide Cells Through Controlled Exsolution of Nanoparticles,” *ChemSusChem*, vol. 10, no. 17, pp. 3333–3341, Sep. 2017, doi: 10.1002/cssc.201700936.
- [19] Y. Sun *et al.*, “A-Site Deficient Perovskite: the Parent for In Situ Exsolution of Highly Active, Regenerable Nano-Particles as SOFC Anodes,” *J. Mater. Chem. A*, vol. 3, no. 20, pp. 11048–11056, 2015, doi: 10.1039/C5TA01733E.
- [20] E. C. Miller, “Synthesis, Characterization, and Optimization of Novel Solid Oxide Fuel Cell Anodes,” Northwestern University, 2015.

## Section 8 – Exsolution for solid oxide $\text{CO}_2$ and/or $\text{H}_2\text{O}$ co-electrolysis

Roelf Maring<sup>1</sup>, Vasileios Kyriakou<sup>1</sup>, Usman Mushtaq<sup>2</sup> and Mihalis N. Tsampas<sup>2</sup>

<sup>1</sup>Engineering & Technology Institute Groningen, University of Groningen, 9747 AG Groningen, the Netherlands

<sup>2</sup>Dutch Institute for Fundamental Energy Research (DIFFER), 5612 AJ Eindhoven, the Netherlands

### 8.1 Status

Solid oxide electrolysis cells (SOECs) are advanced electrochemical energy storage and conversion devices with high energy efficiencies. They offer attractive high-temperature  $\text{CO}_2$  and/or  $\text{H}_2\text{O}$  electrolysis routes that can reduce anthropogenic  $\text{CO}_2$  emissions, enabling large-scale energy storage and facilitate the integration of renewable energy into the electric grid [1]–[3]. A SOEC mainly consists of a fuel electrode, an oxygen electrode and a dense ceramic electrolyte. During operation, the electrode materials offer catalytically active sites for  $\text{CO}_2$  and/or  $\text{H}_2\text{O}$  reduction and oxygen evolution reactions respectively, while the electrolyte provides the required pathway for transporting oxide ions from the fuel to the oxygen electrode.

The electrochemical  $\text{CO}_2$  and/or  $\text{H}_2\text{O}$  conversion and utilization was originally presented as a technique for oxygen regeneration in spacecraft habitats in the US manned spaceflight program in the mid-1960s and as an in-situ resource utilization technology for Mars in the 1970s. In view of energy transition in the beginning of the 21<sup>st</sup> century, the concept has regained momentum as a key

1  
2  
3 technological enabler for renewable energy approach of re-introducing CO<sub>2</sub> in the energy and  
4 chemical cycles [1]–[3].  
5

6  
7 The economic feasibility of transforming CO<sub>2</sub> emissions into value-added products strongly  
8 depends on the decarbonization policies (e.g. carbon taxation), as well as electricity prices.  
9 Technoeconomic studies have highlighted the potential of combining SOECs CO<sub>2</sub> and/or H<sub>2</sub>O  
10 electrolysis with current chemical processes, such as Fischer–Tropsch synthesis for liquid fuels  
11 production and methanation.. In this context, a recent assessment of power-to-gasoline conversion  
12 reported a gasoline price of 2.25 euros/liter [4] Moreover, the production of synthetic natural gas  
13 through co-electrolysis in combination with thermal integration can achieve overall electric  
14 efficiencies of >80% while via low temperature electrolysis the efficiency is limited to 60-70% [5]  
15 However, in such studies the necessity of overcoming material degradations issues is highlighted.  
16  
17  
18

19 The approaches to deal with degradation issues are focused on altering operating conditions  
20 and modifying cell architecture by optimizing or substituting SOEC components, especially electrode  
21 or electrolyte materials. The concept of exsolution has been proposed and successfully implemented  
22 for increasing electrocatalytic activity and stability of electrode materials in SOECs. Due to its unique  
23 feature of probing the electrode interface and bulk, exsolution is considered as an emerging toolbox  
24 for solving electrode material degradation issues , thus bringing the concept to the required maturity  
25 for commercial applications [1]–[3], [6]  
26  
27  
28

## 29 8.2 Current and Future Challenges

30  
31 The technical maturity of CO<sub>2</sub> and/or H<sub>2</sub>O co-electrolysis is high but still not sufficient to reach  
32 the requirements for practical implementation or commercialization. This is due to several major  
33 challenges from which degradation is one of the most noteworthy followed by low  
34 activation/conversion efficiency [1]–[3]. Under practical operations, the lowest degradation reported  
35 at cell level is ~1.7% per 1000 h at ~1 A cm<sup>-2</sup>, while at short stack level degradation is much higher, i.e.  
36 18% per 1000 h [1]. Therefore, to reduce degradation and prolong the lifetime, SOEC studies has been  
37 focused on elucidating the degradation mechanism that can be used as guideline for the development  
38 materials [2], [7].  
39  
40  
41

42  
43 The main technological challenges observed for the SOEC co-electrolysis cell with commonly used  
44 components include [1]–[3], [8]:  
45

- 46 • **Fuel electrode:** limiting long-term performance degradation issues when operating at high current  
47 densities (>1 A.cm<sup>-2</sup>), including nickel agglomeration and depletion, degradation issues due to  
48 chemical interaction with reductive/oxidative (redox) gas atmospheres.
- 49 • **Electrolyte:** maintaining high ionic conductivity and sufficient mechanical strength for lower  
50 operating temperature (<700°C) and thickness.
- 51 • **Oxygen electrode:** mitigating long-term performance degradation issues when operating at high  
52 current densities (>1 A.cm<sup>-2</sup>), including species migration (Sr, Co, etc.), delamination from the  
53 electrolyte (or buffer barrier layer), cracking and poisoning.
- 54 • **Intermediate layer(s):** ensuring physicochemical compatibility with both electrolyte and electrode  
55 materials to allow sufficient performance over long-term operation  
56  
57  
58  
59  
60

- **Poisoning** of the electrode materials from volatile contaminants (Cr, B, S, Si originated from the interconnect, the glass sealant and the inlet streams) damage the stability and activity of electrode performance.

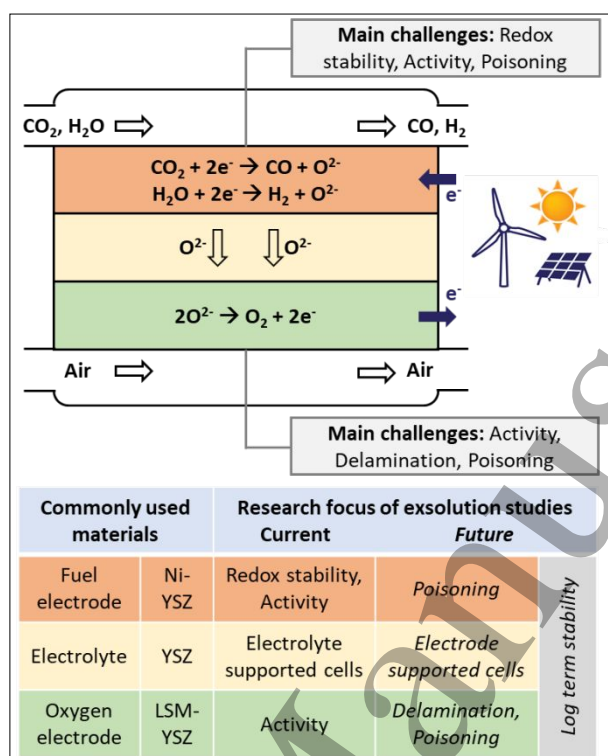


Figure 1 - (Top) Schematic diagram of solid oxide electrolyte cell operating for CO<sub>2</sub> and H<sub>2</sub>O co-electrolysis, with main challenges of the fuel and oxygen electrode. (Bottom) Commonly used materials, current and future research focus of alternative material based on exsolution

There are promising alternative materials that have the potential to address several of the aforementioned challenges, however, their implementation in SOECs will necessitate optimization of alternative fabrication methods. Current, focus has been given in the development of two classes of SOECs i.e. Ni-YSZ (Ytria stabilized zirconia) composite electrode and ScSZ (Scandia-stabilized zirconia) based electrolyte supported cells [8]. These two technologies are distinguished by the thick layer that provides mechanical support to the cell and this leads to operating temperature and performance discrepancies, and thus, it is essential to be able to implement both approaches in SOECs with exsolved electrode materials [8].

### 8.3 Advances in Science and Technology to Meet Challenges

Recent studies in the SOEC field suggests that there has been significant progress towards limiting the aforementioned issues. Some challenges were addressed by modifying the operating conditions. For instance, reactant purification and operation at lower temperature has been shown to hinder poisoning, while the reversible operation could decrease delamination of the oxygen electrode [1]–[3]. Herein, however, we will focus on solutions that could emanate by exploring alternative electrode components.

Regarding the development of SOECs, in addition to fundamental understanding, two main directions for enhancing materials performance include modification or decoration of state-of-the-art (SoA) electrodes, and development of new advanced electrode materials. In both directions, it appears that exsolution could have a pivotal role [1]–[3], [6]. Exsolved nanoparticles display remarkable stability, limited agglomeration while they have low tendency for coking, due to their firm anchoring to the ceramic surface. Furthermore, the method is faster, cheaper and gives better access to hardly reachable locations than conventional impregnation methods, and concurrently maintain exceptional control over the amount and distribution of deposited particles [8]

**Fuel electrode:** Compared to traditional Ni–YSZ electrodes, the perovskite oxides may display mixed ionic –electronic conductivity, superior redox activity and long-term operation stability. Moreover, the socketed nature of the particles offer superior resistance to carbon deposition and sulfur poisoning than their counterparts prepared by wet deposition methods [9]. Perovskites decorated with exsolved nanoparticle of Ni [10], Fe [11], Co [12], NiFe [13] and CoFe [14] have been successfully implemented on increasing electrochemical activity (catalytic activity and conductivity) and redox stability of fuel electrodes for co-electrolysis. It worth to note that perovskites (in contract with Ni-YSZ) can operate in the absence any gaseous reducing agent (e.g. H<sub>2</sub>, CO) hence decreasing the total cost and complexity of the process. Table 1 summarizes recent representative co-electrolysis studies with exsolved fuel electrodes and provides a comparison with Ni-YSZ as fuel electrode on both electrolyte and Ni-YSZ electrode supported cells [10], [15]. The comparison is challenging due to difference in reaction conditions, as well as cell architectures which implies the need for the creation of a protocol for benchmarking the performance of different electrodes. Nevertheless, the table provides evidence that exsolved electrodes are competitive to state-of-the-art materials in terms of electrocatalytic activity even when no protecting gas atmosphere is used.

**Oxygen electrode:** Apart from fuel electrodes either in electrolysis or fuel cell operation, the concept has shown potential for improving the activity of oxygen electrodes [16]–[18]. For instance, Ag exsolved nanocatalysts on perovskites have been reported as highly active oxygen electrodes for SOFCs [17,18]. The excellent performance in terms of electrocatalytic activity and stability is attributed to the synergistic effect of socketed Ag, which acts as a catalytic core to boost surface exchange rates, combined with the promotion of the charge transfer reaction at the Ag-oxide interface. Electrodes with such properties worth to be investigated as a possible solution to delamination, that it is observed in LSM (La<sub>0.8</sub>Sr<sub>0.2</sub>MnO<sub>3-δ</sub>) based electrodes at long term operation.

**SOEC architecture:** Despite the high potential of exsolved electrodes for SOECs their implementation is mainly limited on electrolyte supported cells due to fabrication challenges. Perovskite electrode supported cells have been recently demonstrated for both SOFC and SOEC applications, exhibiting very promising performance, by utilizing a combination of LSM–YSZ oxygen electrode backbone infiltrated with an SrTi<sub>0.3</sub>Fe<sub>0.6</sub>Co<sub>0.1</sub>O<sub>3-δ</sub> perovskite and Sr<sub>0.95</sub>Ti<sub>0.3</sub>Fe<sub>0.63</sub>M<sub>0.07</sub>O<sub>3-δ</sub> (M=Ni or Ru) fuel electrodes nanoengineered with exsolution [19]. This approach could be adapted to expand the concept of exsolution in both fuel and oxygen electrodes for boosting the overall performance and/or decrease the operating temperature.

Table 1 - Summary of recent works in CO<sub>2</sub> and H<sub>2</sub>O solid oxide co-electrolysis with perovskite fuel electrodes decorated with exsolved nanoparticles. The performance of Ni/YSZ electrode and electrolyte supported cells is also given for comparison.

Cell type	Electrolyte	T	Feed composition	Current density (A cm <sup>-2</sup> )
-----------	-------------	---	------------------	---------------------------------------

(Fuel electrode is indicated with bold)	thickness (mm)	(°C)		@1.3 V	@1.6 V
<b>LCTN-Ni</b> //GDC//SCSZ//LSM/YSZ//LSM <sup>[10]</sup>	150	850	25.0% CO <sub>2</sub> -25.0% H <sub>2</sub> O-50.0% N <sub>2</sub>	0.70	1.00
<b>SFM-Fe</b> /SDC//LSGM//SDC/SFM <sup>[11]</sup>	600	850	50.0% CO <sub>2</sub> -50.0% H <sub>2</sub> O	0.58	1.27
<b>SFCM-Co</b> //LSGM//SFCM <sup>[12]</sup>	300	800	45.0% CO <sub>2</sub> -45.0% H <sub>2</sub> O-10.0% H <sub>2</sub>	1.25	2.30
<b>LSFN-NiFe</b> /GDC//LSGM//GDC/PBCC <sup>[13]</sup>	260	800	50.0% CO <sub>2</sub> -50.0% H <sub>2</sub> O	1.00	2.00
<b>STCF-CoFe</b> //LSGM//STCF <sup>[14]</sup>	270	800	50.0% CO <sub>2</sub> -50.0% H <sub>2</sub> O	0.50	0.95
For benchmarking					
Ni/YSZ//GDC//ScCeSZ//LSM/YSZ//LSM <sup>[10]</sup>	150	850	25.0% CO <sub>2</sub> -25.0% H <sub>2</sub> O-50.0% N <sub>2</sub>	0.50	0.75
Ni/YSZ//YSZ//GDC/LSCF <sup>[15]</sup>	15	800	25.0% CO <sub>2</sub> -50.0% H <sub>2</sub> O-25.0% H <sub>2</sub>	1.35	-

#### 8.4 Concluding Remarks

As a powerful toolbox that could combine numerous elements and preparation methods, exsolution is already a proven option to solve a series of challenges in solid oxide co-electrolysis of CO<sub>2</sub> and H<sub>2</sub>O towards upscaling. The solutions identified primarily concern the cell assembly development, such as improved fuel or oxygen electrodes to enhance redox stability and decrease operating temperature towards developing cheaper cell stacks with long-term stability. The reported advances in materials fabrication and exsolution triggering methods (see chapter 1) may be combined with modern machine learning in order to develop high performance electrodes with tailored properties. It is critical that the future works in the field should focus not only on new materials development but also on evaluating exsolved nanoparticles in long-term durability studies in realistic conditions or even in the presence of poisonous compounds. Also, the area can be critically benefited by advances related to perovskite electrode-supported cells to enable high performance cells (where both electrodes will be nanoengineered with exsolution) with thin electrolytes similar to the Ni-YSZ supported cells which have been practically commercialized.

#### 8.5 Acknowledgements

This work has been carried out within the ViSEP program (733.000.006) funded jointly by the Netherlands Organization for Scientific Research (N.W.O.) and Shell.

#### 8.6 References

- [1] Y. Zheng, J. Wang, B. Yu, W. Zhang, J. Chen, J. Qiao, and J. Zhang, 'A review of high temperature co-electrolysis of H<sub>2</sub>O and CO<sub>2</sub> to produce sustainable fuels using solid oxide electrolysis cells (SOECs): Advanced materials and technology', *Chem. Soc. Rev.*, vol. 46, no. 5, pp. 1427–1463, 2017, doi: 10.1039/c6cs00403b.
- [2] A. Hauch, R. Küngas, P. Blennow, A. B. Hansen, J. B. Hansen, B. V. Mathiesen, and M. B. Mogensen, 'Recent advances in solid oxide cell technology for electrolysis', *Science (80-. )*, vol. 370, no. 6513, 2020, doi: 10.1126/science.aba6118.
- [3] A. Hauch, M. L. Traulsen, R. Küngas, and T. L. Skaftø, 'CO<sub>2</sub> electrolysis – Gas impurities and electrode overpotential causing detrimental carbon deposition', *J. Power Sources*, vol. 506, no. June 2021, p. 230108, 2021, doi: 10.1016/j.jpowsour.2021.230108.
- [4] L. Wang, M. Chen, R. Küngas, T. E. Lin, S. Diethelm, F. Maréchal, and J. Van herle, 'Power-to-fuels via solid-oxide electrolyzer: Operating window and techno-economics', *Renew. Sustain. Energy Rev.*, vol. 110, no. May, pp. 174–187, 2019, doi: 10.1016/j.rser.2019.04.071.
- [5] H. Böhm, M. Lehner, and T. Kienberger, 'Techno-Economic Assessment of Thermally Integrated Co-Electrolysis and Methanation for Industrial Closed Carbon Cycles', *Front. Sustain.*, vol. 2, no.



- September, pp. 1–16, 2021, doi: 10.3389/frsus.2021.726332.
- [6] K. Kousi, C. Tang, I. S. Metcalfe, and D. Neagu, 'Emergence and Future of Exsolved Materials', *Small*, vol. 17, no. 21, 2021, doi: 10.1002/smll.202006479.
- [7] J. T. S. Irvine, D. Neagu, M. C. Verbraeken, C. Chatzichristodoulou, C. Graves, and M. B. Mogensen, 'Evolution of the electrochemical interface in high-temperature fuel cells and electrolyzers', *Nat. Energy*, vol. 1, no. 1, pp. 1–13, 2016, doi: 10.1038/nenergy.2015.14.
- [8] A. Nechache and S. Hody, 'Alternative and innovative solid oxide electrolysis cell materials: A short review', *Renew. Sustain. Energy Rev.*, vol. 149, 2021, doi: 10.1016/j.rser.2021.111322.
- [9] D. Neagu, T. S. Oh, D. N. Miller, H. Ménard, S. M. Bukhari, S. R. Gamble, R. J. Gorte, J. M. Vohs, and J. T. S. Irvine, 'Nano-socketed nickel particles with enhanced coking resistance grown in situ by redox exsolution', *Nat. Commun.*, vol. 6, 2015, doi: 10.1038/ncomms9120.
- [10] V. Kyriakou, D. Neagu, E. I. Papaioannou, I. S. Metcalfe, M. C. M. van de Sanden, and M. N. Tsampas, 'Co-electrolysis of H<sub>2</sub>O and CO<sub>2</sub> on exsolved Ni nanoparticles for efficient syngas generation at controllable H<sub>2</sub>/CO ratios', *Appl. Catal. B Environ.*, 2019, doi: 10.1016/j.apcatb.2019.117950.
- [11] S. Hou and K. Xie, 'Enhancing the performance of high-temperature H<sub>2</sub>O/CO<sub>2</sub> co-electrolysis process on the solid oxide Sr<sub>2</sub>Fe<sub>1.6</sub>Mo<sub>0.5</sub>O<sub>6-δ</sub>-SDC/LSGM/Sr<sub>2</sub>Fe<sub>1.5</sub>Mo<sub>0.5</sub>O<sub>6-δ</sub>', *Electrochim. Acta*, vol. 301, pp. 63–68, 2019, doi: 10.1016/j.electacta.2019.01.164.
- [12] Y. Yang, Y. Wang, Z. Yang, Y. Chen, and S. Peng, 'A highly active and durable electrode with in situ exsolved Co nanoparticles for solid oxide electrolysis cells', *J. Power Sources*, vol. 478, no. August, p. 229082, 2020, doi: 10.1016/j.jpowsour.2020.229082.
- [13] L. Bian, C. Duan, L. Wang, Z. Chen, Y. Hou, J. Peng, X. Song, S. An, and R. O'Hayre, 'An all-oxide electrolysis cells for syngas production with tunable H<sub>2</sub>/CO yield via co-electrolysis of H<sub>2</sub>O and CO<sub>2</sub>', *J. Power Sources*, vol. 482, no. June 2020, p. 228887, 2021, doi: 10.1016/j.jpowsour.2020.228887.
- [14] B. Niu, C. Lu, W. Yi, S. Luo, X. Li, X. Zhong, X. Zhao, and B. Xu, 'In-situ growth of nanoparticles-decorated double perovskite electrode materials for symmetrical solid oxide cells', *Appl. Catal. B Environ.*, vol. 270, no. February, p. 118842, 2020, doi: 10.1016/j.apcatb.2020.118842.
- [15] Zhan, Z., Kobsiriphat, W., Wilson, J. R., Pillai, M., Kim, I., & Barnett, S. A. (2009). Syngas production by coelectrolysis of CO<sub>2</sub>/H<sub>2</sub>O: the basis for a renewable energy cycle. *Energy & Fuels*, 23(6), 3089–3096.
- [16] J. H. Kim, J. K. Kim, H. G. Seo, D. K. Lim, S. J. Jeong, J. Seo, J. Kim, and W. C. Jung, 'Ex-Solved Ag Nanocatalysts on a Sr-Free Parent Scaffold Authorize a Highly Efficient Route of Oxygen Reduction', *Adv. Funct. Mater.*, vol. 30, no. 27, pp. 1–9, 2020, doi: 10.1002/adfm.202001326.
- [17] Y. Zhu, W. Zhou, R. Ran, Y. Chen, Z. Shao, and M. Liu, 'Promotion of Oxygen Reduction by Exsolved Silver Nanoparticles on a Perovskite Scaffold for Low-Temperature Solid Oxide Fuel Cells', *Nano Lett.*, vol. 16, no. 1, pp. 512–518, 2016, doi: 10.1021/acs.nanolett.5b04160.
- [18] Y. Chen *et al.*, 'A robust and active hybrid catalyst for facile oxygen reduction in solid oxide fuel cells', *Energy Environ. Sci.*, vol. 10, no. 4, pp. 964–971, 2017, doi: 10.1039/c6ee03656b.
- [19] S. L. Zhang, H. Wang, T. Yang, M. Y. Lu, C. X. Li, C. J. Li, and S. A. Barnett, 'Advanced oxygen-electrode-supported solid oxide electrochemical cells with Sr(Ti,Fe)O<sub>3-δ</sub>-based fuel electrodes for electricity generation and hydrogen production', *J. Mater. Chem. A*, vol. 8, no. 48, pp. 25867–25879, 2020, doi: 10.1039/d0ta06678h.

## Section 9 – Exsolution in solid state protonic systems

Youdong Kim and Ryan O'Hayre

Colorado School of Mines, Golden, CO, USA

### 9.1 Status

Oxide-based solid-state proton conducting systems [1] show significant potential for energy conversion applications including fuel cells/electrolysis cells, membrane reactors, and sensors. Their ability to operate at intermediate temperatures (350°C – 650°C) enables direct integration with important thermochemical processes, relaxes balance-of-plant requirements, and reduces degradation [2]. However, low operating temperatures lead to significant activity challenges, both for the oxygen reduction/evolution reactions facilitated by the air/steam electrode and for the fuel reduction/oxidation reactions facilitated by the fuel electrode. These challenges have led researchers to consider exsolution, first applied to oxygen-ion conductors, to increase electrochemical performance in protonic oxides as well.

Proton-conducting air/steam electrodes are typically based on mixed ionic and electronic-conducting perovskites that incorporate catalytically active transition metal(s) (such as Fe, Co, Ni, and/or Mn) on the B-site. Proton-conducting fuel electrodes generally involve ceramic-metallic (cermet) composites of Ni metal and a ceramic proton conductor. Electrocatalytic activity is generally sufficient at higher operating temperatures but diminishes greatly at lower temperatures (especially < 500 °C) [3]. Conventional electrode formation leads to relatively coarse microstructures and can trigger surface segregation processes that compromise activity, especially at lower temperatures [4-6].

Several strategies can enhance electrode performance, including infiltration [7], one-pot composite synthesis, patterned electrodes, and freeze casting. However, these approaches require additional processing steps and introduce constraints that add complexity and expense to cell fabrication. As a promising alternative, *in-situ* exsolution processes can greatly improve catalytic activity without requiring additional fabrication steps [8]. The approach involves the deliberate substitution of appropriate (typically transition-metal or noble-metal) dopants into a suitable oxide-based parent electrode which, when subjected to appropriate treatment conditions, triggers the exsolution of second phase nanoparticles derived from these dopants that decorate the electrode surface. These exsolved nanoparticles provide additional catalytic surface area and catalytic functionality and exhibit improved stability and cohesion with the parent electrode support relative to infiltrated, composited, or decomposition-derived nanoparticle catalysts. Thus, exsolution promises a new frontier to enhance the stability, functionality, and overall catalytic activity of protonic oxide devices.

Exsolution techniques have been applied to several protonic oxide systems.  $\text{Ba}_{0.95}\text{Ag}_{0.05}\text{Co}_{0.4}\text{Fe}_{0.4}\text{Zr}_{0.1}\text{Y}_{0.1}\text{O}_{3-6}$  air/steam electrode can undergo an Ag exsolution process under oxidizing conditions through a high-temperature steam-mediated air annealing process [9] (Figure 1 a-b). Exsolution of Ni and/or Ni-alloy nanoparticles from various proton-conducting fuel electrodes under reducing conditions has also been demonstrated. As in other systems, these nanoparticles are observed to exsolve in a socket-like fashion, leading to excellent catalytic performance and enhanced durability. For example, a  $\text{Ni}/\text{BaZr}_{0.8}\text{Y}_{0.2}\text{O}_{3-6}$  electrode with exsolved Ni nanoparticles achieved by *in-situ* conditioning of a solid-state reactive-sintered support demonstrated remarkable activity and stability under fuel cell operation with a variety of fuels over thousands of hours of testing [10] (Figure 1 c-d).

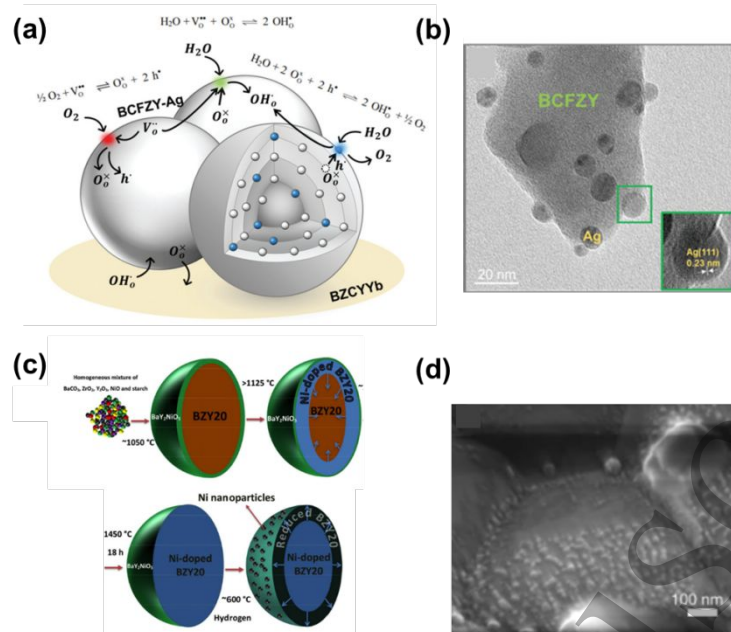
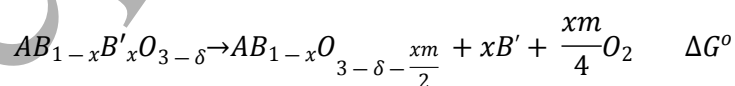


Figure 1 - Exsolution mechanism for positrode and negtrode of PCFCs. (a) schematic diagram of water-mediated exsolution of Ag-doped BCFZY for positrode. (b) SEM image of exsolved Ag on the surface of BCFZY. (c) in-situ exsolution process during solid state reactive sintering of Ni-BZY for negatrode. (d) SEM image of Ni exsolved BZY after 300hrs operation under humidified methane. Reprinted from [9,10]

## 9.2 Current and Future Challenges

Recent exsolution studies in oxygen-ion conductors have established general mechanistic insight [11], however little is known about potential mechanistic differences that might be associated with exsolution in protonic oxide systems. Exsolution represents a chemically driven heterogeneous phase transition, and involves four distinct physical processes of diffusion, reduction, nucleation, and growth. Typically, the chemical potential of oxygen in the gas phase surrounding the electrode (via the imposition of highly reducing conditions) provides the driving force for exsolution, although as previously discussed, the use of steam in mixed proton/electron-conducting oxides can induce exsolution under oxidizing conditions as well. Voltage bias, strain, topotactic conversion, and deliberate non-equilibrium cation deficiency can also serve as potential driving forces for exsolution [11]. For the case of oxygen reduction-driven exsolution, Barnett [12] has proposed a thermodynamic model accommodating both single and multi-cation exsolution processes. Generalized here for a simple perovskite undergoing single-cation exsolution of a reducible B-site dopant B' with oxidation state m, and assuming complete exsolution of the B' dopant:



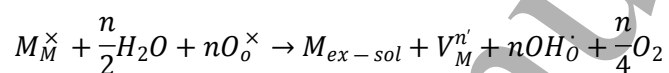
the critical oxygen partial pressure for exsolution ( $P_{O_2}^{Red}$ ) is:

$$(P_{O_2}^{Red})^{\frac{xm}{4}} = \left( \frac{a_{oxide}}{a_{oxide-ex}} \right) e^{-\frac{\Delta G^\circ}{RT}}$$

where  $a_{\text{oxide}}$  is the activity of the oxide before exsolution, and  $a_{\text{oxide-ex}}$  is the activity of the oxide after exsolution. Few oxide systems have sufficient thermodynamic information to establish  $a_{\text{oxide}}$  and  $a_{\text{oxide-ex}}$ , although thermogravimetric (TG) experiments [12] have enabled estimation of these quantities in limited cases. Because thermodynamic information is limited and exsolution models remain underdeveloped, predicting which parent oxide and dopant combinations lead to exsolution under accessible conditions remains a challenge. This challenge is further complicated for multi-cation exsolution processes and for protonic oxides, where competition between more/less reducible cations and/or multiple charge-compensating defects can further complicate analysis.

A germane example of this complexity is given by the aforementioned case of steam-driven exsolution in the mixed proton/electron-conducting  $\text{Ba}_{0.95}\text{Ag}_{0.05}\text{Co}_{0.4}\text{Fe}_{0.4}\text{Zr}_{0.1}\text{Y}_{0.1}\text{O}_{3-6}$  system.

It is hypothesized that proton uptake in steam-rich environments triggers the exsolution of the highly reducible noble metal dopant (M) with metal cation vacancies created for charge compensation:



Importantly, steam is required to trigger exsolution—changes in oxygen partial pressure alone are insufficient. Also, the process only occurs in “triple-conducting oxides”, special materials which accommodate the transport of three mobile charged defects-- protons, oxygen vacancies, and electron holes. The steam-mediated exsolution process is not observed to occur in more conventional oxygen vacancy/electron-hole mixed conducting oxides. This example demonstrates how the unique steam-modulated defect chemistry in protonic oxides represents not only a challenge for implementing exsolution processes— but also an opportunity— as it provides new pathways and mechanisms for exsolution not available in conventional oxygen-ion conducting systems.

Beyond improved mechanistic understanding and the consequent ability to predict suitable parent oxide and dopant systems amenable to exsolution, control over exsolved nanoparticle size and distribution represents another significant challenge. The relative rates of nucleation and growth for exsolved particles depend on many intrinsic and extrinsic properties including surface energies/wetting angles, cation diffusion rates, surface curvature/orientation, grain boundary densities, and mechanical stress/strain. Exsolved particle size and density depend on the strength of the exsolution driving force and exposure time, with larger driving forces and higher exposure times generally leading to larger particle sizes. Furthermore, the shape of exsolved nanoparticles can also be unpredictable. For example, mixtures of exsolved particles composed of Ni and Co can change shape from spherical to square or faceted based on the Kirkendall effect [13]. Recent work has applied classical nucleation and growth theories to describe exsolution, with strain, reactant-concentration, and diffusion-limited growth models proposed [14]. More work in this area is clearly warranted.

Exsolution in protonic systems brings additional challenges not typically present in conventional oxygen-ion conducting systems. Protonic-ceramic devices generally operate at lower temperatures than conventional oxygen-ion conducting devices. Thus, to trigger and control exsolution, initial conditioning may be required at temperatures far higher than the designed

operating temperature of the device, with potentially unknown or unexpected consequences. Furthermore, most protonic oxides involve high concentrations of Barium (often the dominant A-site constituent), which can lead to chemical stability issues during exsolution, as Ba surface segregation or Ba-based second phase decomposition products may compete against or complicate B-site cation exsolution under certain conditions (especially under high steam or CO<sub>2</sub>-rich conditions) [15].

### 9.3 Advances in Science and Technology to Meet Challenges

To further advance scientific understanding, detailed mechanistic studies leveraging advanced (especially *in-situ*) characterization techniques are needed. Physicochemical analysis and computational calculations are also desired to provide fundamental thermodynamic, defect-chemistry, and microstructural information to quantitatively model and predict exsolution behaviour. As identified earlier, special attention must be given to the mixed-ionic conduction character of most protonic oxides, as multiple species can play a role in mediating the exsolution process.

Powerful characterization techniques are needed to probe the fundamental mechanisms of exsolution, including synchrotron-based techniques (structure, bulk chemistry), in-operando XPS (surface chemistry), and in-operando TEM (surface structure, nanoparticle morphology, nucleation and growth kinetics). Synchrotron-based *in-situ* X-ray absorption near edge structure (XANES) and X-ray diffraction (XRD) can reveal the structural evolution and coordination of exsolved metal nanoparticles [16]. *In-operando* electron microscopy can also track exsolved particle evolution in real-time (and with temperature) providing unprecedented insights into the kinetics of exsolution (Figure 2a) [17]. The reader is directed to section 2 of this roadmap for further information. These intensive analytical techniques have not yet been adapted to protonic oxides due to the complex multi-species conduction behaviour and challenges working with water vapour in most analytical systems.

Computational modelling is also essential to inform the rational design of exsolution processes, and is discussed in more detail in section 3 of this roadmap. Basic trends in exsolution propensity from a perovskite lattice have been successfully predicted through density functional theory (DFT), see Figure 2b-c, with co-segregation energy between the host lattice and the exsolved metal as an important predictive factor [18]. Hofu similarly predicted favourable exsolution of bimetallic nanoparticles from a host lattice in an oxide-based CO<sub>2</sub> electrolysis cell by calculating segregation energies [19]. Unfortunately, DFT calculations are confined to relatively small systems (at most a few hundred atoms) and cannot easily incorporate important larger-scale features such as surface curvature or extended defects (grain boundaries, dislocations). To address this issue, the phase-field crystal (PFC) model can potentially link the atomic and mesoscopic scales [20]. Combining PFC models with *in-situ* characterization may be particularly well suited for understanding and predicting exsolution dynamics.

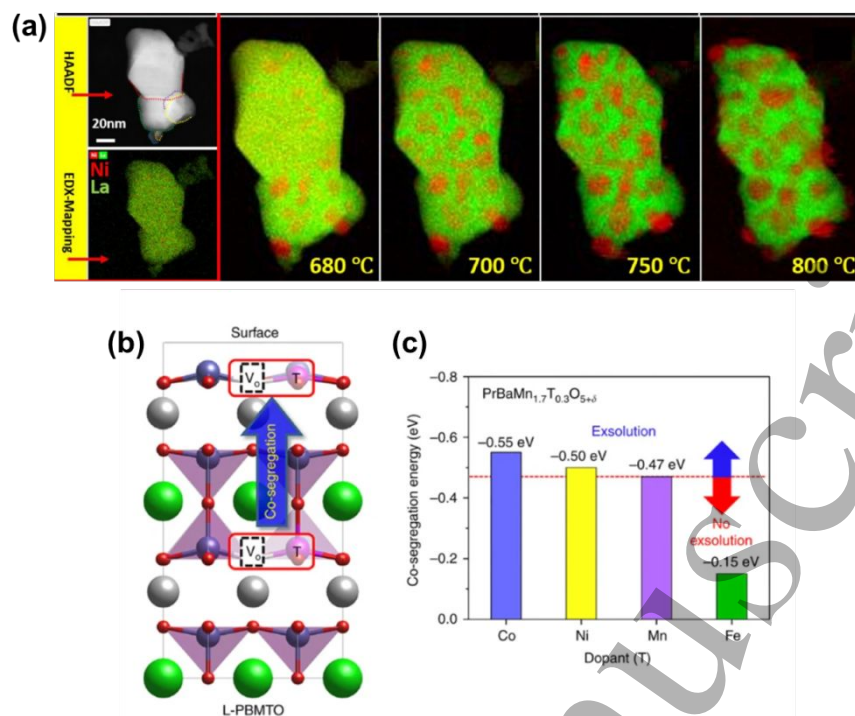


Figure 2 - Revealing exsolution mechanism using in-situ TEM and DFT calculation. (a) EELS maps of Ni and La elements of LaNiO<sub>3</sub> depending on temperature. (b) schematic illustration of DFT calculation model for PrBaMn<sub>1.7</sub>T<sub>0.3</sub>O<sub>5+δ</sub> (T=Mn, Co, Ni and ,Fe). (c) Calculation results of co-segregation energy of the dopant materials such as Co, Ni, Mn, Fe. Reprinted from [17, 18]

#### 9.4 Concluding Remarks

Significant enhancements in electrochemical performance and durability are achieved by employing in-situ exsolution-based strategies in proton-conducting electrode materials. The presence of multiple charge-compensating defects (protons, oxygen vacancies, electron holes) complicates exsolution behaviour. In particular, the steam-modulated defect chemistry in protonic oxides challenges mechanistic understanding but also provides new exsolution pathways not available in oxygen-ion conductors. While analogues from oxygen-ion conductors may provide a baseline for modelling exsolution in protonic oxides, additional insight from in-situ/in-operando characterization, and new mechanisms that capture the role of protonic defects are needed. Here, atomic level (e.g. DFT) and the mesoscale (e.g. PCF) modelling can contribute by informing basic defect-chemistry thermodynamics as well as the longer-range kinetic phenomena that determine exsolution dynamics. There are plenty of opportunities to contribute to this exciting and expanding field of research.

#### 9.5 Acknowledgements

Research supported as part of the Hydrogen in Energy and Information Sciences (HEISs), an Energy Frontier Research Center funded by the U.S. Department of Energy (DOE), Office of Science, Basic Energy Sciences (BES), under award #DE-SC0023450. In addition, Y. K. acknowledges funding from the U.S. Army Research Office through grant number W911NF-22-1-0273.

## 9.6 References

- [1] Takahashi T and Iwahara H 1981 Solid-state ionics: protonic conduction in perovskite type oxide solid solutions *Rev. Chim. Miner* 17 243–53
- [2] C. Duan, J. Huang, N. Sullivan, and R. O’Hayre, 2020 Proton-conducting oxides for energy conversion and storage, *Appl. Phys. Rev.* 7 011314
- [3] W. Bian, W. Wu, Y. Gao, J. Y. Gomez, H. Ding, W. Tang, M. Zhou, and D. Ding 2021 Regulation of cathode mass and charge transfer by structural 3D engineering for protonic ceramic fuel cell at 400 C. *Advanced Functional Materials*, 31, 2102907.
- [4] J. Martynczuk, M. Arnold, H. Wang, J. Caro, and A. Feldhoff, 2007 How  $(\text{Ba}_{0.5}\text{Sr}_{0.5})(\text{Fe}_{0.8}\text{Zn}_{0.2})\text{O}_{3-\delta}$  and  $(\text{Ba}_{0.5}\text{Sr}_{0.5})(\text{Co}_{0.8}\text{Fe}_{0.2})\text{O}_{3-\delta}$  perovskites form via an EDTA/citric acid complexing method. *Advanced Materials*, 19, 2134-2140.
- [5] B. Koo, K. Kim, J. K. Kim, H. Kwon, J. Han, W and W. Jung, 2018 Sr segregation in perovskite oxides: why it happens and how it exists. *Joule*, 2, 1476-1499
- [6] K.Y. Park, Y.D. Kim, J. I. Lee, M. Saqib, J. S. Shin, Y. Seo, J. H. Kim, H. Lim and J.Y. Park, 2018 Operation Protocols To Improve Durability of Protonic Ceramic Fuel Cells. *ACS applied materials & interfaces*, 11, 457-468.
- [7] Irvine J T S, Neagu D, Verbraeken M C, Chatzichristodoulou C, Graves C and Mogensen M B 2016 Evolution of the electrochemical interface in high-temperature fuel cells and electrolyzers *Nat. Energy* 1 15014
- [8] Neagu D, Tsekouras G, Miller D N, Ménard H and Irvine J T S 2013 In situ growth of nanoparticles through control of non-stoichiometry *Nat. Chem.* 5 916–23
- [9] JH. Kim, J. Hong, DK. Lim, S. Ahn, J. Kim, JK. Kim, DH. Oh, SH. Jeon, SJ. Song, and W. Jung 2022 Water as Hole-Predatory Instrumental to Create Metal Nanoparticles on Triple-Conducting Oxides. *Energy & Environmental Science*
- [10] Duan C C et al 2018 Highly durable, coking and sulfur tolerant, fuel-flexible protonic ceramic fuel cells *Nature* 557 217
- [11] O. Kwon, S. Joo, S. Choi, S. Sengodan, and G. Kim, 2020. Review on exsolution and its driving forces in perovskites. *Journal of Physics: Energy*, 2, 032001
- [12] T. Zhu, H. E. Troiani, L. V. Mogni, M. Han, and S. A. Barnett 2018 Ni-substituted Sr (Ti, Fe)  $\text{O}_3$  SOFC anodes: achieving high performance via metal alloy nanoparticle exsolution. *Joule*, 2, 478-496.
- [13] D. Neagu, E. I. Papaioannou, W. K. Ramli, D. N. Miller, B. J. Murdoch, H. Ménard, A. Umar, A. J. Barlow, P. J. Cumpson, J. T. S. Irvine, and I. S. Metcalfe 2017 Demonstration of chemistry at a point through restructuring and catalytic activation at anchored nanoparticles. *Nature communications*, 8, 1-8
- [14] Y. Gao, D. Chen, M. Saccoccio, Z. Lu, and F. Ciucci, 2016 From material design to mechanism study: nanoscale Ni exsolution on a highly active A-site deficient anode material for solid oxide fuel cells. *Nano Energy*, 27, 499-508.
- [15] A. Yan, V. Maragou, A. Arico, M. Cheng, and P. Tsiakaras 2007 Investigation of a  $\text{Ba}_{0.5}\text{Sr}_{0.5}\text{Co}_{0.8}\text{Fe}_{0.2}\text{O}_{3-\delta}$  based cathode SOFC: II. The effect of  $\text{CO}_2$  on the chemical stability. *Applied Catalysis B: Environmental*, 76, 320-327.
- [16] M. A. Naeem, P. M. Abdala, A. Armutlulu, S. M. Kim, A. Fedorov, and C. R. Müller 2019 Exsolution of Metallic Ru Nanoparticles from Defective, Fluorite-Type Solid Solutions  $\text{Sm}_2\text{Ru}_x\text{Ce}_{2-x}\text{O}_7$  To Impart Stability on Dry Reforming Catalysts. *ACS Catalysis*, 10, 1923-1937

- [17] S. De Angelis, P. S. Jørgensen, E. H. R. Tsai, M. Holler, K. Kreka and J. R. Bowen 2018 Three dimensional characterization of nickel coarsening in solid oxide cells via ex-situ ptychographic nano-tomography. *Journal of Power Sources*, 383, 72-79.
- [18] O. Kwon, S. Sengodan, K. Kim, G. Kim, H. Y. Jeong, J. Shin, Y.W. Ju, J. W. Han, and G. Kim 2017 Exsolution trends and co-segregation aspects of self-grown catalyst nanoparticles in perovskites. *Nature communications*, 8, 1-7
- [19] H. Lv, T. Liu, X. Zhang, Y. Song, H. Matsumoto, N. Ta, C. Zeng, G. Wang, and X. Bao 2020 Atomic-Scale Insight into Exsolution of CoFe Alloy Nanoparticles in La<sub>0.4</sub>Sr<sub>0.6</sub>Co<sub>0.2</sub>Fe<sub>0.7</sub>Mo<sub>0.1</sub>O<sub>3-δ</sub> with Efficient CO<sub>2</sub> Electrolysis. *Angewandte Chemie International Edition*, 59, 15968-15973.
- [20] H. Emmerich, H. Löwen, R. Wittkowski, T. Gruhn, G. I. Tóth, G. Tegze, L. Gránásy 2012 Phase-field-crystal models for condensed matter dynamics on atomic length and diffusive time scales: an overview. *Advances in Physics*, 61, 665-743

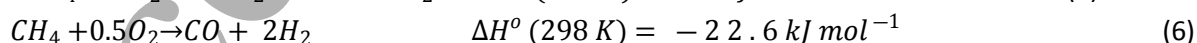
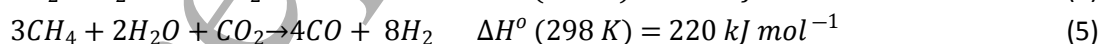
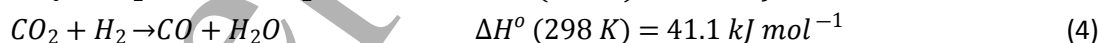
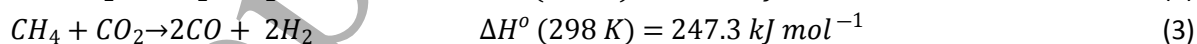
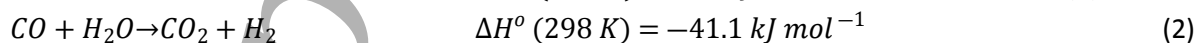
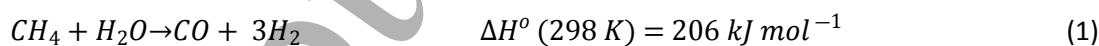
## Section 10 – Exsolution for methane reforming

Alfonso J. Carrillo

Instituto de Tecnología Química (Universitat Politècnica de València – CSIC) Valencia, Spain

### 10.1 Status

Methane reforming encompasses a series of industrially relevant reactions that transform this hydrocarbon into CO and H<sub>2</sub>, a mixture known as syngas, which could be further transformed into liquid fuels in Fischer-Tropsch units. These reactions are steam reforming (SMR), dry reforming (DRM), bi-reforming (BRM) and tri-reforming of methane (TRM). In SMR, methane reacts with steam according to Eq.1. The CO produced in SMR is further transformed via the Water Gas Shift (WGS) reaction (Eq.2) to produce more H<sub>2</sub>, and importantly CO<sub>2</sub>, which is removed through pressure swing absorption to produce pure H<sub>2</sub>. SMR is still nowadays the major technology for hydrogen production worldwide. In DRM, CH<sub>4</sub> reacts with CO<sub>2</sub> to produce syngas in a H<sub>2</sub>:CO molar ratio equal to 1 (Eq.3). Deviations from that ratio are normally caused by the Reverse Water Gas Shift (RWGS) reaction (Eq.4). In bi-reforming, methane reacts with both H<sub>2</sub>O and CO<sub>2</sub>, resulting in syngas with a H<sub>2</sub>:CO ratio of 2 (Eq.5), which is ideal for methanol synthesis [1]. Finally, oxygen can be also incorporated as reactant to adjust the final H<sub>2</sub>:CO in the so-called TRM, which is a combination of steam (Eq.1) and dry reforming (Eq.3), with methane partial oxidation (Eq.6).



Among these technologies, DRM has the advantage of using CO<sub>2</sub> as reagent. In comparison with SMR, using DRM will suppose a decrease of 0.5 Gt year<sup>-1</sup> of CO<sub>2</sub>. [2] In addition, dry, bi and tri-reforming show great promise in the transformation of biogas (a mixture of CH<sub>4</sub>, 50-75%, and CO<sub>2</sub>, 25-50 %) into syngas. [3] All these processes are endothermic and, therefore, require operation at high



temperatures, normally above 700 °C. These harsh conditions generally cause sintering of the catalyst particles, conventionally Ni supported in oxides such as Al<sub>2</sub>O<sub>3</sub>, CeO<sub>2</sub> or MgO. In addition, Ni catalysts are prompt to form carbon depositions, which can cause catalyst deactivation and reactor clogging. Nobel metal catalyst are more resistant to carbon depositions; however, their high cost has prevented its industrial commercialization.

## 10.2 Current and Future Challenges

Based on the above, it is paramount to develop more stable metal-supported catalyst with higher resistance against particle sintering and coking, and high selectivity to syngas, avoiding side reactions. For that reason, nanocatalysts prepared via the exsolution method have gained considerable attention for methane reforming reactions, especially for dry reforming of methane. This technology has not reached the industrial level yet and, therefore, the design and development of more efficient and robust materials remains a fundamental aspect to achieve commercialization. Exsolution, thus, emerges as a promising materials design route, since exsolved nanoparticles show robustness and low tendency to carbon formation [4]. Motivated by the remarkable performance of exsolution-functionalized fuel electrodes in solid oxide fuel cells and electrolyzers, perovskites decorated with exsolved nanoparticles were successfully tested for DRM. Probably, the first work fully devoted to DRM was by Zubenko et al., which exsolved Re-Ni-Fe alloys from LaFeO<sub>3</sub> perovskites, with CH<sub>4</sub> and CO<sub>2</sub> conversions close to 100 % at 900 °C [5]. However, researchers have applied the exsolution concept to other oxides that have been previously used as supports in DRM. Thus, in the last years the study of exsolution has been extended to other oxides rather than perovskites, which has been the most widely oxide host, especially in the solid oxide cell community. For methane reforming, exsolution has been tested in a variety of oxide supports, such as, pyrochlores [6], yttria-stabilized zirconia [7], MgO [8], spinels [9], ceria [10], double perovskite [11] or Ruddlesden-Popper phases [12]. All these studies targeted at long-term catalytic stability while assuring high resistance to sintering and low coking, paying special attention to the fundamental aspects of nanoparticle exsolution and structure-property relationships.

## 10.3 Advances in Science and Technology to Meet Challenges

The benefits of nanoparticle exsolution against more conventional methods, such as impregnation, were soon reported. Naeem et al. prepared catalyst based on Ru exsolution from Sm<sub>2</sub>Ru<sub>0.2</sub>Ce<sub>1.8</sub>O<sub>7</sub> pyrochlores, and compared its activity for DRM versus Ru/Sm<sub>2</sub>Ce<sub>2</sub>O<sub>7</sub> catalysts prepared by impregnation and borohydride reduction (Fig.1a-b)[6]. In Fig.1a, it can be seen that over the course of a 50 h catalytic test, the only material with stable performance was the catalyst prepared via exsolution, exhibiting a 70% of CH<sub>4</sub> conversion. The high temperatures, at which some oxide hosts, e.g., perovskites, are synthesized to obtain pure phases, detrimentally affect to the material's textural properties. For instance, double perovskites used for DRM with exsolved ternary alloyed nanoparticles have specific surface areas (SSA) that lie between 1.2 and 2.3 m<sup>2</sup> g<sup>-1</sup>, [15] whereas for high-performance MgO based catalysts exhibit SSA values around 70 m<sup>2</sup> g<sup>-1</sup> [2]. Thus, increasing the specific surface area of the host oxides, while guaranteeing a pure phase and the ability to exsolve nanoparticles remains then a major challenge in the field. A solution to overcome this problem was recently reported by Xiao and Xie, which fabricated porous single-crystalline CeO<sub>2</sub> monoliths from where Ni nanoparticles were exsolved (Fig.1c-e) [10]. This strategy led to SSA values between 25 and 30 m<sup>2</sup> g<sup>-1</sup> an order of magnitude higher compared to the aforementioned perovskites. The exsolved

1  
2  
3 Ni nanoparticles presented high dispersion and resistance to sintering after a catalytic test of 240 h  
4 (Fig.1c), in which the CH<sub>4</sub> conversion values were very stable (Fig.1e). Xiao and Xie, studied several Ni  
5 contents, which is limited by the low solubility of Ni in the CeO<sub>2</sub> lattice, finding that CeO<sub>2</sub> with 2.31%wt.  
6 of Ni reached almost 100% CO<sub>2</sub> conversion at 650 °C [10]. These results illustrated the prospect of  
7 nanoparticle exsolution in porous oxides.  
8  
9

10 An additional attractive feature of exsolution is the possibility of exsolving metallic alloys in a  
11 facile manner [13]. This is especially linked to the ability of perovskite oxides to host several transition  
12 metal cations in the B-site of the crystal lattice while maintaining a pure phase. These cations can  
13 recombine under certain exsolution conditions under metallic alloys, which can unlock unprecedented  
14 catalytic properties compared to single-element metallic nanoparticles. Several works have reported  
15 exsolution of metallic alloys for DRM, e.g. Re-Fe-Ni [5], FeNi<sub>3</sub> [11], [14] or Fe-Ni-Co[15]. In this last  
16 case, Joo et al. fabricated these ternary metallic alloy nanoparticles via topotactic exsolution in  
17 PrBaMn<sub>1.7</sub>Co<sub>0.1</sub>Ni<sub>0.2</sub>O<sub>5+δ</sub>, infiltrated with a solution of Fe precursors to obtain the multi-elemental alloy  
18 (Fig.1f). Importantly, the authors observed that the ternary exsolved alloy outperformed the bimetallic  
19 CoNi and metallic Ni and Fe exsolved nanoparticles as DRM catalysts (Fig1.g) [15]. Based on DFT  
20 calculations, Joo et al. ascribed this improvement to an increase charge donation ability for the ternary  
21 alloy, which facilitates the dissociation of CO<sub>2</sub>. [15]  
22  
23  
24  
25  
26

27 Finally, a third approach (together with oxide porosity and exsolved metallic alloys) that  
28 exhibits great potential is shape-controlled nanoparticle exsolution [16]. Very recently, Kim et al.  
29 reported on the possibility of changing the morphology of the exsolved nanoparticles by adjusting the  
30 exsolution conditions [16]. Namely, by increased time (24 h) and temperature (900-1000 °C) it was  
31 possible to obtained pyramidal exsolved Ni nanoparticles. [16] These shape-controlled exsolved  
32 nanoparticles exhibited higher resistance to coking than the spherical shape ones, and higher CH<sub>4</sub> and  
33 CO<sub>2</sub> conversion over the course of a 390 h DRM catalytic test [16].  
34  
35  
36  
37  
38  
39  
40  
41  
42  
43  
44  
45  
46  
47  
48  
49  
50  
51  
52  
53  
54  
55  
56  
57  
58  
59  
60

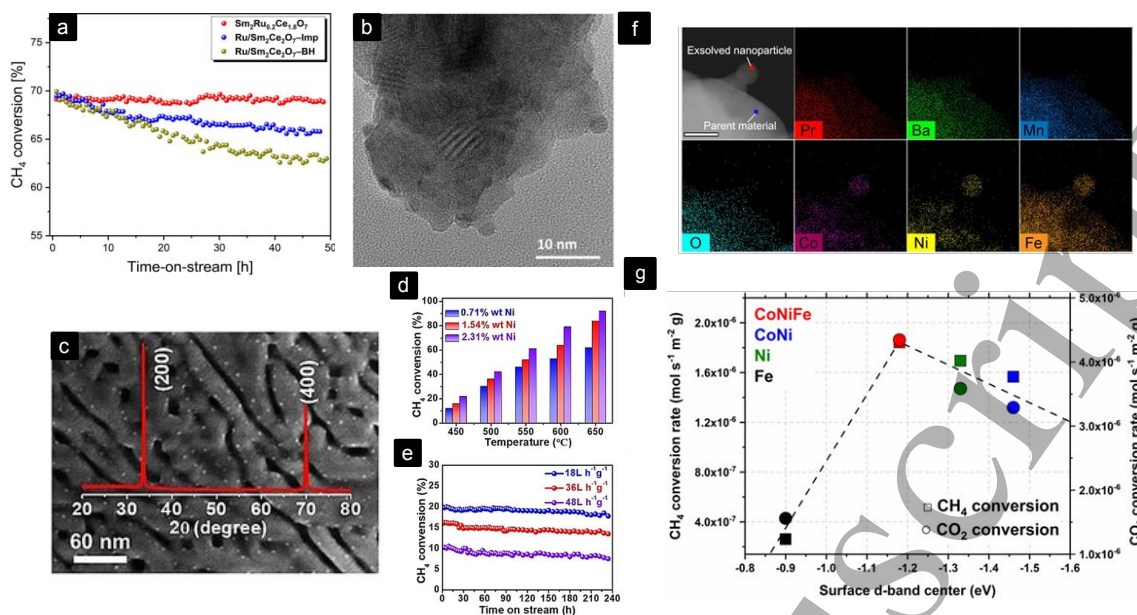


Figure 1 - (a) Methane conversion comparison for a material with Ru exsolution (red symbols), Ru impregnation (blue symbols) and Ru prepared via sodium borohydride reduction (yellow symbols). (b) TEM micrograph of Ru exsolution on  $\text{Sm}_2\text{Ru}_{0.2}\text{Ce}_{1.8}\text{O}_7$ . Both reprinted with permission from ACS Catal. 2020, 10, 3, 1923–1937. Copyright 2020 American Chemical Society. (c) SEM micrograph of exsolved Ni nanoparticles on  $\text{CeO}_2$  after 240 h dry reforming test. (d) Methane conversion at different temperatures for exsolved Ni catalyst on ceria with different Ni loading. (e) Methane conversion over 240 h test at different space velocity conditions. Reproduced with permission from John Wiley & Sons. (f) HAADF-EDX maps of illustrating Ni-Fe-Co ternary alloy topotactic exsolution from  $\text{PrBaMn}_{1-x}\text{Co}_x\text{Ni}_{0.2}\text{O}_{5+\delta}$  + 15 wt% infiltration of Fe. (g) Volcano plot of DFT-calculated d-band center and the  $\text{CH}_4$  and  $\text{CO}_2$  conversion in dry reforming of methane comparison for Fe, Ni,  $\text{Co}_3\text{Ni}$  and  $\text{CoNiFe}$  exsolved nanoparticles, from ref.[15]. Reproduced with permission from John Wiley & Sons.

#### 10.4 Concluding Remarks

Exsolution enables the formation of highly stable nanoparticles with remarkable resistance to sintering and coking, the two main issues that catalysts face in methane reforming reactions. This fact has prompted the development of advanced catalysts with improved performance over prolonged operation. Recent advances in which oxide porosity is increased and nanoparticle shape and composition are easily controlled by exsolution can contribute to expand the application of exsolved nanocatalysts in dry reforming reactions, which still seeks for more efficient and robust materials to reach industrial development.

#### 10.5 Acknowledgements

The project that gave rise to these results received the support of a fellowship from “la Caixa” Foundation (ID 100010434). The fellowship code is LCF/BQ/PI20/11760015.

#### 10.6 References

- [1] G. A. Olah, A. Goepfert, M. Czaun, and G. K. S. Prakash, “Bi-reforming of methane from any source with steam and carbon dioxide exclusively to metgas ( $\text{CO}-2\text{H}_2$ ) for methanol and

- hydrocarbon synthesis," *J. Am. Chem. Soc.*, vol. 135, no. 2, pp. 648–650, 2013, doi: 10.1021/ja311796n.
- [2] Y. Song *et al.*, "Dry reforming of methane by stable Ni–Mo nanocatalysts on single-crystalline MgO," *Science (80-. )*, vol. 367, no. 6479, pp. 777–781, Feb. 2020, doi: 10.1126/science.aav2412.
- [3] X. Zhao, B. Joseph, J. Kuhn, and S. Ozcan, "Biogas Reforming to Syngas: A Review," *iScience*, vol. 23, no. 5, p. 101082, 2020, doi: 10.1016/j.isci.2020.101082.
- [4] D. Neagu *et al.*, "Nano-socketed nickel particles with enhanced coking resistance grown in situ by redox exsolution," *Nat Commun*, vol. 6, p. 8120, 2015, doi: 10.1038/ncomms9120.
- [5] D. Zubenko, S. Singh, and B. A. Rosen, "Exsolution of Re-alloy catalysts with enhanced stability for methane dry reforming," *Appl. Catal. B Environ.*, vol. 209, pp. 711–719, 2017, doi: 10.1016/j.apcatb.2017.03.047.
- [6] M. A. Naeem, P. M. Abdala, A. Armutlulu, S. M. Kim, A. Fedorov, and C. R. Müller, "Exsolution of Metallic Ru Nanoparticles from Defective, Fluorite-Type Solid Solutions  $\text{Sm}_2\text{Ru}_x\text{Ce}_{2-x}\text{O}_7$  To Impart Stability on Dry Reforming Catalysts," *ACS Catal.*, vol. 10, no. 3, pp. 1923–1937, Feb. 2020, doi: 10.1021/acscatal.9b04555.
- [7] S. Joo *et al.*, "The first observation of Ni nanoparticle exsolution from YSZ and its application for dry reforming of methane," *Mater. Reports Energy*, vol. 1, no. 2, p. 100021, 2021, doi: 10.1016/j.matre.2021.100021.
- [8] Y. S. Park *et al.*, "Fabrication of a regenerable Ni supported NiO–MgO catalyst for methane steam reforming by exsolution," *J. Power Sources*, vol. 397, no. March, pp. 318–324, 2018, doi: 10.1016/j.jpowsour.2018.07.025.
- [9] Y. J. Wong, M. K. Koh, N. F. Khairudin, S. Ichikawa, Y. Morikawa, and A. R. Mohamed, "Development of Co Supported on Co–Al Spinel Catalysts from Exsolution of Amorphous Co–Al Oxides for Carbon Dioxide Reforming of Methane," *ChemCatChem*, vol. 11, no. 22, pp. 5593–5605, Nov. 2019, doi: 10.1002/cctc.201901098.
- [10] Y. Xiao and K. Xie, "Active Exsolved Metal–Oxide Interfaces in Porous Single-Crystalline Ceria Monoliths for Efficient and Durable  $\text{CH}_4/\text{CO}_2$  Reforming," *Angew. Chemie Int. Ed.*, vol. 61, no. 1, pp. 1–8, Jan. 2022, doi: 10.1002/anie.202113079.
- [11] A. J. Carrillo and J. M. Serra, "Exploring the Stability of Fe–Ni Alloy Nanoparticles Exsolved from Double-Layered Perovskites for Dry Reforming of Methane," *Catalysts*, vol. 11, no. 6, p. 741, Jun. 2021, doi: 10.3390/catal11060741.
- [12] S. Vecino-Mantilla, E. Quintero, C. Fonseca, G. H. Gauthier, and P. Gauthier-Maradei, "Catalytic Steam Reforming of Natural Gas over a New Ni Exsolved Ruddlesden-Popper Manganite in SOFC Anode Conditions," *ChemCatChem*, vol. 12, no. 5, pp. 1453–1466, 2020, doi: 10.1002/cctc.201902306.
- [13] C. Tang, K. Kousi, D. Neagu, and I. S. Metcalfe, "Trends and Prospects of Bimetallic Exsolution," *Chem. – A Eur. J.*, vol. 27, no. 22, pp. 6666–6675, Apr. 2021, doi: 10.1002/chem.202004950.
- [14] D. Papargyriou, D. N. Miller, and J. T. S. Irvine, "Exsolution of Fe–Ni alloy nanoparticles from  $(\text{La,Sr})(\text{Cr,Fe,Ni})\text{O}_3$  perovskites as potential oxygen transport membrane catalysts for methane reforming," *J. Mater. Chem. A*, vol. 7, no. 26, pp. 15812–15822, 2019, doi: 10.1039/c9ta03711j.
- [15] S. Joo *et al.*, "Enhancing Thermocatalytic Activities by Upshifting the d-Band Center of Exsolved Co–Ni–Fe Ternary Alloy Nanoparticles for the Dry Reforming of Methane," *Angew.*

- Chemie Int. Ed.*, vol. 19104, pp. 2–10, 2021, doi: 10.1002/anie.202101335.
- [16] Y. H. Kim, Y. Kang, S. Jo, H. Jeong, D. Neagu, and J. Myung, "Shape-Shifting Nanoparticles on a Perovskite Oxide for Highly Stable and Active Heterogeneous Catalysis," *SSRN Electron. J.*, pp. 1–29, 2022, doi: 10.2139/ssrn.4032434.

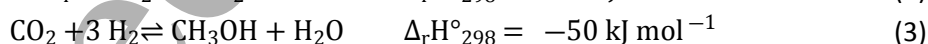
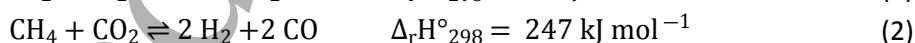
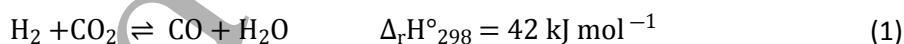
## Section 11 – Exsolution for CO<sub>2</sub> utilization applications

Thomas Ruh, Lorenz Lindenthal, Florian Schrenk, and Christoph Rameshan  
Chair of Physical Chemistry, Montanuniversität Leoben, 8700 Leoben, Austria

### 11.1 Status

To achieve a future where both economy and social prosperity are sustainable, independence from depletable resources is indispensable. Thus, it is necessary to establish a closed carbon cycle for industrial and energy processes. One way is to capture CO<sub>2</sub> from flue gas and transform it back into value added chemicals (CCU – carbon capture and utilisation) [1]. In addition to general technologies for CO<sub>2</sub> utilisation [2], exsolution materials represent a novel promising alternative [3]. The compositional flexibility of e.g. perovskites opens the possibility for a materials design approach [4].

One of the core strengths of exsolution catalysts for CO<sub>2</sub> utilization is their bifunctional nature: The exsolution process creates a surface decorated with metal nanoparticles embedded in a highly reactive oxide surface [3]. This makes them suitable for bifunctional reaction mechanisms, which are often required for CO<sub>2</sub> valorisation; with one type of active centres for CO<sub>2</sub> adsorption and activation, e.g. in the form of oxygen vacancies, located at the oxide support, and a second type for hydrogen or methane dissociation on exsolved nanoparticles, e.g. metallic Ni, Fe, or Co (Figure 1). Furthermore, the close vicinity of both types at the interface between host lattice and exsolved nanoparticles is crucial for the enhanced performance. Prominent examples for CO<sub>2</sub> utilization processes which benefit from this bifunctionality are reverse water-gas shift (rWGS, Equation 1), dry reforming of methane (DRM, Equation 2), or methanol synthesis (Equation 3):



For thermodynamic and selectivity reasons, the first two processes are operated at high temperatures. For rWGS, higher operation temperatures (i.e. 700–800 °C) shift the equilibrium to the product side. Even higher reaction temperatures (800–1000 °C) are required to shift selectivity towards DRM [5]. Methanol synthesis is operated at much lower temperatures (200–300 °C), but requires high pressures (>30 bar) to shift the equilibrium to the products [6].

Perovskite oxide catalysts are prime candidates for the high temperature reactions (rWGS + DRM), due to their enhanced thermal stability and tuneable exsolution properties. Their rich surface oxygen chemistry (i.e. easy formation and refilling of oxygen vacancies) furthermore prevents catalyst deactivation by e.g. coking or carbon nanotube formation (via oxidation of deposited carbon). From an industrial point of view, rWGS is the preferred CO<sub>2</sub> utilisation method, as it can be integrated in already established large-scale processes [7]. Moreover, exsolution catalysts display high intrinsic selectivity towards rWGS.

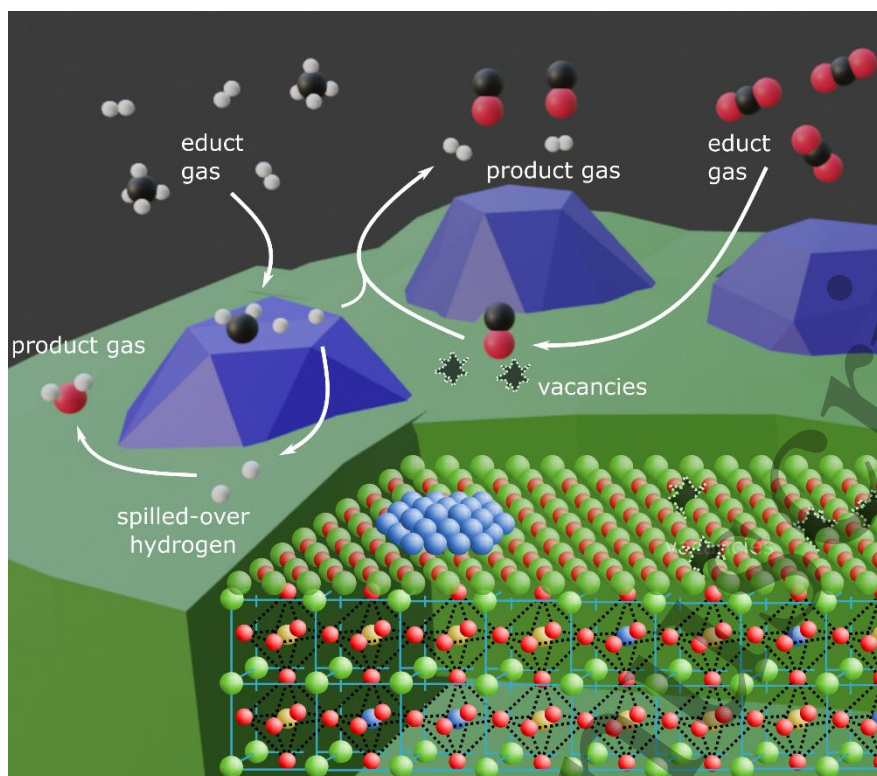


Figure 1 - Representation of the bifunctional nature of exsolution catalysts.

Different educt gases adsorb at different sites: (i)  $H_2$  and methane dissociate at metallic nanoparticles (blue). Consequently, H atoms spill over to the oxide surface where they react further. (ii)  $CO_2$  adsorbs at the perovskite, where it fills a vacancy (grey star-like shapes) and desorbs as CO.

## 11.2 Current and Future Challenges

Due to high necessary reaction temperatures for efficient rWGS and DRM, requirements regarding properties and stability of the exsolution materials are demanding. The composition of e.g. doped perovskites has a huge influence on their lattice stability, surface chemistry, and exsolution properties. Different material classes (e.g. titanates, ferrites, cobaltites etc.) feature different base catalytic properties and stabilities. Commercial WGS catalysts are for instance  $Fe_2O_3/Cr_2O_3$  mixtures, making particularly ferrites interesting for rWGS. The proper choice of the A-site cation (e.g. redox-capability) with additional A-site doping can significantly improve the oxygen surface chemistry (i.e. vacancy dynamics) for  $CO_2$  activation, figure 2A. B-site doping for preferential exsolution of e.g. Co (also highly active for rWGS) can further improve catalytic performance. In summary, a huge parameter space needs to be examined to optimize the catalytic properties via a materials design approach [8]. Predictions via theoretical modelling (including machine learning and Density Functional Theory) to efficiently determine the optimum between material stability and catalytic performance is of increasing importance [9].

For industrial applicability, exsolution catalysts additionally must be stable in varying gas environments, as in large-scale reactors gas compositions and temperatures, and hence chemical potentials, change across the catalyst bed (from product-lean at the entrance to product-rich at the

1  
2  
3 end of the reactor). For DRM reactions at high conversions (i.e. high H<sub>2</sub> content), this can lead to  
4 strongly reductive conditions that might result in decomposition of the host lattice. Even without  
5 complete decomposition, A-site cation segregation is often observed at high temperatures, thus  
6 causing deactivation (e.g. carbonate formation, figure 2C).  
7  
8

9  
10 How nanoparticle exsolution is achieved constitutes an important question: Size, shape and  
11 distribution of the formed nanoparticles strongly depend on process parameters, such as  
12 temperature, time, and gas phase (i.e. either reductive pre-treatment or *in-situ* exsolution in a  
13 reaction environment) [10]. This can have a huge effect on the achievable CO<sub>2</sub> utilization efficiency, as  
14 has been shown by recent studies that prove the beneficial effect of *in-situ* exsolution on the reactivity  
15 [3,11]. Also, additional growth of nanoparticles during operation is possible. For structure sensitive  
16 chemical reactions this needs to be considered.  
17  
18

19  
20 Another particularly important challenge is to increase the active surface area of exsolution  
21 catalysts. Classical synthesis routes, e.g. Pechini synthesis, sol-gel methods, or solid-state reactions,  
22 lead to materials with relatively low surface areas (below 10 m<sup>2</sup> g<sup>-1</sup>). Usually, high temperature  
23 calcination steps are required to achieve phase purity; however, this decreases the surface area.  
24 Therefore, novel synthesis routes that enable the production of larger quantities of high surface area  
25 (50–100 m<sup>2</sup>) exsolution catalysts need to be developed.  
26  
27

### 28 **11.3 Advances in Science and Technology to Meet Challenges**

29  
30 *In-situ* or *operando* studies (e.g. spectroscopy, diffraction, microscopy) are required to  
31 optimize exsolution catalysts with respect to surface structure and composition and to correlate  
32 structure and surface chemistry, figure 2D. However, the high operation temperatures of rWGS and  
33 DRM make these investigations particularly challenging. Hence, customized measurement cells have  
34 to be developed that allow precise control of the process parameters (even at high temperatures –  
35 e.g. above 800 °C – and in strongly reducing gas atmospheres; exact determination of the temperature  
36 at the sample surface is often particularly challenging) and still deliver excellent *in-situ/operando* data,  
37 which is needed to monitor possible intermediate species, reaction pathways, and possible  
38 deactivation phenomena [12].  
39  
40  
41  
42

43  
44 Detailed studies regarding long-term performance and stability of exsolution catalysts under  
45 realistic operating conditions (high T and high p) are also missing; however, this information is crucial  
46 for further development of industrially relevant catalysts. Especially the behaviour under realistic gas  
47 streams (often complex mixtures or containing contaminants) needs to be addressed for efficient  
48 application of industrial scale CO<sub>2</sub> utilization processes [13], e.g. issues connected to sulphur  
49 poisoning.  
50  
51

52  
53 Transitioning from fundamental scientific investigations to first real applications necessitates  
54 additional prerequisites to be met. As exsolution properties can strongly vary with small compositional  
55 variations, e.g. stoichiometry, A-site deficiency, or lattice strain [14], novel synthesis strategies are  
56 needed that enable highly reproducible production of doped perovskites; especially on an industrial  
57 scale. A promising approach is e.g. synthesis via flame spray pyrolysis [15], which would produce  
58 catalysts with high surface area as well. As a further step, the powder materials usually used in  
59 fundamental studies need to be transformed into structured catalysts that can be utilized in industrial  
60

1  
2  
3 processes (e.g. by mixing and supporting the perovskite on high surface area alumina) [16].  
4 Furthermore, the issue of integrating exsolution catalysts for CO<sub>2</sub> utilization into existing industrial  
5 processes needs to be addressed.  
6  
7

8 For catalyst optimization, comparable data is urgently needed, especially regarding catalytic  
9 performance of different materials – for instance in the form of unified turn over frequencies (TOF) or  
10 specific activities with detailed documentation of reaction and exsolution parameters.  
11  
12

13 In terms of industrial applicability, chemical looping is a further interesting topic, as it can be  
14 paired with discontinuous CO<sub>2</sub>-intense processes [17]. Although the rich redox chemistry of exsolution  
15 catalysts makes them promising materials, detailed performance studies for extended looping is rare.  
16 Especially the continued phase changes (and the more extreme conditions, e.g. pure H<sub>2</sub> instead of a  
17 mixture) may lead to pronounced performance loss over time due to sintering and phase separation  
18 processes.  
19  
20  
21  
22  
23  
24  
25  
26  
27  
28  
29  
30  
31  
32  
33  
34  
35  
36  
37  
38  
39  
40  
41  
42  
43  
44  
45  
46  
47  
48  
49  
50  
51  
52  
53  
54  
55  
56  
57  
58  
59  
60



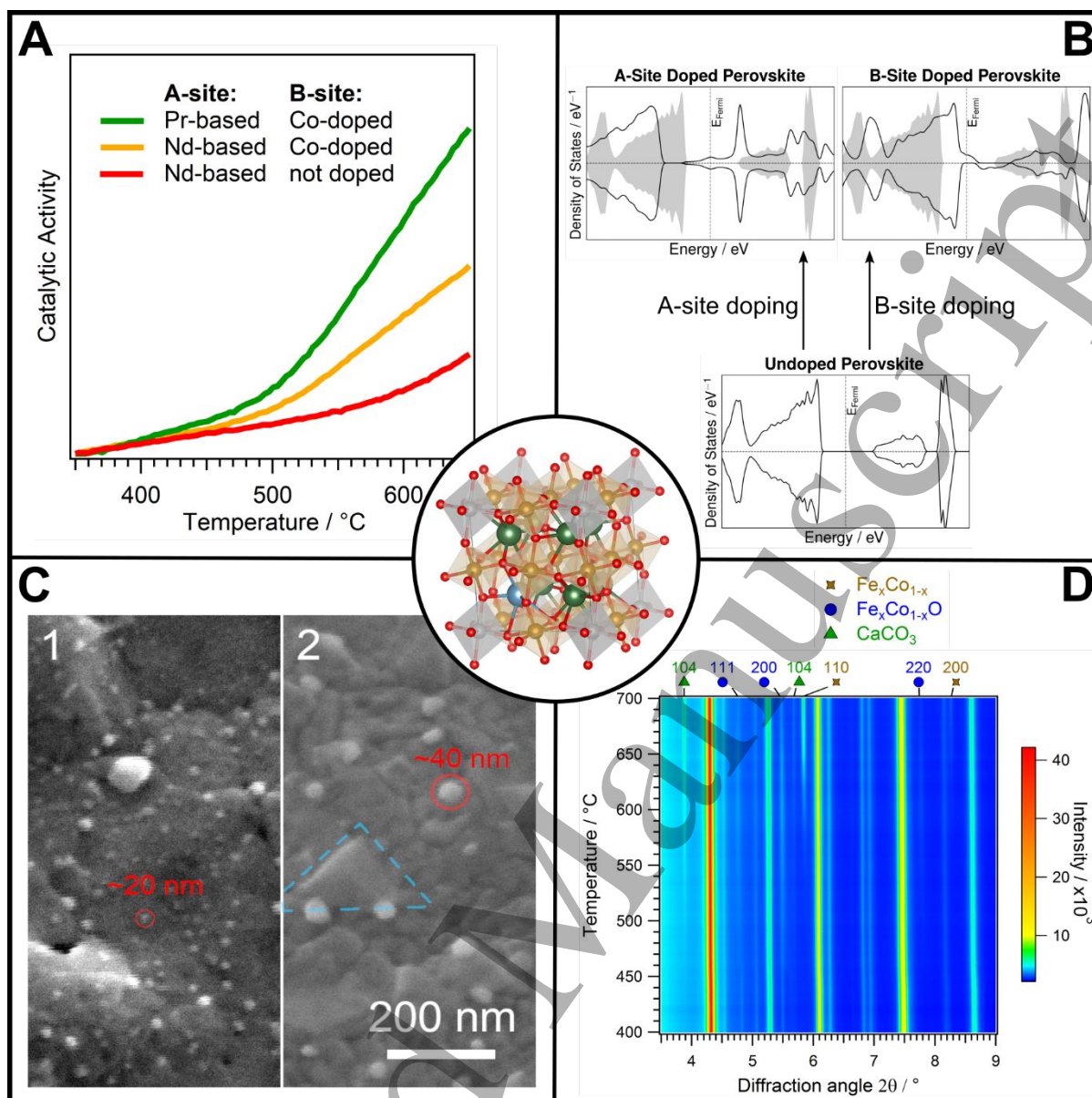


Figure 2 - Opportunities and challenges of perovskite-based exsolution catalysts used in CO<sub>2</sub> utilization.

Top: Changing the A-site base element and/or B-site doping allow tuning of catalytic properties (e.g. performance optimization for rWGS reaction; **A**). The electronic structure of the catalysts can be influenced via doping as well:

Depending on the respective dopants, the fermi level ( $E_{Fermi}$ ) can be shifted up or down

(see densities of states calculated with Density Functional Theory shown in **B**).

Bottom: The same material (a Co-doped perovskite) shows differently sized exsolved nanoparticles (highlighted with red circles in SEM images; **C**), depending on the conditions during exsolution (**C1**: lower temperature, **C2**: higher temperature). Additionally, unwanted triangular carbonate crystallites can be seen in **C2** (blue marking), which formed during high temperature rWGS reaction. Operando XRD data (taken during rWGS at a synchrotron facility; **D**) support those findings and confirm the formation of additional phases (metallic/oxidic nanoparticles, unwanted carbonaceous species) with increasing temperature.

#### 11.4 Concluding Remarks

CO<sub>2</sub> utilization via exsolution catalysts is a rapidly emerging field. The reasons are diverse and include:

- (i) High temperature stability of the host lattice (e.g. perovskites) which is necessary to withstand the high operation temperatures of CO<sub>2</sub> conversion processes, as required for rWGS and DRM.
- (ii) Intrinsic CO<sub>2</sub> activation capability of the reducible host lattice through surface oxygen vacancies.
- (iii) Catalyst surfaces with exsolved nanoparticles with highly improved H<sub>2</sub> or CH<sub>4</sub> dissociation on the metallic nanoparticles.
- (iv) A bifunctional reaction pathway as a result of the combination of (ii) and (iii).
- (v) A materials design approach via selective doping of the A- and B-site of the host lattice enables tailoring catalysts materials to industrial process conditions (e.g. optimized operating temperatures and pressures).

However, several challenges (e.g. long-term stability of the catalysts under operating conditions) have yet to be met on the pathway to industrial applications. First, novel synthesis routes need to be developed that allow the synthesis of larger quantities of high surface area materials. Especially achieving and maintaining high surface areas is challenging. Finally, exsolution materials have to be transformed into a shape (structured catalysts) that is applicable in industrial processes.

### 11.5 Acknowledgements

This work was funded by the European Research Council (ERC) under the European Union's Horizon 2020 research and innovation programme, grant agreement no. 755744/ERC—Starting Grant TUCAS.

The authors acknowledge DESY (Hamburg, Germany), a member of the Helmholtz Association HGF, for the provision of experimental facilities. Parts of this research were carried out at PETRA III, and the authors would like to thank Henrik Jeppesen for assistance in using beamline P02.1. Beamtime was allocated for proposal I-20211526 EC.

### 11.6 References

- [1] R. Schlögl, "Synthetic Fuels," in *Zukünftige Kraftstoffe: Energiewende des Transports als ein weltweites Klimaziel*, W. Maus, Ed., Wiesbaden, Germany: Springer Vieweg, 2019, pp. 191–223.
- [2] E. Alper and O. Y. Orhan, "CO<sub>2</sub> utilization: Developments in conversion processes," *Petroleum*, vol. 3, no. 1, pp. 109–126, Mar. 2017, doi: 10.1016/j.petlm.2016.11.003.
- [3] L. Lindenthal, J. Popovic, R. Rameshan, J. Huber, F. Schrenk, T. Ruh, A. Nanning, S. Löffler, A. K. Opitz, and C. Rameshan, "Novel perovskite catalysts for CO<sub>2</sub> utilization - Exsolution enhanced reverse water-gas shift activity," *Appl. Catal. B*, vol. 292, Sep. 2021, Art no. 120183, doi: 10.1016/j.apcatb.2021.120183.
- [4] H. Tanaka and M. Misono, "Advances in designing perovskite catalysts," *Curr. Opin. Solid State Mater. Sci.*, vol. 5, no. 5, pp. 381–387, Oct. 2001, doi: 10.1016/s1359-0286(01)00035-3.
- [5] D. Pakhare and J. Spivey, "A review of dry (CO<sub>2</sub>) reforming of methane over noble metal catalysts," *Chem. Soc. Rev.*, vol. 43, no. 22, pp. 7813–7837, Nov. 2014, doi: 10.1039/c3cs60395d.

- 1  
2  
3 [6] S. Dang, H. Yang, P. Gao, H. Wan, X. Li, W. Wei, and Y. Sun, "A review of research progress on  
4 heterogeneous catalysts for methanol synthesis from carbon dioxide hydrogenation," *Catal.*  
5 *Today*, vol. 330, pp. 61–75, Jun. 2019, doi: 10.1016/j.cattod.2018.04.021.
- 6  
7 [7] Y. A. Daza and J. N. Kuhn, "CO<sub>2</sub> conversion by reverse water gas shift catalysis: comparison of  
8 catalysts, mechanisms and their consequences for CO<sub>2</sub> conversion to liquid fuels," *RSC Adv.*,  
9 vol. 6, no. 55, pp. 49675–49691, Apr. 2016, doi: 10.1039/c6ra05414e.
- 10  
11 [8] J. H. Kim, J. K. Kim, J. Liu, A. Curcio, J.-S. Jang, I.-D. Kim, F. Ciucci, and W. Jung, "Nanoparticle  
12 Ex-solution for Supported Catalysts: Materials Design, Mechanism and Future Perspectives,"  
13 *ACS Nano*, vol. 15, no. 1, pp. 81–110, Jan. 2021, doi: 10.1021/acsnano.0c07105.
- 14  
15 [9] J. Hwang, R. R. Rao, L. Giordano, Y. Katayama, Y. Yu, and Y. Shao-Horn, "Perovskites in  
16 catalysis and electrocatalysis," *Science*, vol. 358, no. 6364, pp. 751–756, Nov. 2017, doi:  
17 10.1126/science.aam7092.
- 18  
19 [10] Y. H. Kim, Y. Kang, S. Jo, H. Jeong, D. Neagu, and J.-h. Myung, "Shape-shifting nanoparticles  
20 on a perovskite oxide for highly stable and active heterogeneous catalysis," *Chem. Eng. J.*,  
21 vol. 441, Aug. 2022, Art no. 136025 doi: <https://doi.org/10.1016/j.cej.2022.136025>.
- 22  
23 [11] F. Schrenk, L. Lindenthal, H. Drexler, G. Urban, R. Rameshan, H. Summerer, T. Berger, T. Ruh,  
24 A. K. Opitz, C. Rameshan, "Impact of nanoparticle exsolution on dry reforming of methane:  
25 Improving catalytic activity by reductive pre-treatment of perovskite-type catalysts" *Applied*  
26 *Catalysis B*, Volume 318, December 2022, 121886, doi: 10.1016/j.apcatb.2022.121886
- 27  
28 [12] R. Rameshan, A. Nanning, J. Raschhofer, L. Lindenthal, T. Ruh, H. Summerer, A. K. Opitz, T.  
29 M. Huber, and C. Rameshan, "Novel Sample-Stage for Combined Near Ambient Pressure X-  
30 ray Photoelectron Spectroscopy, Catalytic Characterization and Electrochemical Impedance  
31 Spectroscopy," *Crystals*, vol. 10, no. 10, Oct. 2020, Art no. 947, doi: 10.3390/cryst10100947.
- 32  
33 [13] F. Wang, H. Kishimoto, T. Ishiyama, K. Develos-Bagarinao, K. Yamaji, T. Horita, and H.  
34 Yokokawa, "A review of sulfur poisoning of solid oxide fuel cell cathode materials for solid  
35 oxide fuel cells," *J. Power Sources*, vol. 478, Dec. 2020, Art no. 228763, doi:  
36 10.1016/j.jpowsour.2020.228763.
- 37  
38 [14] D. Neagu, G. Tsekouras, D. N. Miller, H. Menard, and J. T. S. Irvine, "In situ growth of  
39 nanoparticles through control of non-stoichiometry," *Nat. Chem.*, vol. 5, no. 11, pp. 916–  
40 923, Nov. 2013, doi: 10.1038/nchem.1773.
- 41  
42 [15] S. Angel, J. Neises, M. Dreyer, K. F. Ortega, M. Behrens, Y. Wang, H. Arandiyan, C. Schulz, and  
43 H. Wiggers, "Spray-flame synthesis of La(Fe, Co)O<sub>3</sub> nano-perovskites from metal nitrates,"  
44 *AIChE J.*, vol. 66, no. 1, Jan. 2020, Art no. e16748, doi: 10.1002/aic.16748.
- 45  
46 [16] S. Mitchell, N. L. Michels, and J. Perez-Ramirez, "From powder to technical body: the  
47 undervalued science of catalyst scale up," *Chem. Soc. Rev.*, vol. 42, no. 14, pp. 6094–6112,  
48 July 2013, doi: 10.1039/c3cs60076a.
- 49  
50 [17] D. Sastre, D. P. Serrano, P. Pizarro, and J. M. Coronado, "Chemical insights on the activity of  
51 La<sub>1-x</sub>Sr<sub>x</sub>FeO<sub>3</sub> perovskites for chemical looping reforming of methane coupled with CO<sub>2</sub>-  
52 splitting," *J. CO<sub>2</sub> Util.*, vol. 31, pp. 16–26, May 2019, doi: 10.1016/j.jcou.2019.02.013.
- 53  
54  
55  
56  
57  
58  
59  
60

## Section 12 – Exsolution for CO Oxidation

Evangelos I. Papaioannou

School of Engineering, Newcastle University, Newcastle, United Kingdom

### 12.1 Status

The reaction between CO and O<sub>2</sub> (CO oxidation reaction) is seemingly straightforward and is one of the most widely studied chemical reactions. Although seemingly uncomplicated, it still attracts wide scientific interest, not only because it serves as an excellent model reaction for surface science investigations but also because CO oxidation finds a wide range of applications in air purification, automotive exhausts, fuel cells, gas sensors and lasers among others [1]. Up to now noble metals like platinum, palladium and iridium are frequently used as catalytic materials for CO oxidation while transition metals and metal oxides were proposed as lower cost alternatives [2]. Redox exsolution has emerged over the past decade as an alternative and simple synthetic platform for supported nanoparticles synthesis. Exsolved nanoparticles demonstrate enhanced activity across a wide range of application areas combined with high stability over thermal agglomeration and poisoning as opposed to their deposited analogues, owing to their partially socketed nature which results in a strained particle-oxide interface [3]. The recent years a number of different types of design elements (such as crystal structures, host lattice and exsolvable elements) and synthesis routes have been reported aiming for high catalytic activity and stability at a variety of operating conditions. Particularly for the CO oxidation reaction Co, Fe and Ti have been incorporated as B-site host lattice elements, while Ni, Co, Rh, Ir and Pd have been reported as exsolvable elements [4-10]. The solid state and the sol-gel methods were the two most prominent synthesis techniques used with the aim to achieve either strict control of stoichiometry (a critical parameter for preparation of materials with large amount of point defects) or phase formation at low temperatures (~700 °C) when smaller grains are desired [6]. Recently the redox exsolution efforts in CO oxidation have focused on the design of compositionally diverse transition metal oxide nanoparticles capable of achieving site activities previously observed in their noble metal analogues. Simultaneous exsolution of two or more reducible metal species or post synthesis morphological and chemical transformations are two representative examples of novel methods to unlock superior functionality and stability of such catalyst systems [4, 11]. This concept paved the way for a step change in the design of earth-abundant metal catalysts rivalling noble metals for the CO oxidation reaction.

### 12.2 Current and Future Challenges

There is no doubt that the redox exsolution concept has demonstrated that creating and manipulating confined particles enhances the intrinsic site activities of base metals by several orders of magnitude, leading to nanostructures capable of rivalling platinum-group catalysts on a per-site or per-weight basis for CO oxidation [4,9]. Understanding and controlling the physical and chemical properties of exsolved nanoparticles at the surface as well as the bulk of functional oxide supports is critical for further enhancing the activity and stability. Recent studies demonstrated that the shape and chemistry of exsolved nanoparticles can be tuned by controlling the gas environment the particles are exsolved from [4, 15]. Even though controlling extrinsic parameter for particle growth is intriguing, more research is required to model the resulting structures and establish links between specific facets and catalytic activity. For example, even though the mechanism of CO oxidation is well studied in conventionally prepared supported nanoparticles, i.e. a balance between Mars Van Krevelen mechanism on the interface and Langmuir-Hinshelwood mechanism on the metal surface, there are currently no reported studies for the exsolved analogues to interpret the higher catalytic activity apart

1  
2  
3 from limited reports on strong metal-support interactions which would facilitate ion and electron  
4 transport at strained interfaces [18, 19].  
5

6 Furthermore, it has been recently shown that exsolved nanoparticles can be dispersed throughout  
7 the bulk of oxide supports unlocking new dimensions in materials functionalisation [12, 13]. These  
8 developments are very important as strain engineering can be tuned via particle immersion in a  
9 controlled manner [14]. Nevertheless, there is still a great deal of work that needs to be done for  
10 understanding the links between lattice/particle strain and active sites for the CO oxidation  
11 reaction. Even though the developments on the fundamental studies on redox exsolution are  
12 profound, the scale-up of the exsolution method so that the exsolved catalyst structures can be used  
13 in large-scale catalytic applications is not trivial and present major challenges. Firstly, very few studies  
14 have focused on low loadings of the catalytic element present on the B-site and usually only a small  
15 fraction of these elements can emerge on the surface as exsolved nanoparticles [17]. Also, the internal  
16 surface area of the supporting oxide used for exsolution tend to be low, so once scaled up, the  
17 available specific surface area will be low and hence impact the resulting catalytic activity. Finally, in  
18 the large majority of studies, the exsolution takes place at high temperatures (>600°C) and under  
19 highly reducing conditions (99.9%+ purity H<sub>2</sub>), making the cost for upscale forbidden for further  
20 industrial implementation.  
21  
22  
23  
24  
25  
26  
27

### 28 **12.3 Advances in Science and Technology to Meet Challenges**

29  
30 Further scientific advances are required in the areas of modelling, operando and in-situ techniques  
31 for mechanistic understanding of particle growth as well as morphological and chemical  
32 transformations, the use of model systems under realistic conditions and manufacturing advances for  
33 scale-up. A holistic approach to modelling of the resulting nanostructures is crucial if one was to link  
34 materials characteristics (such as grain properties, surface and bulk structure and defects, particle  
35 properties etc) with intrinsic and extrinsic control parameters. Recent work has investigated the  
36 exsolution of individual nanoparticles with high spatial and temporal resolution and the results  
37 revealed the mechanisms that underpin the socketing and straining of the exsolved nanoparticles [15].  
38 High resolution scanning electron microscopy in conjunction with nanoparticle tracking and kinetic  
39 experiments (Figure 1, [4] ) has shown that exsolved particles do not re-dissolve back to the parent  
40 oxide and this can serve as a platform and alter their structure, composition and functionality while  
41 preserving their initial spatial arrangement for the CO oxidation reaction [4]. Such techniques,  
42 although complicated and expensive, could be used more routinely to provide insight into the in-situ  
43 formation and morphological and chemical transformations of exsolved nanoparticles.  
44  
45

46  
47 New methods need to be developed to address the challenges for scaling up exsolution. It is  
48 likely that thin-film heterostructures on low cost and high surface area supports can present several  
49 advantages as opposed to traditional synthesis methodologies. Exsolution from thin films if successful  
50 can achieve more efficient use of precursor materials and lower synthesis temperatures. To date only  
51 a few preliminary studies on this area have been reported [16]. The use of non-thermal atmospheric  
52 plasma as the driving force for exsolution can also be explored to induce exsolution in milder and more  
53 economical conditions which are more favourable for industrial implementation of the exsolution  
54 method.  
55  
56  
57  
58  
59  
60

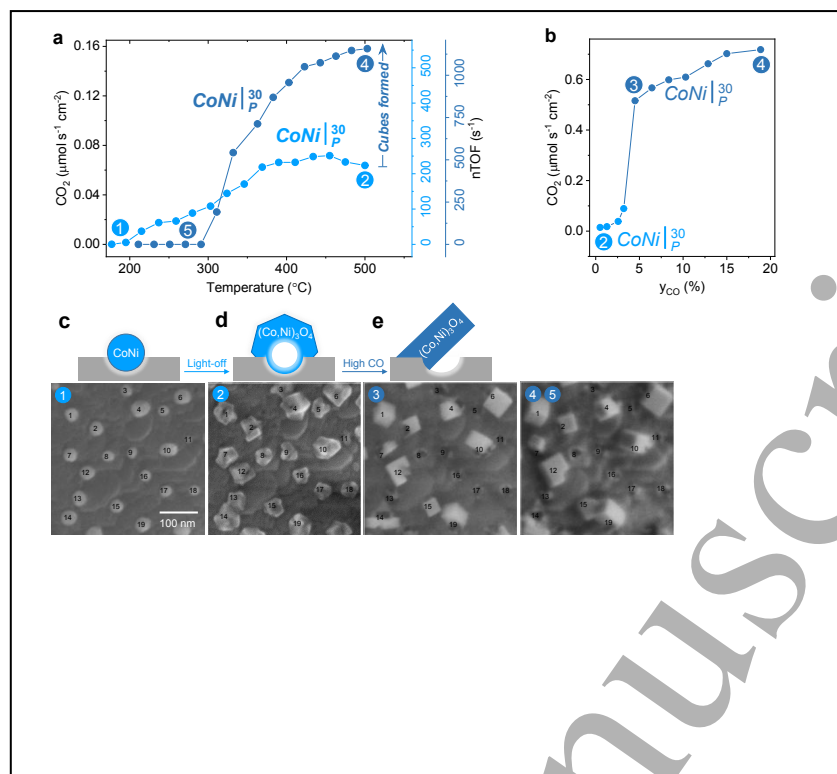


Figure 1 - Restructuring and catalytic activation at CoNi exsolved particles for the CO oxidation reaction. Selected regions of the samples are shown, tracking an average of 20 individual particles during the light-off experiment (points 1-2), before (points 2-4) and after (points 4-5) the CO kinetic experiment: **a** CO<sub>2</sub> production rate and nominal turnover frequencies (nTOF) from the CO oxidation reaction before and after the CO kinetic experiment, as a function of temperature (light-off experiment). **b** CO<sub>2</sub> production rate as a function of the partial pressure of CO ( $y_{CO}$ ) at 520 °C. **c-e** microstructure evolution showing: **c** as-prepared metal particles; **d** particles after the light-off experiment; **e** morphological transformations during the CO kinetic experiment. Adapted from [4] CC-BY-4.0.

## 12.4 Concluding Remarks

Undoubtedly the scientific advances in fundamental research and understanding of the exsolution mechanisms and structure-property relationships has demonstrated that exsolved systems with enhanced activity, stability as well as emergent functionality can satisfy the need for low cost and efficient catalysts for the CO oxidation reaction. In addition, with further simplification of the exsolution process requirements it is also possible to pave the way for industrial implementation of this revolutionary materials design concept.

## 12.5 Acknowledgements

The author is grateful for the financial support from the UK Catalysis Hub funded by EPSRC grant reference EP/R027129/1.

## 12.6 References

- [1] M. A. van Spronsen, J. W. M. Frenken, and I. M. N. Groot, "Surface science under reaction conditions: CO oxidation on Pt and Pd model catalysts," *Chem Soc Rev*, vol. 46, no. 14, pp. 4347-4374, Jul 17 2017, doi: 10.1039/c7cs00045f.

- 1  
2  
3 [2] L. Zhou et al., "Transition-Metal Doped Ceria Microspheres with Nanoporous Structures for CO  
4 Oxidation," *Sci Rep*, vol. 6, p. 23900, Mar 31 2016, doi: 10.1038/srep23900.
- 5 [3] D. Neagu et al., "Nano-socketed nickel particles with enhanced coking resistance grown in situ by  
6 redox exsolution," *Nat Commun*, vol. 6, p. 8120, Sep 11 2015, doi: 10.1038/ncomms9120.
- 7 [4] D. Neagu, E. I. Papaioannou, W.K.W. Ramli, D.N. Miller, B.J. Murdoch, H. Ménard, A. Umar, A.J.  
8 Barlow, P.J. Cumpson, J.T.S. Irvine, I.S. Metcalfe, "Demonstration of chemistry at a point through  
9 restructuring and catalytic activation at anchored nanoparticles" *Nature Communications*, vol. 8,  
10 no. 1855, 2017, doi: 10.1038/s41467-017-01880-y.
- 11 [5] C. Tang, K. Kousi, D. Neagu, J. Portolés, E. I. Papaioannou and I. S. Metcalfe, "Towards efficient use  
12 of noble metals via exsolution exemplified for CO oxidation" *Nanoscale*, vol. 11, p. 16935, Sep 1  
13 2019, doi: 10.1039/c9nr05617c.
- 14 [6] X. Zhang, H. Li, Y. Li and W. Shen, "Dynamic Behavior of Pd Species in an LaFe<sub>0.95</sub>Pd<sub>0.05</sub>O<sub>3</sub>  
15 Perovskite" *Catal. Lett.* Vol. 142, p. 118 Nov. 2 2012, doi: 10.1007/s10562-011-0735-7.
- 16 [7] M. Kurnatowska, L. Kepinski and W. Mista, "Structure evolution of nanocrystalline  
17 Ce<sub>1-x</sub>Pd<sub>x</sub>O<sub>2-y</sub> mixed oxide in oxidizing and reducing atmosphere: Reduction-induced activity in low-  
18 temperature CO oxidation", *Appl. Catal.*, vol. 117-118, p. 135, Jan 14 2012, doi:  
19 10.1016/j.apcatb.2011.12.034.
- 20 [8] S. Liu, W. Zhang, T. Deng, D. Wang, X. Wang, X. Zhang and C. W. Zheng, "Mechanistic Origin of  
21 Enhanced CO Catalytic Oxidation over Co<sub>3</sub>O<sub>4</sub>/LaCoO<sub>3</sub> at Lower Temperature", *ChemCatChem*, vol.  
22 9, p. 3102, Aug 7 2017, doi: 10.1002/cctc.201700937.
- 23 [9] E. I. Papaioannou, D. Neagu, W. K. W. Ramli, J. T. S. Irvine and I. S. Metcalfe, "Sulfur-Tolerant,  
24 Exsolved Fe–Ni Alloy Nanoparticles for CO Oxidation" *Top. Catal.*, vol. 62, p. 1149, Oct 5 2018, doi:  
25 10.1007/s11244-018-1053-8.
- 26 [10] E. Cali, G. Kerherve, F. Naufal, K. Kousi, D. Neagu, E. I. Papaioannou, M. P. Thomas, B. S. Guiton, I.  
27 S. Metcalfe, J. T. S. Irvine and D. J. Payne, "Exsolution of Catalytically Active Iridium Nanoparticles  
28 from Strontium Titanate" *ACS Appl. Mater. Interfaces*, vol. 12, p. 37444, Jul 23 2020, doi:  
29 10.1021/acsami.0c08928.
- 30 [11] C. Tang, K. Kousi, D. Neagu, I. S. Metcalfe, "Trends and Prospects of Bimetallic Exsolution" *Chem.*  
31 *Eur. J.*, vol. 27, p. 6666, Jan 11 2021, doi: 10.1002/chem.202004950.
- 32 [12] K. Kousi, D. Neagu, L. Bekris, E. I. Papaioannou and I. S. Metcalfe, "Endogenous Nanoparticles  
33 Strain Perovskite Host Lattice Providing Oxygen Capacity and Driving Oxygen Exchange and CH<sub>4</sub>  
34 Conversion to Syngas" *Angew. Chem., Int. Ed.*, vol. 59, p. 2510, Dec 5 2019, doi:  
35 10.1002/anie.201915140.
- 36 [13] K. Kousi, D. Neagu, L. Bekris, E. Cali, G. Kerherve, E. I. Papaioannou, D. J. Payne and I. S. Metcalfe,  
37 "Low temperature methane conversion with perovskite-supported exo/endo-particles" *J. Mater.*  
38 *Chem. A*, vol. 8, p. 12406, Jun 9 2020, doi: 10.1039/d0ta05122e.
- 39 [14] H. Han, J. Park, S. Y. Nam, K. J. Kim, G. M. Choi, S. S. P. Parkin, H. M. Jang and J. T. S. Irvine, "Lattice  
40 strain-enhanced exsolution of nanoparticles in thin films" *Nat. Commun.*, vol. 10, p. 1471, Apr 1  
41 2019, doi: 10.1038/s41467-019-09395-4.
- 42 [15] D. Neagu, V. Kyriakou, I. L. Roiban, M. Aouine, C. Tang, A. Caravaca, K. Kousi, I. Schreur, I. S.  
43 Metcalfe, P. Vernoux, M. C. M. van de Sanden and M. Tsampas, "In Situ Observation of  
44 Nanoparticle Exsolution from Perovskite Oxides: From Atomic Scale Mechanistic Insight to  
45 Nanostructure Tailoring", *ACS Nano*, vol. 13, p. 12996, Nov 19 2019, doi:  
46 10.1021/acs.nano.9b05652.
- 47 [16] K. J. Kim, H. Han, T. Defferriere, D. Yoon, S. Na, S. J. Kim, A. M. Dayaghi, J. Son, T. S. Oh, H. M. Jang  
48 and G. M. Choi, "Facet-Dependent in Situ Growth of Nanoparticles in Epitaxial Thin Films: The Role  
49 of Interfacial Energy" *J. Am. Chem. Soc.*, vol. 141, p. 7509, Apr 16 2019, doi: 10.1021/jacs.9b02283.
- 50 [17] D. Neagu, T. S. Oh, D. N. Miller, H. Ménard, S. M. Bukhari, S. R. Gamble, R. J. Gorte, J. M. Vohs and  
51 J. T. S. Irvine, "Nano-socketed nickel particles with enhanced coking resistance grown in situ by  
52 redox exsolution", *Nat. Commun.*, vol. 6, no 8120, Sep 11 2015, doi: 10.1038/ncomms9120.
- 53  
54  
55  
56  
57  
58  
59  
60

[18]Sun X, Chen H J, Yin YM, T. Curnan M, Han J W, Chen Y and Ma Z F 2021 Progress of exsolved metal nanoparticles on oxides as high performance (electro)catalysts for the conversion of small molecules *Small* **17** 2005383-419

[19]Sun X, Chen H J, Yin YM, T. Curnan M, Han J W, Chen Y and Ma Z F 2021 Progress of exsolved metal nanoparticles on oxides as high performance (electro)catalysts for the conversion of small molecules *Small* **17** 2005383-419

## Section 13 – Exsolution for Chemical Looping Hydrogen Production

Kalliopi Kousi<sup>1</sup> and Ian S. Metcalfe<sup>2</sup>

<sup>1</sup> Department of Chemical and Process Engineering, University of Surrey, United Kingdom

<sup>2</sup> Department of Chemical Engineering and Advanced Materials, Newcastle University, United Kingdom

### 13.1 Status

Chemical looping (CL) is a process in which individual reactions are divided into sub-reactions, either in different reactors, or in the same reactor but separated by time, with the reaction being mediated by a carrier material. Here we focus on the most common type, an oxygen carrier material (OCM). CL employing OCMs has received increased attention for hydrogen production as an alternative to the conventional process of steam methane reforming, followed by shift and separation, because of the ability of CL processes to produce separated product streams (Fig1).

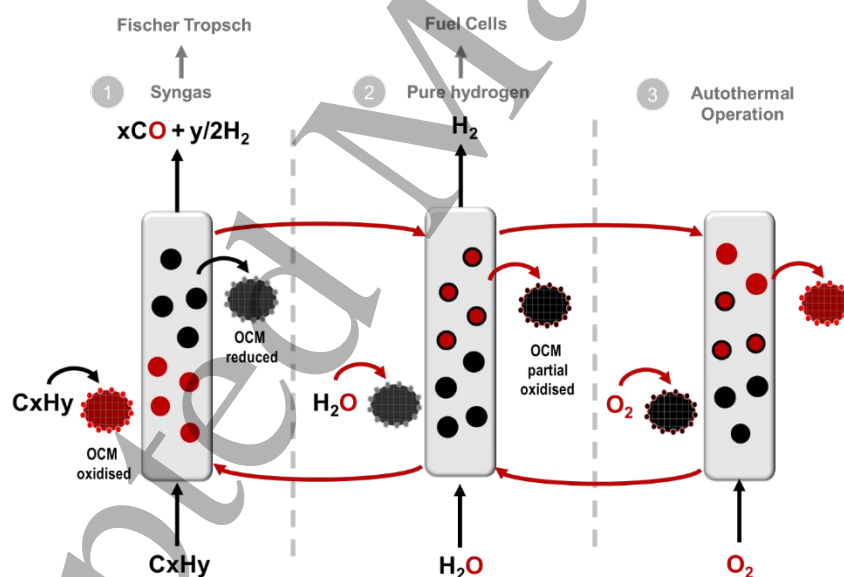


Figure 1 - Schematic representation of chemical looping and the use of an exsolved material as an OCM

A suitable OCM needs to possess a number of characteristics including but not limited to, oxygen exchange ability, oxygen storage capacity, redox stability, catalytic activity and poison, sintering and coking resistance. The OCM is often a metal/metal oxide (M/MO) system that undergoes reversible redox reactions and displays suitable thermodynamics for the application. More complex materials such as non-stoichiometric oxides have been the subject of interest permitting conversions in excess of conventional 'mixed' reaction equilibria[1]. Mixtures of the two above categories can also



be employed. However, OCM deactivation due to agglomeration, sintering, carbon deposition and matrix mismatch under redox conditions must be considered.

Recently the concept of exsolution has been used to address some of the above requirements. Exsolved systems exhibit redox stability, are catalytically active and possess resistance to poisons, sintering and coking[2]. Reversible exsolution and reincorporation of metal nanoparticles in the perovskite structure is thought to be the key to increase redox stability[3–5], avoid particle sintering and deactivation[6,7] and provide improved activity due to possible synergetic effects between the particles and the oxide support material[8]. In contrast, in irreversible exsolution the stable host matrix together with the exsolved particles form a metal-ceramic composite that due to the crystallographic alignment and socketing of the metallic particles overcomes the traditional limitations posed by deactivation due to matrix mismatch[9].

While exsolution has been used to decorate the surface of the host matrix, recently titanates were used to exsolve epitaxially aligned particles not only on the surface but also throughout the bulk[10,11]. For these structures, while the perovskite remains responsible for mediating oxygen exchange between the surface and the embedded nanoparticles, its oxygen transport capabilities are modified, in this case favourably, by the introduction of strain via the bulk particles (Fig2).

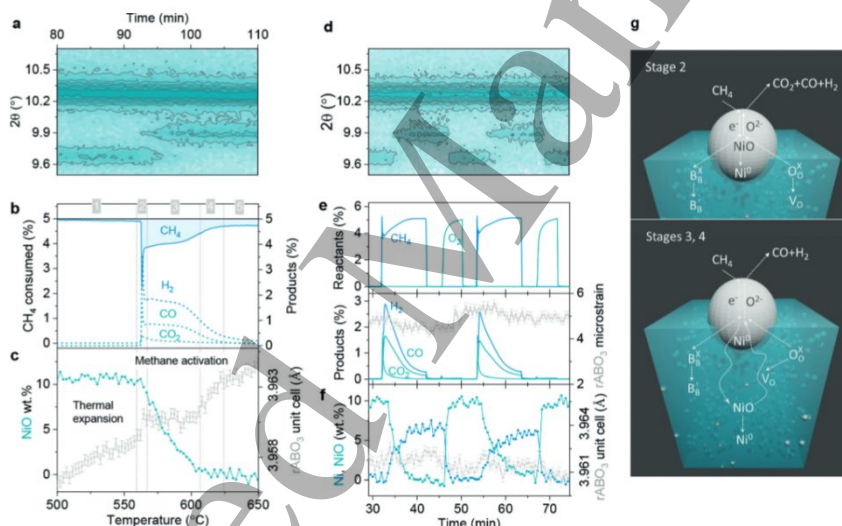


Figure 2 - Operando mechanistic insight into  $\text{CH}_4$  conversion with submerged nanoparticles in CL methane partial oxidation. Reproduced with permission [10].

### 13.2 Current and Future Challenges

The challenges in achieving a leap forward in the area of exsolution for CL belong in three main areas: design and synthesis of new materials, characterisation techniques and long-term stability. All should ideally be supported by computational modelling.

Many materials that have been used for CL processes take advantage of a M/MO phase change for the oxygen capacity needed, which is usually not easily tuneable to the process itself. Recently, non-stoichiometric oxides have been employed in order to provide more favourable thermodynamic strategies. However, such materials usually lack the capacity of a M/MO phase transition. Additionally, activation of hydrocarbon fuels, i.e.,  $\text{CH}_4$ , is often very slow and becomes the

1  
2  
3 rate limiting step. Hence, combining a non-stoichiometric oxide with a catalyst could allow for systems  
4 that demonstrate these desired properties. This approach comes with challenges in terms of stability,  
5 due to the presence of separate phases, different deactivation mechanisms and interphases.  
6 Exsolution can be used as a technique that can introduce the catalytic activity needed within a non-  
7 stoichiometric perovskite, in what could be considered to be a single material. However, preparation  
8 of exsolved systems has so far been dominated by solid-state methods which leads to low surface  
9 areas. Hence, new synthesis techniques are needed that would allow for tuneable surface and  
10 microstructural characteristics. This could in turn allow for increased surface exchange kinetics leading  
11 to potentially lower operation temperatures.  
12  
13  
14

15  
16 The lack of thermodynamic and kinetic data for exsolved systems in CL both when it comes to  
17 controlling key parameters ie particle size and population of said materials but also their  
18 thermodynamic behaviour when used as oxygen carrier materials is inhibiting wider application. In  
19 order to acquire this missing data, we need to invest in developing correlated in-situ characterisation  
20 techniques. This will allow us to monitor the way the materials function and evolve during operation  
21 and allow us to set the basis of designing materials tailored to specific applications.  
22  
23

24  
25 However, for all the above cases it will still be difficult to establish a well-defined set of rational  
26 design principles unless we aim to further develop computational modelling.  
27

28  
29 Lastly, the use of exsolved materials at scale is pretty much still at its infancy. By default,  
30 exsolution would allow for protecting against deactivation mechanisms such as agglomeration, carbon  
31 deposition, sulphur poisoning. However, long term studies under realistic conditions to evaluate the  
32 structural and chemical evolution of the materials are yet to be explored.  
33

### 34 **13.3 Advances in Science and Technology to Meet Challenges**

35  
36 Advances needed to address the challenges are divided into three main categories;  
37 understand, modify, and demonstrate.  
38

39  
40 To understand the origin of materials' performance, advances are required. In-situ techniques  
41 such as XRD (bulk composition, dynamic changes during operation), XPS (surface species – catalytic  
42 activators), EXAFS (coordination environment) especially at synchrotron sources coupled with detailed  
43 thermodynamic and kinetic data as well as the development of computational modelling at all length-  
44 scales, from materials design to process, would allow us to establish a detailed set of rational design  
45 principles[12]. The use of correlated in-situ techniques would provide an insight into the possibility of  
46 exsolution under reaction conditions and appropriate oxygen potentials. Additionally, different  
47 surface techniques that measure oxygen exchange as well as surface exchange and diffusion, would  
48 be of high interest because they would provide an insight into improving the design of these systems.  
49 Such techniques could include but are not limited to the use of Secondary Ion Mass Spectrometry  
50 (SIMS) or Nuclear Reaction Analysis (NRA) to determine isotopic exchange[13,14], conductivity  
51 relaxation experiments to determine ionic conductivity or in situ optical transmission relaxation  
52 coupled with impedance spectroscopy for oxygen surface exchange kinetics determination[15]. New  
53 methods might also need to be developed for measuring kinetic rates since in such materials these  
54 could potentially be dominated by interfaces[16].  
55  
56  
57  
58  
59  
60

1  
2  
3 Additionally, employing extrinsic techniques to control the crystal faces on the surface ie  
4 particle shape would make possible the design of highly active, selective and tailored materials[17–  
5 19], enabling a functional diversity that will allow for more efficient CL processes. As mentioned above,  
6 preparation method plays a key role in the nano and microstructure of these materials and  
7 modification of the current synthesis methods would impact on the microstructure of the backbone  
8 matrixes. This in turn would lead to the development of appropriate structures, ie smaller grain size,  
9 hierarchically ordered perovskites, in order to facilitate not only extent of exsolution, which is  
10 important for any application, but also oxygen exchange essential for CL processes[16]. Additionally,  
11 developing synthetic methods to prepare large batches of exsolved materials controllably, would  
12 facilitate their transition to pilot scale and ultimately commercial application.  
13  
14  
15  
16

17 Lastly, the integration of machine learning models with the above techniques may help  
18 uncover important structure-property relationships and guide further exploration and upscaling of  
19 these materials. The use of high-throughput testing would also accelerate the use of those materials  
20 at lab and pilot scale and eventually the transition to commercial processes[20].  
21  
22

### 23 **13.4 Concluding Remarks**

24  
25 There is no doubt that the use of exsolved materials in CL processes will lead to smarter more  
26 efficient chemical conversions for a sustainable future. However, challenges still remain. The key to  
27 exploitation is a combination of materials engineering and long-term real-life testing. The  
28 development of in-situ characterisation techniques as well as computational modelling will aid the  
29 design of improved materials with low cost, high activity and cyclability for clean hydrogen production  
30 via chemical looping.  
31  
32  
33

### 34 **13.5 Acknowledgements**

35  
36 The authors wish to thank EPSRC for funding via grant EP/R023921/1. ISM's position was  
37 supported by the Royal Academy of Engineering under the Chairs in Emerging Technologies scheme.  
38  
39

### 40 **13.6 References**

- 41  
42 [1] Metcalfe I S, Ray B, Dejoie C, Hu W, Leeuwe C de, Dueso C, García-García F R, Mak C-M,  
43 Papaioannou E I, Thompson C R and Evans J S O 2019 Overcoming chemical equilibrium  
44 limitations using a thermodynamically reversible chemical reactor *Nat. Chem.* **11** 638  
45  
46 [2] Neagu D, Oh T-S, Miller D N, Ménard H, Bukhari S M, Gamble S R, Gorte R J, Vohs J M and Irvine J  
47 T S 2015 Nano-socketed nickel particles with enhanced coking resistance grown *in situ* by redox  
48 exsolution *Nat. Commun.* **6** 8120  
49  
50 [3] Cui D, Li M, Qiu Y, Ma L, Zeng D and Xiao R 2020 Improved hydrogen production with 100% fuel  
51 conversion through the redox cycle of ZnFeAlOx oxygen carrier in chemical looping scheme  
52 *Chem. Eng. J.* **400** 125769  
53  
54 [4] Carrillo A J, Kim K J, Hood Z D, Bork A H and Rupp J L M 2020 La<sub>0.6</sub>Sr<sub>0.4</sub>Cr<sub>0.8</sub>Co<sub>0.2</sub>O<sub>3</sub> Perovskite  
55 Decorated with Exsolved Co Nanoparticles for Stable CO<sub>2</sub> Splitting and Syngas Production *ACS*  
56 *Appl. Energy Mater.* **3** 4569–79  
57  
58  
59  
60

- 1  
2  
3 [5] Zeng D, Qiu Y, Peng S, Chen C, Zeng J, Zhang S and Xiao R 2018 Enhanced hydrogen production  
4 performance through controllable redox exsolution within CoFeAlO<sub>x</sub> spinel oxygen carrier  
5 materials *J. Mater. Chem. A* **6** 11306–16  
6  
7 [6] Zeng D, Cui D, Lv Y, Qiu Y, Li M, Zhang S and Xiao R 2020 A mixed spinel oxygen carrier with both  
8 high reduction degree and redox stability for chemical looping H<sub>2</sub> production *Int. J. Hydrog.*  
9 *Energy* **45** 1444–52  
10  
11 [7] Hosseini D, Donat F, Abdala P M, Kim S M, Kierzkowska A M and Müller C R 2019 Reversible  
12 Exsolution of Dopant Improves the Performance of Ca<sub>2</sub>Fe<sub>2</sub>O<sub>5</sub> for Chemical Looping Hydrogen  
13 Production *ACS Appl. Mater. Interfaces*  
14  
15 [8] Lindenthal L, Popovic J, Rameshan R, Huber J, Schrenk F, Ruh T, Nanning A, Löffler S, Opitz A K  
16 and Rameshan C 2021 Novel perovskite catalysts for CO<sub>2</sub> utilization - Exsolution enhanced  
17 reverse water-gas shift activity *Appl. Catal. B Environ.* **292** 120183  
18  
19 [9] Otto S-K, Kousi K, Neagu D, Bekris L, Janek J and Metcalfe I S 2019 Exsolved Nickel Nanoparticles  
20 Acting as Oxygen Storage Reservoirs and Active Sites for Redox CH<sub>4</sub> Conversion *ACS Appl. Energy*  
21 *Mater.* **2** 7288–98  
22  
23 [10] Kousi K, Neagu D, Bekris L, Papaioannou E I and Metcalfe I S 2020 Endogenous Nanoparticles  
24 Strain Perovskite Host Lattice Providing Oxygen Capacity and Driving Oxygen Exchange and CH<sub>4</sub>  
25 Conversion to Syngas *Angew. Chem. Int. Ed.* **59** 2510–9  
26  
27 [11] Kousi K, Neagu D, Bekris L, Cali E, Kerherve G, Papaioannou E I, Payne D J and Metcalfe I S 2020  
28 Low temperature methane conversion with perovskite-supported exo/endo-particles *J. Mater.*  
29 *Chem. A*  
30  
31 [12] Yeo B C, Nam H, Nam H, Kim M-C, Lee H W, Kim S-C, Won S O, Kim D, Lee K-Y, Lee S Y and Han S  
32 S 2021 High-throughput computational-experimental screening protocol for the discovery of  
33 bimetallic catalysts *Npj Comput. Mater.* **7** 1–10  
34  
35 [13] Anon Isotopic oxygen exchange study to unravel noble metal oxide/support interactions: The  
36 case of RuO<sub>2</sub> and IrO<sub>2</sub> nanoparticles supported on CeO<sub>2</sub>, TiO<sub>2</sub> and YSZ - Hajar - - ChemCatChem  
37 - Wiley Online Library  
38  
39 [14] Sabioni A C S, Freire F L Jr, Barros Leite C V, Amami B A, Dolin C, Monty C and Millot F 1993 Study  
40 of oxygen self-diffusion in oxides by ion beam techniques: comparison between nuclear reaction  
41 analysis and SIMS *Nucl. Instrum. Methods Phys. Res. Sect. B* **73** 85–9  
42  
43 [15] Perry N H, Kim J J and Tuller H L 2018 Oxygen surface exchange kinetics measurement by  
44 simultaneous optical transmission relaxation and impedance spectroscopy: Sr(Ti,Fe)O<sub>3-x</sub> thin  
45 film case study *Sci. Technol. Adv. Mater.* **19** 130–41  
46  
47 [16] Irvine J, Rupp J, Liu G, Xu X, Haile S M, Qian X, Snyder A, Freer R, Ekren D, Skinner S, Celikbilek O,  
48 Chen S, Tao S, Shin T H, O'Hayre R, Huang J, Duan C, Papac M, Li S, Russel A, Celorrio V, Hayden  
49 B, Nolan H, Huang X, Wang G, Metcalfe I, Neagu D and Martin S G 2021 Roadmap on inorganic  
50 perovskites for energy applications *J. Phys. Energy*  
51  
52 [17] Neagu D, Kyriakou V, Roiban I-L, Aouine M, Tang C, Caravaca A, Kousi K, Schreur-Piet I, Metcalfe I  
53 S, Vernoux P, van de Sanden M C M and Tsampas M N 2019 In Situ Observation of Nanoparticle  
54 Exsolution from Perovskite Oxides: From Atomic Scale Mechanistic Insight to Nanostructure  
55 Tailoring *ACS Nano* **13** 12996–3005  
56  
57 [18] Kim Y H, Kang Y, Jo S, Jeong H, Neagu D and Myung J 2022 Shape-shifting nanoparticles on a  
58 perovskite oxide for highly stable and active heterogeneous catalysis *Chem. Eng. J.* **441** 136025  
59  
60

- [19] Khalid H., Haq U A., Alessi B., Wu J., Savaniu D C., Kousi K., Metcalfe S I., Parker C S., Irvine T S J., Maguire P., Papaioannou I E., Mariotti D. 2022 Rapid Plasma Exsolution from an A-site Deficient Perovskite Oxide at Room Temperature *Adv. Energy Mater.* **12** 2201131
- [20] Ortega C, Otyuskaya D, Ras E-J, Virla L D, Patience G S and Dathe H 2021 Experimental methods in chemical engineering: High throughput catalyst testing — HTCT *Can. J. Chem. Eng.* **99** 1288–306

## Section 14 – Exsolving functional nanoparticles from semiconductor matrix to expedite efficient photocatalysis

Xiaoxiang Xu<sup>1</sup> and Gang Liu<sup>2,3</sup>

<sup>1</sup>Shanghai Key Lab of Chemical Assessment and Sustainability, Tongji University, Shanghai, China

<sup>2</sup>Shenyang National Laboratory for Materials Science, Institute of Metal Research, CAS, Shenyang, China

<sup>3</sup>School of Materials Science and Engineering, University of Science and Technology of China, Shenyang, China

### 14.1 Status

The photocatalytic reactions generally involve, sequentially, the generation, separation, and transferring of photocarriers ( $e^-$  and  $h^+$ ). The large time-scale differences among these processes have raised severe challenges to modulate the photocarrier flow smoothly. For instance, the photocarrier separation normally occurs at a time scale of picoseconds to microseconds ( $10^{-12}s \sim 10^{-6}s$ ) while photocarrier transfer at the surface takes milliseconds to seconds ( $10^{-3}s \sim 10^0s$ )[1]. This renders strong implications for the photocatalysts to encompass different functional units which work synergistically. For instance, a photocatalyst normally comprises a semiconductor substrate for photocarrier generation and supported nanoparticles as cocatalysts to facilitate interfacial charge transfer[2]. Presumably, a strong interconnection between different functional units is indispensable to keep charge flows but usually cannot be guaranteed through conventional methods[3]. Directly growing nanoparticles from their supported substrates, known as exsolution processes[4], offers an ideal means to fabricate nanoparticles with strong interactions with the semiconductor matrix. This has been ascribed in part to the crystallographic alignment between the exsolved nanoparticles and semiconductor matrix and in part to the peculiar microstructures where exsolved nanoparticles are partially socketed into the supporting substrate[5]. In 2015, Xu et al introduced this exsolution tactic to fabricate  $AgTaO_3$  anchored with Ag-nanoparticles (i.e.  $Ag@AgTaO_3$ )[6]. The exsolved Ag nanoparticles have a size of around 40 nm whose plasmonic frequency falls into the visible light region and are capable of delivering hot electrons to the  $AgTaO_3$  substrate through localized surface plasmon resonance (LSPR) (Figure 1A). The  $Ag@AgTaO_3$  hybrid system not only owns visible light absorption but also shows improved photocatalytic activity for  $H_2$ -evolution under both UV and visible light illumination. Following these findings, many Ag-exsolved photocatalytic systems have been fabricated and have demonstrated intriguing performance for different applications, e.g. photodegradation, water splitting,  $CO_2$  reduction, etc.[7-9] Apart from noble-metal Ag, non-noble metals have also been exsolved from semiconductor substrates as hybrid photocatalytic systems. For instance, Cu nanoparticles have been exsolved from  $Cu_2O$  which contribute to a much-improved  $CO_2$  photoreduction activity even under near-infrared irradiation (Figure 1B) [10]. Likewise, Bi nanoparticles can be exsolved from  $BiOCl$  and deliver enhanced photocatalytic activity and stability for  $NO$  removal (Figure 1C) [11]. Currently, the research on nanoparticles exsolved from semiconductor matrix is at its infancy but has demonstrated exciting results in different photocatalytic applications. With ongoing exploration and understanding of the mechanism underpinning

semiconductor exsolution, one can foresee flourishing outcomes from photocatalysis involving exsolved nanoparticles.

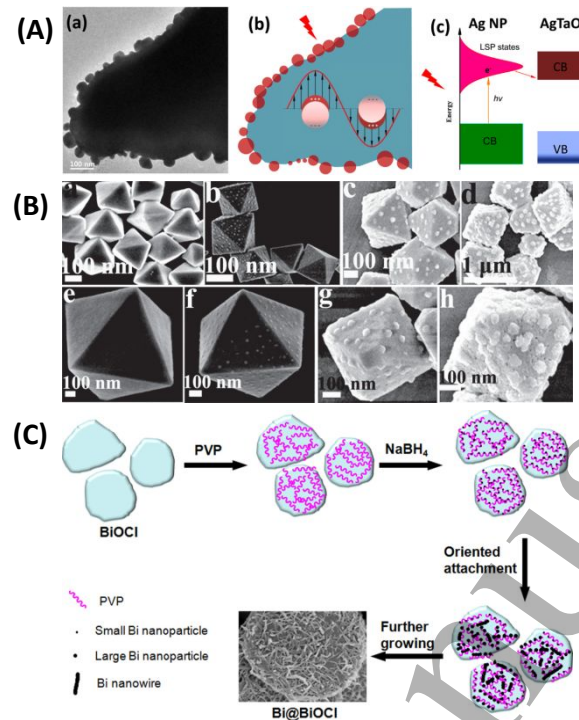


Figure 1 - (A) TEM image of AgTaO<sub>3</sub> exsolved with Ag nanoparticles (a), schematic representation of Ag exsolved from AgTaO<sub>3</sub> (b), schematic illustration of hot electron injection from Ag nanoparticles to AgTaO<sub>3</sub> (c) [6]; (B) Cu nanoparticles evolved from Cu<sub>2</sub>O at different stages: pristine Cu<sub>2</sub>O (a, e), Cu<sub>2</sub>O calcined in N<sub>2</sub> for 1 h (b, f), Cu<sub>2</sub>O calcined in N<sub>2</sub> for 2 h (c, g), Cu<sub>2</sub>O calcined in N<sub>2</sub> for 3 h (d, h) [10]; (C) schematic diagrams of the formation of Bi nanowires on BiOCl with the aid of PVP [11].

## 14.2 Current and Future Challenges

Although exsolved nanoparticles have shown promising applications in the field of photocatalysis, there are many questions and challenges to solve. Firstly, the role of exsolved nanoparticles is yet to be clarified during photocatalytic processes. Previous investigations have suggested that the exsolved metal nanoparticles participate in photocatalytic reactions through their LSPR. The LSPR can either inject hot electrons into the semiconductor substrate or can enhance photocarrier generation by an amplified near-field electromagnetic field and resonant photon scattering. As metal nanoparticles are also known as active catalysts for chemical reactions, it is unknown whether these metal nanoparticles also collect photocarriers from the semiconductor substrate and promote interfacial charge transfer (i.e. as a cocatalyst). It should be emphasized here that the charge flow direction is distinct for the two mechanisms: electrons migrate from metal nanoparticles to the semiconductor in LSPR and conversely in cocatalyst. Secondly, the type of nanoparticles that can be exsolved and semiconductor substrates suitable for exsolution awaits further exploration. Currently, nanoparticles exsolved from semiconductor substrates are mostly metals that can be easily reduced, e.g. Ag, Cu, Bi, etc. Only a few non-metal nanoparticles have been exsolved from semiconductors including WS<sub>2</sub> and Mn<sub>3</sub>O<sub>4</sub>. [12, 13] It would be of great interest to extend the categories of nanoparticles exsolvable to meet the diverse applications in the field of photocatalysis. On the other hand, the semiconductor substrates used to exsolve nanoparticles need

more investigation. In particular, the tolerance and capability of different crystal structures for exsolution have not been systematically studied. This is critical for semiconductor photocatalysis as any structural changes such as non-stoichiometry, defects, strains, etc. would dramatically modify the fundamental properties of the semiconductor, i.e. optical absorption, charge recombination, charge mobility, etc. Thirdly, the strategies to precisely control nanoparticle exsolution from semiconductors should be extended. From the viewpoint of photocatalysis, the activity would substantially hinge on the exsolved nanoparticles in terms of their location, density, particle size, crystal facets exposed, etc.

### 14.3 Advances in Science and Technology to Meet Challenges

The photocatalysts containing nanoparticles exsolved from semiconductor substrates are essentially heterogeneous multiphase systems. Knowledge about the location of photocarriers within the systems would be very helpful to understand the roles of different functional units and provides some clues to disclose the underlying mechanisms. There are some chemical and physical techniques that are spatially resolved for the detection of photocarriers. For instance, photo-deposition techniques can be used to identify the position of different photocarriers.  $\text{MnO}_x$  and  $\text{CoO}_x$  can be photo-deposited to the place where holes are accumulated whilst Pt and Ag are frequently used to probe the location of electrons[14]. In addition, recent advances in spatially resolved surface photovoltage (SPSPV) method have shown powerful capability in mapping the charge distribution at the nanoscale over heterogeneous photocatalysts and in revealing their charge separation mechanism [15] (Figure 2A). It would be very informative to apply the SPSPV method to study photocatalytic systems with nanoparticles exsolved from semiconductor substrates. With regard to the control of exsolution, a number of new synthetic methods or strategies have shown great potential to exquisitely tailor the composition and microstructures of nanoparticles exsolved. For instance, modifying the driving force needed for exsolution serves as a useful tool to modify the microstructures. Alternatively, some post-treatments can be used to prepare nanoparticles that cannot be directly exsolved from semiconductors [12] (Figure 2B). In the meantime, altering the properties of the semiconductor substrates can add another dimension to the design target of nanoparticles exsolved. In particular, perovskite-based semiconductors are well-known for their flexibility in structure and composition which provides copious possibilities in shaping the exsolved nanoparticles [9, 16].

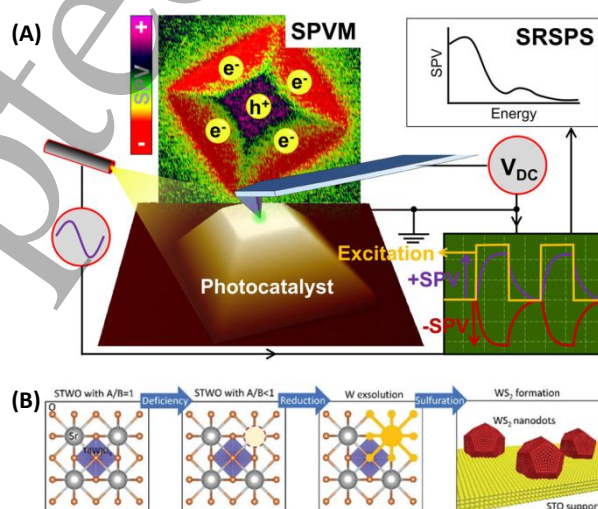


Figure 2 - (A) Schematic diagram of the spatially resolved SPV technique. The technique includes SPVM, which directly maps surface-charge distribution, and SRSPS, which measures modulated SPV signals with spectral

dependence [15]; (B) Schematic illustration of the new formation strategy of a  $WS_2$ -anchored- $SrTiO_3$  heterostructure via *in situ* exsolution [12].

#### 14.4 Concluding Remarks

Exsolution of nanoparticles from semiconductors is an appealing phenomenon and is very useful in fabricating photocatalytic systems which involve different functional units with strong interconnection. Compared with conventional nanoparticles, the exsolved ones clearly have many advantages such as good dispersion against agglomeration, robustness against poisoning, exceptional durability and stability under various reaction conditions, etc. These desirable properties have endowed exsolved nanoparticles with broad applications in the field of photocatalysis. Although the properties of exsolved nanoparticles need further investigation, previous encouraging results have proven their usefulness in achieving superior photocatalytic activities. With the ongoing investigation of their catalytic mechanisms with the state-of-art analytic techniques as well as the development of various new preparation protocols, we ought to witness more exciting outcomes in the photocatalytic systems involving nanoparticles exsolved from semiconductors.

#### 14.5 Acknowledgements

We thank the National Natural Science Foundation of China (Grant No. 51972233, 52172225, 51825204), Natural Science Foundation of Shanghai (Grant No. 19ZR1459200), Science and Technology Commission of Shanghai Municipality (Grant No. 19DZ2271500) and the Fundamental Research Funds for the Central Universities for funding.

#### 14.6 References

- [1] K. Takanabe, "Photocatalytic Water Splitting: Quantitative Approaches toward Photocatalyst by Design," *Acs Catalysis*, vol. 7, pp. 8006-8022, Nov 2017.
- [2] A. Kudo and Y. Miseki, "Heterogeneous photocatalyst materials for water splitting," *Chemical Society Reviews*, vol. 38, pp. 253-278, 2009.
- [3] J. H. Yang, D. G. Wang, H. X. Han, and C. Li, "Roles of Cocatalysts in Photocatalysis and Photoelectrocatalysis," *Accounts of Chemical Research*, vol. 46, pp. 1900-1909, Aug 20 2013.
- [4] D. Neagu, G. Tsekouras, D. N. Miller, H. Menard, and J. T. S. Irvine, "In situ growth of nanoparticles through control of non-stoichiometry," *Nature Chemistry*, vol. 5, pp. 916-923, Nov 2013.
- [5] K. Kousi, C. Y. Tang, I. S. Metcalfe, and D. Neagu, "Emergence and Future of Exsolved Materials," *Small*, vol. 17, May 2021.
- [6] X. X. Xu, G. Liu, and A. K. Azad, "Visible light photocatalysis by in situ growth of plasmonic Ag nanoparticles upon  $AgTaO_3$ ," *International Journal of Hydrogen Energy*, vol. 40, pp. 3672-3678, 2015.
- [7] Y. X. Dai, Y. T. Wang, G. C. Zuo, J. J. Kong, Y. Guo, C. Sun, and Q. M. Xian, "Photodegradation of acenaphthylene over plasmonic  $Ag/Ag_3PO_4$  nanopolyhedrons synthesized via in-situ reduction," *Applied Surface Science*, vol. 572, Jan 15 2022.



- 1  
2  
3  
4  
5  
6  
7  
8  
9  
10  
11  
12  
13  
14  
15  
16  
17  
18  
19  
20  
21  
22  
23  
24  
25  
26  
27  
28  
29  
30  
31  
32  
33  
34  
35  
36  
37  
38  
39  
40  
41  
42  
43  
44  
45  
46  
47  
48  
49  
50  
51  
52  
53  
54  
55  
56  
57  
58  
59  
60
- [8] J. X. Yu, L. Zhang, J. Qian, Z. R. Zhu, S. Ni, G. Liu, and X. X. Xu, "In situ exsolution of silver nanoparticles on AgTaO<sub>3</sub>-SrTiO<sub>3</sub> solid solutions as efficient plasmonic photocatalysts for water splitting," *Applied Catalysis B-Environmental*, vol. 256, p. 117818, 2019.
- [9] L. Zhang, Y. L. Yang, J. S. Tian, J. H. Li, G. Chen, L. J. Zhou, Y. F. Sun, and Y. F. Qiu, "Selective Photocatalytic Reduction of CO<sub>2</sub> to Syngas Over Tunable Metal-Perovskite Interface," *Chemsuschem*, Feb 23 2022.
- [10] M. Sayed, L. Y. Zhang, and J. G. Yu, "Plasmon-induced interfacial charge-transfer transition prompts enhanced CO<sub>2</sub> photoreduction over Cu/Cu<sub>2</sub>O octahedrons," *Chemical Engineering Journal*, vol. 397, Oct 1 2020.
- [11] F. Dong, T. Xiong, S. Yan, H. Q. Wang, Y. J. Sun, Y. X. Zhang, H. W. Huang, and Z. B. Wu, "Facets and defects cooperatively promote visible light plasmonic photocatalysis with Bi nanowires@BiOCl nanosheets," *Journal of Catalysis*, vol. 344, pp. 401-410, Dec 2016.
- [12] Y. F. Sun, Y. L. Yang, J. Chen, M. Li, Y. Q. Zhang, J. H. Li, B. Hua, and J. L. Luo, "Toward a rational photocatalyst design: a new formation strategy of co-catalyst/semiconductor heterostructures via in situ exsolution," *Chemical Communications*, vol. 54, pp. 1505-1508, Feb 11 2018.
- [13] J. J. Li, M. Zhang, E. A. Elimian, X. L. Lv, J. Chen, and H. P. Jia, "Convergent ambient sunlight-powered multifunctional catalysis for toluene abatement over in situ exsolution of Mn<sub>3</sub>O<sub>4</sub> on perovskite parent," *Chemical Engineering Journal*, vol. 412, May 15 2021.
- [14] R. G. Li, F. X. Zhang, D. G. Wang, J. X. Yang, M. R. Li, J. Zhu, X. Zhou, H. X. Han, and C. Li, "Spatial separation of photogenerated electrons and holes among {010} and {110} crystal facets of BiVO<sub>4</sub>," *Nature Communications*, vol. 4, p. 1432, Feb 2013.
- [15] R. T. Chen, F. T. Fan, and C. Li, "Unraveling Charge-Separation Mechanisms in Photocatalyst Particles by Spatially Resolved Surface Photovoltage Techniques," *Angewandte Chemie-International Edition*, p. e202117567, Feb 21 2022.
- [16] O. Kwon, S. Joo, S. Choi, S. Sengodan, and G. Kim, "Review on exsolution and its driving forces in perovskites," *Journal of Physics-Energy*, vol. 2, Jul 2020.